Author/s:
Xu, Bangyan

Title:
Application of activity-based probes to interrogate the contribution of cathepsin X to dendritic cells

Date:
2023-08

Persistent Link:
https://hdl.handle.net/11343/337948

Application of activity-based probes to interrogate the contribution of cathepsin X to dendritic cells

Bangyan Xu

ORCID ID: 0000-0002-2156-9074

Submitted in total fulfilment of the requirements of the degree of

Doctor of Philosophy

June 2023

Department of Biochemistry and Pharmacology

Faculty of Medicine, Dentistry and Health Sciences

The University of Melbourne

Abstract:

Cathepsin X/Z/P (Cat X) is a lysosomal cysteine protease that exhibits mono-carboxypeptidase activity. Increased cathepsin X expression is associated with cancer and inflammation; however, its roles in normal physiology are poorly understood. Cathepsin X is highly expressed by antigen-presenting cells such as dendritic cells (DCs). DCs undergo functional changes upon agonism of pattern recognition receptors (e.g., Toll-like receptors) by pathogen-associated molecular patterns (e.g., bacterial DNA – CpG). Mature DCs can secrete cytokines and present antigens to activate adaptive immunity. We hypothesised that cathepsin X contributes to DC function.

Using activity-based probes, immunoblotting, and immunofluorescence imaging, we measured active and total levels of cathepsin X in naïve immortalised DCs (DC1940) or those stimulated with TLR-1/2, 2/6, 3, 4, 7/8, and 9 agonists (Pam3, FSL-1, Poly I:C, LPS, R-848, and CpG, respectively). Lysosomal and secreted cathepsin X levels were significantly elevated in response to TLR-9 agonist CpG treatment and to a much lesser extent with the other agonists. We further investigated this mechanism and found that IL-6 secreted upon TLR-9 agonism promotes cathepsin X upregulation.

To examine the impact of cathepsin X on DC function, we generated cathepsin X-deficient DC1940 cells using CRISPR-Cas9. DC maturation, antigen uptake and antigen presentation were not affected by cathepsin X deficiency. We also investigated cytokine secretion and found that IL-6, IL-10, IL-12, TNFα, and MCP-11 were not affected by cathepsin X deficiency, while secretion of IL-1β was impaired. We further conducted shotgun proteomics to broadly investigate the impact of cathepsin X deficiency on DC immune function. We discovered that the expression of TMEM176B was significantly elevated in cathepsin X-deficient cells. TMEM176B has been reported to be a negative regulator of inflammasome activation. We hypothesise that the impaired secretion of IL-1β was due to the upregulation of TMEM176B in cathepsin X-deficient cells.

We next investigated the impact of cathepsin X deficiency on the overall lysosomal proteolytic environment. Cathepsin X-deficient cells exhibited altered processing of cathepsin L, while the processing and activities of other lysosomal proteases and their inhibitors were unaffected. We further found that cathepsin X deficient cells exhibited lower levels of nuclear cathepsin L. Whether or not the altered processing of cathepsin L was related to nuclear localisation is still under investigation. Furthermore, lower nuclear cathepsin L in the absence of cathepsin X resulted in reduced processing of its nuclear substrate, lamin B1.

Collectively, our data indicate that cathepsin X was strongly upregulated by TLR-9 agonism in DCs. While it may not be essential for DC maturation, antigen uptake, and antigen presentation, cathepsin X may regulate IL-1β secretion through TMEM176B. In addition, the processing of cathepsin L was altered in cathepsin X-deficient cells, and the level of nuclear cathepsin L was reduced. Future studies will focus on the mechanistic interaction between cathepsin X and TMEM176B and investigate the impact of reduced nuclear cathepsin L on nuclear proteolysis to better understand the role of cathepsin X in pathophysiology.

Declaration:

This is to certify that:

1. This thesis comprises only my original work towards the PhD except where indicated in the preface.
2. Due acknowledgements have been made in the text to all other materials used.
3. This thesis is less than 100,000 words in length, excluding tables, bibliographies, and appendices.

Bangyan Xu

August 2023

Preface

The work presented in this thesis was conducted in the laboratory of Dr Laura Edgington-Mitchell. The work was funded by the following grants awarded to Laura Edgington-Mitchell:

- Priority-Driven Collaborative Cancer Research Scheme Young Investigator Award (co-funded by Cancer Australia and Cure Cancer) (GNT1157171)
- Grimwade Fellowship (Russell and Mab Grimwade Miegunyah Fund, the University of Melbourne)
- Australian Research Council Discovery Early Career Research Award Fellowship (DE180100418)
- National Health and Medical Research Council Ideas Grant (GNT2011119)

My study was supported by the Research Training Program scholarship from the Australian Commonwealth Government. I wrote the original draft of the thesis and edited chapters in response to feedback from supervisor Dr Laura Edgington-Mitchell.

The contributions of others are acknowledged below, with the proportion of my original work indicated.

Chapter 3: Mutu DC1940 cells, primary splenic dendritic cells, cell media, TLR agonists, and the antibodies for detecting surface CD86 expression were generously provided by the Mintern Lab (the University of Melbourne). Proportion of original work by the Author: 100%.

Chapter 4: I generated the cathepsin X-deficient DC1940 cell line, antigen presentation, and endocytosis OVA-Cy5 in the Mintern Lab. The Mintern Lab also provided the materials for the experiments mentioned above. The Gleeson Lab (the University of Melbourne) generously provided Lucifer Yellow dye. I conducted the shotgun proteomic experiments in the Stroud Lab (the University of Melbourne), and the Stroud Lab generously provided the materials involved in the mass-spec. The proteomic data analysis and the acquisition were performed by Roopasingam Kugapreethan and David Robison. Proportion of original work by the Author: 98%.

Chapter 5: I generated the stable cathepsin X-expressing cell lines in the Stroud Lab with the assistance of Dr Joanna Sacharz. The Stroud Lab also generously provided some materials for generating the cell lines, including viral vectors, Gibson Assembly® Cloning Kit, Lipofectamine™ 2000 Transfection Reagent, and Opti-MEM™ media. Proportion of original work by the Author: 99%.

Publications resulting from candidature.

1. Liu, H., Wilson, K. R., Firth, A. M., Macri, C., Schriek, P., Blum, A. B., Villar, J., Wormald, S., Shambrook, M., **Xu, B.,** Lim, H. J., McWilliam, H. E. G., Hill, A. F., Edgington-Mitchell, L. E., Caminschi, I., Lahoud, M. H., Segura, E., Herold, M. J., Villadangos, J. A., Mintern, J. D., (2022). Ubiquitin-like protein 3 (UBL3) is required for MARCH ubiquitination of major histocompatibility complex class II and CD86. Nature Communications. 13. 1934. 10.1038/s41467-022-29524-w.

   Contribution by the author:

   Liu et al. discovered that UBL3 deficient cDC1 and cDC2 dendritic cells exhibited impaired antigen presentation to T cells. They demonstrated that impaired antigen presentation was due to the reduced capacity of antigen degradation. I applied activity-based probes to investigate the activity of lysosomal cathepsins and demonstrated that reduced proteolysis in the absence of UBL3 was not due to loss of cathepsin activity.

2. Wilson, K.R., Jenika, D., Blum, A. B., Macri, C., **Xu, B.,** Liu, H., Schriek, P., Schienstock, D., Francis, L., Makota, F. V., Ishido, S., Mueller, S. N., Lahoud, M. H., Caminschi, I., Edgington-Mitchell, L. E., Villadangos, J.A., Mintern, J. D., (2021). MHC Class II Ubiquitination Regulates Dendritic Cell Function and Immunity. The Journal of Immunology. 207. ji2001426. 10.4049/jimmunol.2001426.

   Contribution by the author:

   Wilson et al. reported that the lack of MHC-II ubiquitination impaired the immune function of the splenic dendritic cells. They discovered that the cells lacking MHC-II ubiquitination exhibited a reduction in antigen processing and, as a consequence, impaired antigen presentation to T cells. I characterised the activity of lysosomal proteases, including cathepsin B, L, S and X, as well as the expression of cystatin C, and demonstrated that reduced proteolysis in the absence of MHC-II ubiquitination was not due to loss of cathepsin activity.

3. Newton, P., Thomas, D.R., Reed, S. C. O., Lau, N., **Xu, B.,** Ong, S. Y., Pasricha, S., Madhamshettiwar, P. B., Edgington-Mitchell, L. E., Simpson, K. J., Roy, C. R., Newton, H. J., (2020). Lysosomal degradation products induce Coxiella burnetii virulence. Proceedings of the National Academy of Sciences. 117. 201921344. 10.1073/pnas.1921344117.

Contribution by the author:

Newton et al. reported that the optimal replication of *Coxiella burnetii* in host cells depends on low-density lipoprotein receptor-related protein 1 (LRP1) and cation-dependent M6PR receptors. They aimed to validate that loss of LRP1 and M6PR would reduce the degradative ability of lysosomes. I characterized the activities of lysosomal proteases using activity-based probes and did not observe any differences in the activities of several lysosomal proteases. We then used DQ-BSA to analyse the degradative ability of lysosomes, showing that loss of LRP1 and M6PR reduced lysosomal hydrolytic activity. This supported the conclusion that the tripeptidyl peptidase 1 (TPP1) is transported to the lysosomes in an LRP1/M6P receptor-dependant manner and is crucial for Coxiella effector translocation and virulence of *C. burnetii*.

4. Mountford, S. J., Anderson, B. M., **Xu, B.,** Tay, E. S. V., Szabo, M., Hoang, M-L., Diao, J., & Aurelio, L., Campden, R. I., Lindström, E., Sloan, E. K., Yates, R. M., Bunnett, N. W., Thompson, P. E., Edgington-Mitchell, L. E., (2020). Application of a Sulfoxonium Ylide Electrophile to Generate Cathepsin X-Selective Activity-Based Probes. ACS Chemical Biology. XXXX. 10.1021/acschembio.9b00961.

Contribution by the author:

This manuscript describes a series of novel activity-based probes with increased potency and specificity for cathepsin X. I characterised the efficacy of the probes in live RAW264.7 cells and cell lysates. This led to the identification of the best cathepsin X-selective probe to date, sCy5-Nle-SY, which was used heavily in my PhD project.

Awards and scholarships

1. 2019-2023 Research Training Program Scholarship, the University of Melbourne.
2. Jun 2021 3-minute thesis competition winner, Department of Biochemistry and Pharmacology, the University of Melbourne.

Conference presentations:

1. 2019 ASMR VIC Student Research Symposium – Oral presentation
2. 2019 Melbourne Cell Biology and Signalling (MCBS) Conference – Poster presentation
3. 2019 MPG Student Symposium – Poster presentation
4. 2020 Lorne Infection and Immunity Conference – 3-minute oral and poster presentation
5. 2020 MDHS Graduate Research Conference – Poster presentation
6. 2021 Lorne Infection and Immunity Conference – Poster presentation
7. 2021 MPG Student Symposium - Poster presentation
8. 2022 Gordon Research Seminar – Oral presentation
9. 2022 Gordon Research Conference – Poster presentation
10. 2022 MPG Student Symposium – Poster presentation
11. 2022 ComBio – Onsite poster presentation

Acknowledgements

As I am approaching the end of my PhD, I wish to acknowledge all the supporting people involved in this unforgettable journey.

Foremost, I would like to acknowledge my principal supervisor, Dr Laura Edgington-Mitchell. I feel grateful for working in your lab. We started from zero and witnessed the growth of our lab. You have always been extremely caring and supportive in the past five years. Under your supervision, I learned to think critically, design rigorous experiments, deliver extraordinary presentations, and many more. Apart from scientific skills, you also helped me develop better personalities. I was a shy person and not very confident. I surprisingly found that I gradually became more confident in delivering public speeches. I genuinely appreciate your supervision throughout my PhD journey. You are the best supervisor and will always be.

Thank you, LEM members, for making a collaborative and enjoyable lab environment. There is a saying that people with similar personalities will gather. We are all very caring and willing to help each other. Thank you, Beth, for your support all the way. We both started when LEM lab was just settled. As the only senior scientist in our lab for most of the time, you are always willing to take responsibility for helping me solve problems. Your hard work made our lab operate smoothly. Apart from that, I enjoy having conversations with you and learning Australian slang. Thank you, Umar, our previous post-doc, for teaching me various techniques, including animal-related and PCR-related skills. Those skills equipped me and helped my PhD journey. Thanks to Alex for being very supportive and helpful in the lab. I enjoyed our conversations about our common hobbies. If I had a second chance, I would not hesitate to work in the LEM lab again.

I would like to thank my co-supervisor, Prof Justine Mintern and the Mintern lab members. Thank you, Justine, for allowing me to attend your lab meeting, from which I learned valuable knowledge in immunology. At the beginning of my PhD, our lab was just settled. Therefore, I did many experiments in the Mintern lab. I met many friends and fantastic scientists. I learned most immunological techniques in your lab. To Gerry and Christophe, thank you for teaching me many immunological techniques. Thanks to Jo, Haiyin, Kayla, Annabelle, Devi, Nishma, Bjorn, Ashley and Hew for generously offering help when I was conducting experiments in your lab. I could not have done my PhD without all your help.

Thank you, Stroud Lab. I conducted a few experiments in your lab and learned a lot from many of you. I would like to thank Joanna for teaching me cloning and genetic editing techniques and Kugan and David for helping me with mass-spectrometry and data analysis. It was a great experience working with you, and I benefited greatly.

To my research committee: thank you, Kristin, for always being supportive and encouraging. Thank you, Jose, for giving me feedback on my data and giving me ideas for future experiments. Thank you, Hayley, for allowing me to collaborate on an exciting and interesting project with your lab.

I would like to acknowledge the Department of Biochemistry and Pharmacology for the travel support. Therefore, I was extremely fortunate to attend the Gordon Research Conference in Lucca (Barga), LU, Italy. During the conference, I presented my PhD work and received valuable feedback.

Thank you, my family members, Mom, Dad, and my sister Winnie, for all your support. Especially for Mom, you have sacrificed a lot taking care of Winnie and me since we moved to Melbourne. Thanks, Dad, for always working hard to create the best life for us.

Thank you, my fiancé Coco. Your company is invaluable. I feel grateful that you stayed with me throughout my highs and lows. I could not have imagined life without you.

To my friends, Yapeng, Shengzhu, Yafei, Anna, Jiaqi, and Minghui, I appreciate your company over the past few years. I enjoyed our road trips and weekly gatherings, which gave me emotional support to overcome obstacles during my PhD journey.

I would also like to acknowledge my guild and friends in the World of Warcraft for all the fun time.

Contents

List of Figures

List of Tables

List of Abbreviations:

ABP – Activity-based probe

AF – Alexa Fluor

ALR – Absent in melanoma 2 (AIM2)-like receptors

APC – Antigen Presentation Cell

APC – Allophycocyanin dye

ATP – Adenosine Triphosphate

ASMase – Acid Sphingomyelinase

BCA – Bicinchoninic Acid Assay

BSS – Balanced Salt Solution

CatB/C/D/H/L/S/X – Cathepsin B/C/D/H/L/S/X

CARD – Caspase Activation and Recruitment Domain

CD – Cluster of Differentiation

CFP – Cyan Fluorescent Protein

CHAPS – 3-[(3-cholamidopropyl) dimethylammonio]-1-propanesulfonic acid

cNLS – Canonical Nuclear Localisation Signal

CTV – Cell Tracer Violet

CpG – The " 5'—C—phosphate—G—3' " sequence of nucleotides

DAMPs – Damage-associated Molecular Patterns

DC – Dendritic cells

DMEM – Dulbecco's Modified Eagle Medium

DMSO – Dimethylsulfoxide

DTT – Dithiothreitol

EDTA – Ethylenediaminetetraacetic acid

EDTA-BSS - Ethylenediaminetetraacetic acid – balanced salt solution

ER – Endoplasmic Reticulum

FBS – Fetal Bovine Serum

Flt3 – Fms Like Tyrosine Kinase 3

GM-CSF – Granulocyte-macrophage Colony-stimulating Factor

GsdmD – Gasdermin-D

HEPES – N-2-hydroxyethylpiperazine-N-2-ethane sulfonic acid

HSV-1 – Herpes Simplex Virus I

IMDM – Iscove's Modified Dulbecco's Medium

IRF8 – IFN regulatory factor 8

KDS-RPMI – Potassium dodecyl sulphate – Roswell Park Memorial Institute

LRR – Leucine-rich Repeat

Mac-1 – Macrophage Antigen-1

MPU – Media Preparation Unit

NAIP – Neuronal Apoptosis Inhibitor Protein

NBD – Nucleotide-binding Domain

NF water – Nanofiltered water

NHS – Normal Horse Serum

Nle – Norleucine

NLR – Nucleotide-binding Oligomerization Domain (NOD)-like receptors

NLRP – Leucine-rich Repeat

NLS – Nuclear Localization Signals

OVA – Ovalbumin

PAMPs – Pathogen-associated Molecular Patterns

PBS – Phosphate-buffered Saline

PBST – Phosphate-buffered Saline Solution with 0.05% Tween™ 20

PDI – The Peter Doherty Institute for Infection and Immunity

PE – Phycoerythrin

PI – Propidium Iodide

PPR – Pattern Recognition Receptor

RPMI – Roswell Park Memorial Institute

RUSH – Retention Using Selective Hooks

sCy5 – Sulfo-Cyanine5

SY – Sulfoxonium ylides

TLR – Toll-Like Receptor

TWIK2 – Two-pore Domain Weak Inwardly Rectifying K+ Channel 2

WEHI – Walter and Eliza Hall Institute of Medical Research

Chapter 1. Introduction

1.1 Cathepsin X

1.1.1 Cathepsins are a unique family of proteases.

Proteases are hydrolytic enzymes that cleave the peptide bonds of protein substrates and are responsible for protein degradation and turnover. Proteases contribute to diverse biological processes, including antigen processing, cell signalling, migration, maturation, and proliferation [1-4]. Abnormal regulation of proteases is linked to various diseases, including cancer, inflammation, and cardiovascular diseases [5].

Cathepsins are a unique family of proteases with broad pathophysiological roles. The name "cathepsin" is derived from ancient Greek, meaning "boiling down" or "soften", indicating its role as an enzyme. Cathepsins can be classified into three groups based on their action of mechanism, including cysteine, serine, and aspartic cathepsins. Of particular interest for this thesis, there are 11 human cysteine cathepsins, including cathepsin B, C, F, H, K, L, O, S, V, X, and W. Cathepsin V (also named as cathepsin L2) is only expressed in human. Human cathepsin V has about 75% sequence identity with mouse cathepsin L; they are found to be functionally overlapping with each other [6]. Mice have a unique cysteine cathepsin, called cathepsin J, that is 59.3% homologous to cathepsin L [7].

1.1.2 Trafficking and localisation of cathepsins

Cathepsins are initially synthesised as zymogens in the ER and trafficked to endosomes via the mannose-6-phosphate receptor (M6PR) pathway [8]. Upon reaching the acidic environment, they are activated through autoactivation or cleavage by other proteases. Lysosomal cathepsins contribute to various vital cellular processes, including cell signalling, antigen processing, maturation of the MHC-II complex and TLR receptor processing and will be discussed in detail later in the introduction [9-12].

Most cysteine proteases have optimal activity within the acidic environment of lysosomes. However, a few notable exceptions include cathepsin B and S, which retain activity at neutral pH, indicating their potential roles in cell compartments other than the lysosomes [13, 14]. There is increasing evidence of extra-lysosomal roles for cathepsins (**Table. 1.1**), including in the cytosol, extracellular environment, and the nucleus. With proper chaperons, such as the glycosaminoglycans (GAGs), structures of cathepsins can be stabilised in a neutral or even

alkaline pH in vitro, indicating cathepsins may properly fold and function other than in the lysosomes [15].

Cytosolic cathepsins are primarily associated with inflammation during lysosomal rupture [16]. Cathepsin B, C, L, S, and X leaked from the lysosome during oxidative stress have been shown to impact the secretion of IL-1β and pyroptosis [17-20].

Cathepsins are also secreted into the extracellular environment, mainly in their inactive pro-forms [21]. The pathway of how cathepsins are secreted is still under debate. One possible route of cathepsin secretion is via the exosomes. A study conducted by Jiang and colleagues showed that pro-cathepsin L was contained by exosomes released by microglia and exacerbated Parkinson's disease [22]. In addition to that, glycosylation on lysosomal proteases may play a role in protease secretion: A disruption of the mannose 6-phosphate tagging may result in the mislocalisation of lysosomal proteases, making them secreted instead of transported to the lysosomes [23, 24].

When lysosomal proteases are secreted within exosomes, the exosomes may be endocytosed by other cells to modulate signalling pathways [25, 26]. Alternatively, in the context of the cancer microenvironment, the increased anaerobic glycolysis acidifies the local environment and subsequently facilitates the autoactivation of secreted pro-cathepsins. The secreted cathepsins can degrade the extracellular matrix and mediate cancer cell invasion [27, 28]. In addition, some lysosomal proteases possess an RGD motif and can bind to αVβ3 integrin receptors to trigger downstream signalling pathways independent of their proteolytic activity [29, 30].

Cathepsins have also been reported to reside in the nucleus, including cathepsin L, cathepsin V, and legumain [31-33]. Cathepsin L is reported to translocate into the nucleus through the importin β1 pathway [32], where it can modify the nuclear environment by cleaving nuclear substrates, including transcription factors and nuclear membrane proteins [34, 35]. Nuclear cathepsin L also modulates the cell cycle and ultimately contributes to colorectal carcinoma progression [36]. Similarly, nuclear cathepsin V (L2) is found in normal thyroid epithelial and carcinoma cells and may have a role in cancer cell hyperproliferation [31]. Legumain, a lysosomal cysteine endopeptidase that cleaves after an asparagine residue, has also been

characterised in the nucleus and found to cleavage histone H3.1 in colorectal cancer and Foxp3 transcription factor in regulatory T cells [33, 37].

Nonetheless, the cytosolic, nuclear, and extracellular environments significantly differ from the lysosomes. It is crucial to understand how lysosomal proteases (cathepsins) are trafficked into cellular locations other than lysosomes. Whether cathepsins are first localised in the lysosomes and subsequently trafficked into other subcellular locations or are directly trafficked to other locations from the ER remains to be investigated.

Table 1.1 Subcellular localisation of lysosomal proteases.

Localisations	Pathways	Function	References
Lysosomes	Mannose-6-phosphate (M6PR) pathway	Cell signalling Immune function Protein turnover	[12] [38] [39]
Cytosol	Lysosomal rupture	Pyroptosis	[17-20]
Extracellular space	Disruption of glycosylation Exosomes	Cleavage of extracellular matrix Cell communication Integrin binding	[27, 28] [25, 26] [29, 30]
Nucleus	Importin β1	Cleavage of nuclear proteins Cell cycle/cell progression	[33-35, 37] [31, 36]

1.1.3 Cathepsin X is a cysteine protease.

Cathepsin X (Z/P, CTSZ) is a papain-like cysteine protease that mainly resides in the lysosomes in cells of monocyte/macrophage lineage [40]. Like other cysteine proteases, cathepsin X mediates substrate hydrolysis through a catalytic triad (Cys–His–Asn). However, cathepsin X shares only 26–35% of overall homology and has a relatively short pro-peptide region compared to other cysteine proteases [41]. Most cathepsins are endopeptidases that cleave substrates in the middle of the peptide chain [42]. Although it has been published that cathepsin X may have low endopeptidase and dipeptidase activity, cathepsin X is generally considered a monocarboxy-exopeptidase at the optimal pH of 5.0 [43], meaning that it cleaves one amino acid at a time from the carboxy terminus of its substrates (**Figure 1.1**) [43-45]. This unique activity is due to a “mini-loop” structure corresponding to residue His23 to Tyr27. The “mini-loop” restricts the accessibility of endopeptidase substrates into the active site of cathepsin X and, therefore, mediates the substrate preference of cathepsin X [43].

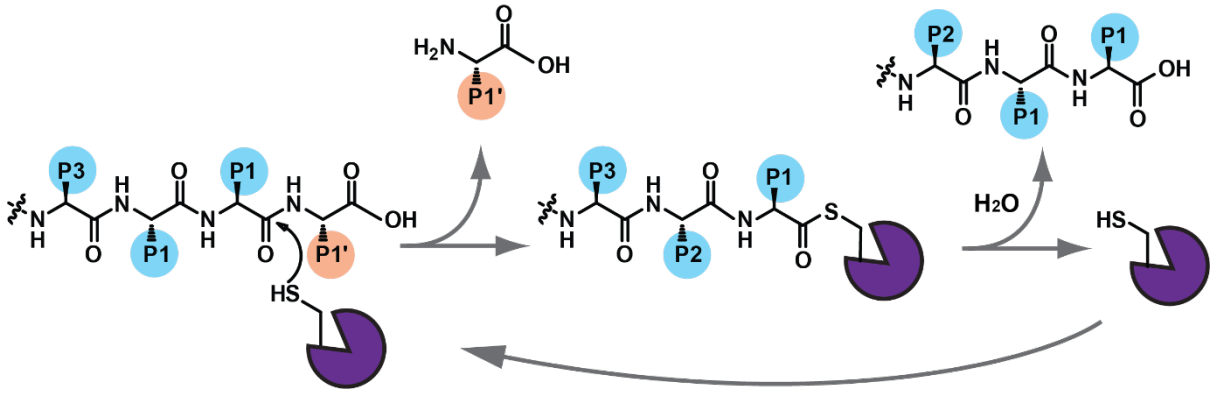

Figure 1.1 Mechanism of cathepsin X proteolysis. Cathepsin X cleaves off one amino acid at a time from the carboxy terminus of its substrates. The active cysteine on cathepsin X conducts a nucleophilic attack on the carbonyl group of the P1 amino acid. The P1' amino acid is subsequently released. Figure modified from Edgington et al. 2011 [46].

Cathepsin X is subject to complex post-translational regulation (**Figure 1.2**). It is first synthesised as an inactive zymogen and is transported to lysosomes via the mannose-6-phosphate receptor pathway like most other lysosomal proteins [47]. The pro-peptide sequence of cathepsin X contains three consecutive amino acids: an arginine, a glycine, and an aspartic acid to form an RGD motif **(Figure 1.2**). This RGD motif can bind to extracellular domains of integrins to trigger downstream signalling pathways involving focal adhesion kinase (FAK) and Src kinase and ultimately promote cell proliferation [48]. Most cysteine proteases have active proforms and can autoactivate themselves into mature forms in the lysosome. However, the crystal structure of cathepsin X showed its active cysteine was linked to a cysteine in the pro-peptide region with a disulphide bridge, thus making the proform inactive [49]. As a result, the activation of cathepsin X requires the removal of the pro-peptide region by other proteases. It has been shown that pro-cathepsin X could be processed into mature active cathepsin X by cathepsin L in a reducing environment in an in vitro setting [43]. There is little evidence of how cathepsin X is activated in normal physiological conditions.

Once activated, many proteases are kept in check by endogenous inhibitors, including the cystatin family (e.g., Cystatin C). However, cathepsin X does not appear to be inhibited by cystatin C, possibly due to the unique “mini-loop” structure preventing access of cystatin C to the cathepsin X active site [43]. Whether cathepsin X is subject to regulation by other endogenous inhibitors remains unknown.

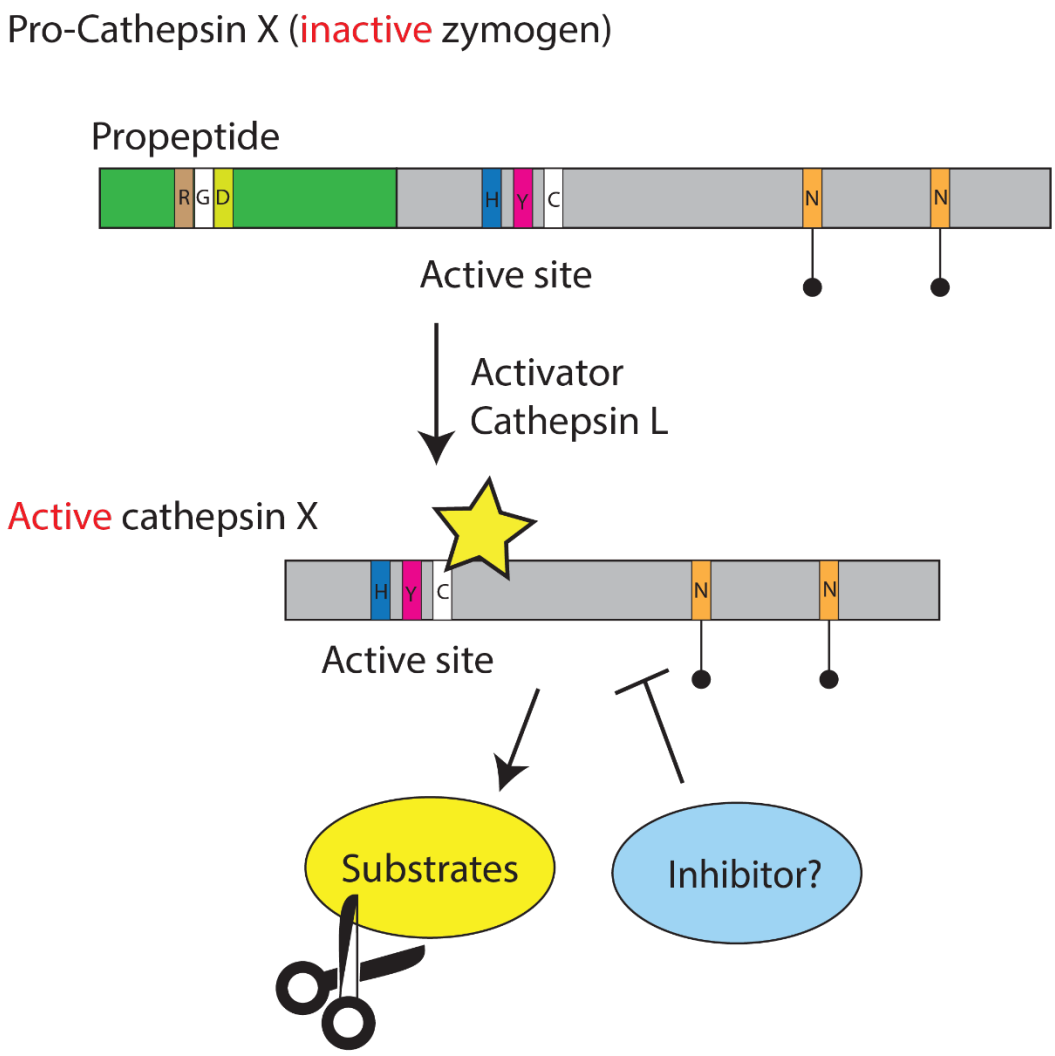

Figure 1.2 Post-translational regulation of cathepsin X. Cathepsin X is first synthesised as an inactive zymogen. The pro-peptide sequence is removed by proteolysis to activate cathepsin X. Cathepsin L has been used to activate cathepsin X in vitro. The active cathepsin X can cleave substrates in a mono-carboxypeptidase manner. Proteases are subject to the regulation of endogenous inhibitors; whether or not cathepsin X has an endogenous inhibitor is unknown.

According to in vitro analyses, cathepsin X can accommodate a broad range of amino acid residues. Among the P2, P1, and P1′ sites, proline is not favoured at P1, P2 or P1′ sites. Glycine is not favoured at the P2 site but preferred at P1 and P1′ sites (**Figure 1.1**) [50, 51]. Its broad substrate specificity suggests that cathepsin X may cleave a wide range of substrates [51] (**Table. 1.2**). Cathepsin X is reported to cleave cxcl-12, enolase, and β2-integrin [3, 50, 52, 53]. Cleavage of these substrates was demonstrated only in an in vitro setting, however, and thus requires further validation to confirm that they are indeed physiological substrates. Cathepsin X can also cleave profilin and limit its neutrophilic function. The discovery of cathepsin X substrates must be coupled with more advanced technologies, such as C-terminomics [54]. This technique provides insight into protein degradation/processing under physiological conditions.

Table 1.2 Cathepsin X substrates.

Substrates	Function/Pathophysiology	Reference
CXCL-12	Cell adhesion and migration	[50]
Profilin	Clathrin-Mediated Endocytosis	[53]
Enolase	Impaired survival and neuritogenesis of neuronal cells	[52]
β2-integrin	Dendritic cell maturation	[3]

1.1.4 Using chemical probes to measure protease activity.

Due to the complexity of the post-translational regulation of protease activity, conventional techniques such as immunoblotting, ELISA or immunofluorescence only reveal the total level of proteases. They do not report on the proportion of active, functional enzymes. For example, a highly expressed protease may have low activity in the presence of endogenous inhibitors, or the protease might exist predominantly in its proform. Therefore, measures of protease levels should be coupled with assessments of their activity. For this purpose, activity-based probes (ABPs) have been developed for various proteases. ABPs consist of three major features: a warhead, a recognition sequence, and a reporter group **(Figure 1.3AB**). The warhead is an electrophile that reacts and subsequently forms a covalent linkage with the nucleophilic residue within the active site of the protease. The recognition sequence mimics the substrate, incorporating an amino acid that guides selectivity towards specific proteases. The reporter group is typically a fluorophore but can also be modified to fit other applications (e.g., biotin) **(Figure 1.3AB)**. Using imaging techniques, probe binding can be visualised at multiple levels, including whole organisms, tissues, and cells. As the probe binds covalently to the protease of interest, the binding survives the reducing conditions of SDS-PAGE (sodium dodecyl sulphate polyacrylamide gel electrophoresis); protease binding can be detected by measuring in-gel fluorescence using flat-bed laser scanners [55].

The Edgington-Mitchell Lab has recently developed a series of activity-based probes for cathepsin X [56]. The most potent and selective probe, sCy5-Nle-SY, has a sulfoxonium ylide warhead, a norleucine amino acid as the recognition site and a sulfo-Cy5 fluorophore **(Figure 1.3B)**. sCy5-Nle-SY exhibits high specificity to cathepsin X when applied to acidified cell or tissue lysates **(Figure 1.3C left)**. However, when applied to living cells, it also targets cathepsin S. The molecular weight discrepancy between cathepsin X and S allows facile differentiation of the two proteases by in-gel fluorescence (**Figure 1.3C right**).

A

sCy5-Nle-SY

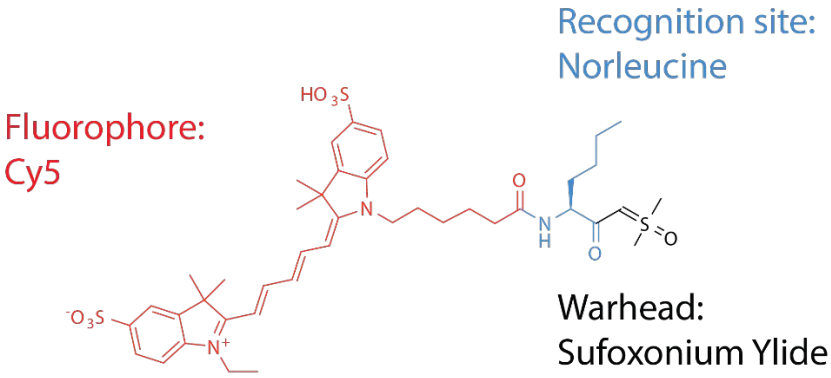

B

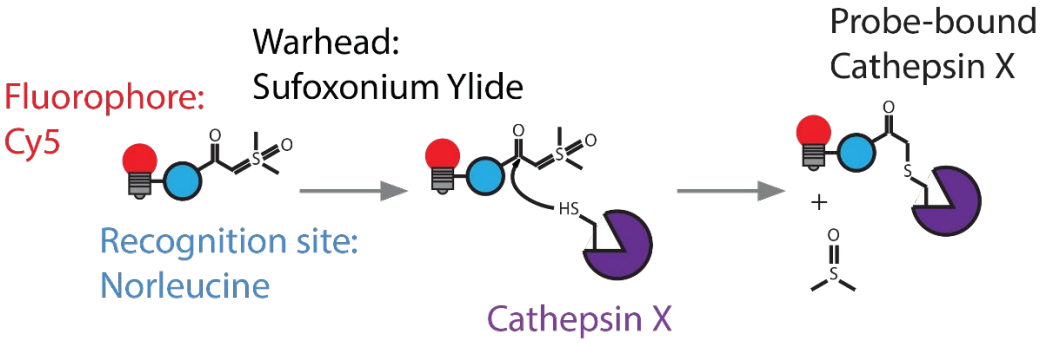

C

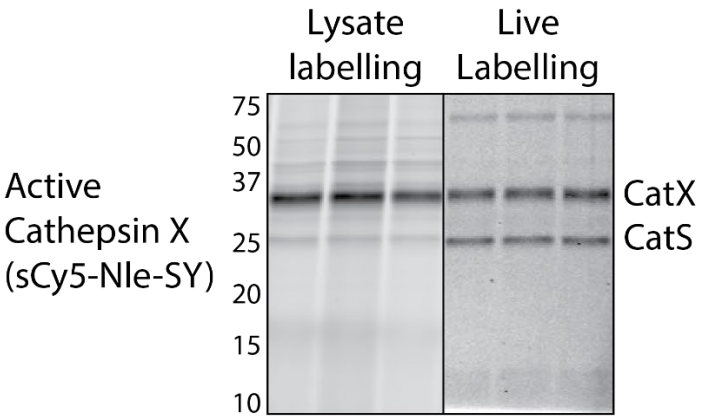

Figure 1.3 Mechanism and structure of the activity-based probe for cathepsin X. A. Structure of cathepsin X ABP, sCy5-Nle-SY. **B.** Mechanism of cathepsin X ABP. **C.** Acidified dendritic cell lysates (left) and live dendritic cells (right) were labelled by sCy5-Nle-SY as shown in gel-fluorescence.

1.2 Dysregulation of Cathepsin X is associated with diseases.

Increased expression of cathepsin X has been associated with various diseases, including cancer, neurodegenerative diseases, and neuroinflammation [30, 57, 58] (**Table 1.3**). In addition, cathepsin X can promote disease development either through its proteolytic or integrin-binding functions. The following examples will discuss the role of cathepsin X in disease progression in both the catalytic and the RGD-motif-dependent manner.

In pancreatic cancer, the total level of cathepsin X was significantly elevated and correlated with cancer malignancy [48, 57]. Thus, the level of cathepsin X could be used as an indication for cancer diagnosis and prognosis [59]. Furthermore, cathepsin X may also contribute to cancer progression: in pancreatic and breast cancer, overexpression of cathepsin X has been shown to induce epithelial-mesenchymal transition (EMT), a critical marker for cancer invasiveness [57, 60]. Administration of a specific cathepsin X inhibitor Z9 resulted in breast tumour shrinkage and significantly reduced metastases [61]. However, another group showed that the increased cancer cell proliferation and invasiveness were not caused by the catalytic activity of cathepsin X as was once proposed. Instead, the RGD motif is responsible for its oncogenic property. When pro-cathepsin X is secreted into the tumour microenvironment by cancer cells or infiltrating immune cells, its integrin motif binds to β2 integrin receptors, promoting cancer progression by activating Srk and FAK signalling pathways [48].

The role of cathepsin X in cancers is not always detrimental [62]. Cathepsin X was reported to be protective in *H. pylori*-induced gastric cancer. Cathepsin X-deficient mice developed more severe metaplasia, accompanied by more macrophage infiltration and prolonged cytokine secretion, compared to wild-type mice. While the mechanism of how cathepsin X mediates *H. pylori*-induced gastric cancer is still largely unknown, this study highlights contrasting roles for cathepsin X across tumour types.

Cathepsin X has also been reported to have a role in propagating neuroinflammation. Inflamed brain tissue exhibits increased cathepsin X expression and activity in mice and rats in experiment-induced neuroinflammation models [30, 63]. In vitro, cathepsin X has been shown to cleave two amino acids from the C-terminus of a neurotrophic factor enolase, which limits its neurotrophic activity. Administration of a cathepsin X inhibitor prevented this cleavage, leading to increased neuritogenesis and reduced serum-deprived cell death [52]. Cathepsin X

knockout mice exhibit reduced neuroinflammation symptoms due to reduced IL-1β and IL-18 secretion by immune cells, including macrophages and dendritic cells [30]. Cathepsin X was further found to promote IL-1β secretion through RGD-dependent activation of α5 integrin, which regulates NLRP3 inflammasome and caspase-1 activation [64].

To understand the contribution of cathepsin X to disease and to ultimately validate it as a target for treatments, more information is needed about its roles during basic immunological processes, which are still largely unknown.

Table 1.3 Cathepsin X is associated with various diseases.

Diseases	Function	Reference
***H. pylori*-induced gastric cancer**	Cathepsin X has a protective role in *H. pylori*-induced gastric cancer.	[62]
Pancreatic cancer	The RGD motif of cathepsin X contributes to cancer proliferation and invasiveness.	[48]
Hepatocellular carcinoma	Cathepsin X induces epithelial-mesenchymal transition.	[65]
Breast cancer	Cathepsin X, along with cathepsin B, induces epithelial-mesenchymal transition.	[60]
Neuroinflammation and Glioblastoma	Cathepsin X cleaves enolase and impairs neuritogenesis.	[52, 66]
Multiple Sclerosis	The RGD motif of cathepsin X regulates IL-1β secretion and subsequently affects neuron inflammation.	[30, 64]

1.3 Dendritic cell biology:

1.3.1 Cathepsin X is expressed by dendritic cells.

Cathepsin X is predominantly expressed by antigen-presenting cells such as macrophages and dendritic cells. Dendritic cells act as a bridge between the innate and adaptive immune systems. Naïve dendritic cells have a high phagocytic capacity and scavenge antigens in tissues. Once dendritic cells interact with antigens, they are activated. Activated dendritic cells migrate to lymphoid organs, secrete cytokines, and present antigens loaded onto major histocompatibility complexes (MHC) to $CD8^+$ cytotoxic T cells or $CD4^+$ T-helper cells. Those T cells can further differentiate into various T helper cell subtypes with distinct functions [11, 67]. Related cathepsin family members have been reported to contribute to dendritic cell function: Lysosomal cathepsins play a role in the uptake of exogenous antigens [53], activation of TLR receptors [68], antigen processing/presentation [11, 69], and cytokine regulation [70]. These functions of cathepsins will be discussed in more detail in the following paragraphs.

1.3.2 Dendritic cell subtypes:

Dendritic cells have a complex lineage (**Table 1.4**). They are divided into myeloid DCs (conventional DCs in mice) and plasmacytoid DCs based on surface markers. Myeloid DCs (mDCs/cDCs) express high levels of CD11c, CD13, CD33 and CD11b and can further be split into $CD1c^+$ or $CD141^+$ lineage. These two lineages are homologous to murine $CD11b^+$ (cDC2) or $CD8^+$ (cDC1) lineage, respectively. Plasmacytoid DCs (pDCs) lack cDC surface markers and express high CD123, CD303, and CD304. There are also other minor subtypes of DCs, the monocyte-like DCs ($CD1c^+$, $CD14^+$ DCs) [71, 72] and Langerhans DCs [73]. The monocyte-like DCs belong to a subtype of $CD11b^+$ and can be found in inflamed tissues or cancers [74-76]. The classification of Langerhans cells is controversial. Langerhans cells reside in the epidermis and are commonly associated with tissue macrophages and microglia in the brain [77]. However, they are functionally more similar to conventional dendritic cells as they capture antigens, mature and migrate to the lymph nodes [78].

$CD8^+$ cDCs were found to exhibit lower expression of lysosomal proteases, including cathepsin B, L, and S, in comparison to $CD11b^+$ cDCs, implying that $CD8^+$ cDCs are generally considered to be less proteolytic [79]. However, our preliminary data indicated a specific increase in

cathepsin X activity and total expression in $CD8^+$ cDCs. This suggests a potential role for cathepsin X in the distinctive features of $CD8^+$ cDCs.

Furthermore, $CD8^+$ cDCs are characterized by a unique ability known as antigen cross-presentation. This process involves a unique mechanism of antigen presentation that will be discussed in more detail in the following introduction. In brief, $CD8^+$ cDCs possess lysosomes with increased permeability, allowing exogenous antigens they engulf to be released into the cytosol for degradation and subsequent presentation to T cells [80]. However, the precise mechanism underlying antigen cross-presentation remains to be fully understood. Given the heightened activity and expression of cathepsin X, along with the remarkable lysosomal characteristics, $CD8^+$ cDCs were chosen as the primary focus of our study.

Table 1.4 Dendritic cells lineage

Dendritic cell lineage		**Characteristics**	
Myeloid/Conventional DCs	$CD11b^+$ Myeloid DCs (cDC2)	$CD11c^+$, $CD13^+$, $CD33^+$, $CD11b^+$	$CD11b^+$ (Human $CD1c^+$)
	$CD8^+$ Myeloid DCs (cDC1)		$CD8^+$ (Human $CD141^+$)
Plasmacytoid DCs		$CD123^+$, $CD303^+$, and $CD304^+$	
Monocyte-like DCs		$CD14^+$	
Langerhans DCs		Epidermis-resident	

1.3.3 Conventional $CD8^+$ dendritic cell line:

Because of the vulnerability of primary dendritic cells and the difficulties in obtaining enough $CD8^+$ DCs from mice spleens, the DC1940 cell line is often used to study DC function *in vitro* [81]. This cell line preserves most characteristics of primary conventional $CD8^+$ dendritic cells. They can be activated by Toll-like receptor agonists, including TLR1/2, TLR2/6, TLR3, and TLR9 ligands (Pam3, FSL-1, Poly I:C and CpG, respectively) and express similar patterns of surface markers, cytokines, and chemokines as the primary splenic $CD8^+$ cells do. Upon TLR activation, the expression of surface markers (co-stimulatory molecules) CD40, CD80, and CD86 were significantly upregulated along with a slight increase in MHC-I, MHC-II, PD-L1 and PD-L2 surface markers [81].

1.3.4 Toll-like receptors (TLRs):

To mount an immune response, APCs such as dendritic cells are first activated by toll-like receptor agonists (**Figure 1.4**). Toll-like receptors are a family of pattern-recognition receptors (PRRs) that reside either on the surface of immune cells or within the endocytic pathway (e.g., endosomes). They can recognise pathogen-associated molecular patterns (PAMPs) derived from exogenous pathogens, including bacterial walls and DNA, or damage-associated molecular patterns (DAMPs) derived from endogenous tissue damage. Upon interacting with TLR agonists, the receptors dimerise and couple with adaptor proteins, including: translocating chain-associated membrane protein (TRAM) for endocytosed TLR4 receptor; Myeloid differentiation primary response 88 (MYD88) for TLR1/2, TLR2/6, surface TLR4, TLR7/8, and TLR9 receptors; TIR-domain-containing adapter-inducing interferon-β (TRIF) for endocytosed TLR4 and TLR3; or Mal/toll-interleukin 1 receptor (TIR) domain-containing adaptor protein (TIRAP) for TLR1/2, TLR2/6, and TLR4. The signalling cascade ultimately transduces to the nucleus, where nuclear factor- κB (NF-κB) is activated to stimulate the synthesis of proinflammatory cytokines or interferon regulatory factors (IRFs) to boost the synthesis of type 1 interferons (IFNα and IFNβ) [82].

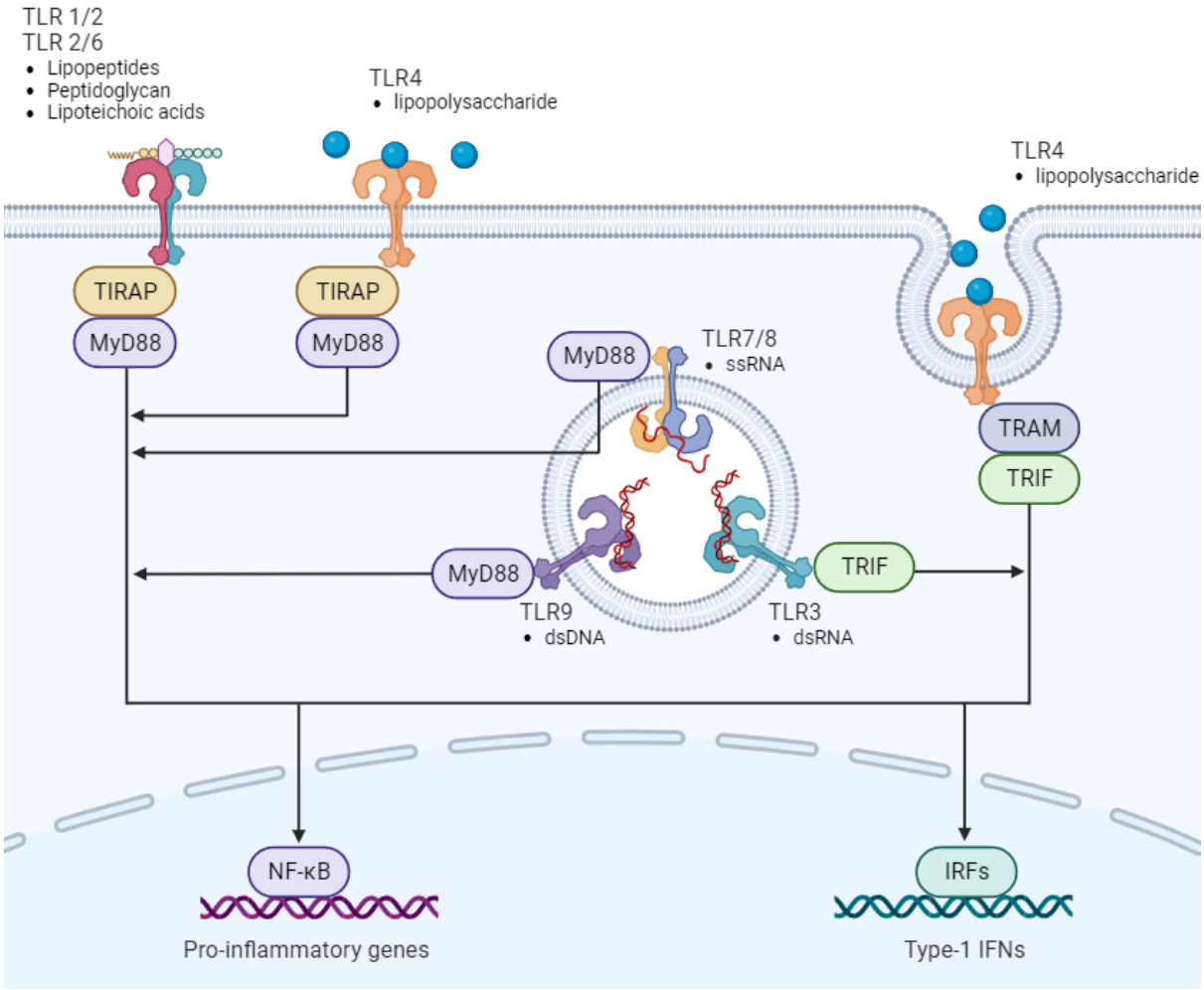

Figure 1.4 Overview of TLR signallings. When TLR receptors are stimulated by their respective ligands, they first go through dimerisation. The dimerised receptors then recruit adaptor proteins such as TIR Domain Containing Adaptor Protein (TIRAP), Toll/interleukin (IL)-1 receptor (TIR)-domain-containing adaptor-inducing interferon-β (TRIF), myeloid differentiation primary-response protein 88 (MyD88), and TRIF-related adaptor molecule (TRAM). The adaptor proteins can activate the downstream signalling cascade and eventually activate transcription factors, including nuclear factor kappa-light-chain-enhancer of activated B cells (NF-κB) for the expression of the pro-inflammatory genes and Interferon regulatory factors (IRFs) for the expression of type-interferons. Created with BioRender.com

1.3.5 Inflammasome activation:

Apart from the surface Pattern Recognition Receptors (PRRs) such as the TLRs, as mentioned earlier, immune cells also possess intracellular supramolecular protein receptors that can sense the toxins released by invading pathogens or damaged tissues in the cytosol. These receptors include nucleotide oligomerization domain (NOD)-like receptors (NLRs), Absent in melanoma 2 (AIM2)-like receptors (ALRs), pyrin receptors and caspase-11 (caspase-4/5 in humans) (**Table 1.5**). The engagement of the contributors with pathogenic or physiologic stimuli contributes to inflammasome activation [83, 84]. Upon inflammasome activation, caspase-1 is recruited by the inflammasome complex and undergoes autoactivation. The activated caspase-1 then cleaves pro-IL-1β and IL-18 for their secretion. The inflammasome activation also induces cell pyroptosis by activating Gasdermin D (GSDMD). The whole process plays a vital role in combating exogenous pathogens and getting rid of infected/damaged cells.

Table 1.5 Types of inflammasome activation

Family	Types	Features	Stimuli	Reference
NLRs	NLRP1 inflammasome	The first cytosolic sensor identified to form a caspase-1 activating inflammasome.	*Bacillus anthracis* lethal toxin	[85]
	NLRP3 inflammasome	Activation involves both the priming and activation steps.	Signal 1: TLR agonists. Signal 2: Crystalline, extracellular ATP, pore-forming toxins, viral/fungal protozoan pathogens	[86, 87]
	NLRP6 inflammasome	Highly expressed in nonhematopoietic cells Involved with intestinal homeostasis.	Microbiota	[88, 89]
	NLRP12 inflammasome	Involved with intestinal homeostasis. Non-canonical NF-κB inhibitor.	*Yersinia pestis*	*[90, 91]*
	NAIP/NLRC4 inflammasome	NLRC4 partners with another NLR family member – NAIP	PAMPs including bacterial flagellin and type III secretion system (T3SS) components.	[92, 93]
Non-NLRs	AIM2 inflammasome	Consists of an N-terminal PYD and a C-terminal HIN200 domain	Bacterial, viral, or self-leaked DNA	[94]
	IFI16 inflammasome	The isolated IFI16 HIN200 domain has a weaker affinity to DNA. The DNA binding affinity is associated with protein length.	Viral DNA	[95]
	Pyrin	Sense Rho GTPase-inactivation induced by bacterial toxins.	detects inactivation of the Rho GTPase RHOA	[96]
	Non-canonical inflammasomes	Independent of caspase 1	LPS	[97, 98]

The NLRP3 inflammasome is the most well-characterised pathway. The activation of the NLRP3 inflammasome requires two signals. The first signal involved the activation of TLR receptors. The TLR receptor signalling pathway eventually leads to the activation of the NF-κB transcription factor and upregulates the expression of inflammasome genes, including NLRP3, pro-IL-1β and pro-caspase-1 [86]. The assembled NLRP3 inflammasome responds to the second signal. The second signal covers a wide range of stimuli which contains extracellular PAMPs, including toxins released by bacteria, viral, fungal, and protozoan pathogens, and host-derived DAMPs, including ATP, uric acid crystals, and amyloid-β fibrils [87]. The activation of the NLRP3 inflammasome is also restrictedly regulated by ion flux. Potassium efflux and calcium influx are two major ion mobilizations that regulate NLRP3 inflammasome activation. The K^+ efflux is mediated by the two-pore domain weak inwardly rectifying K^+ channel 2 (TWIK2). The necessary environment for NLRP3 activation requires a low concentration of cytosolic potassium [99]. Ca^{2+} influx has been reported to be the other crucial upstream regulator of NLRP3 inflammasome activation [100]. Unlike potassium, extracellular calcium influx is mediated by the P2X7 receptor [101]. Calcium influx can also come from the ER calcium storage by C/EPB homologous protein [102]. TMEM176B has been reported to be a negative regulator of the cytosolic level of calcium. When TMEM176B was genetically deleted, the cytosolic calcium concentration increased, resulting in a more profound secretion of IL-1β [103].

NLRP3 inflammasome is expressed by innate immune cells, especially macrophages [104]. Some dendritic cells are also thought to exhibit inflammasome activation. Most researchers use BMDCs derived from bone marrow progenitor cells culturing with GM-CSF, which generates a mixture of cell populations containing bone marrow-derived macrophages (BMDM) and bone marrow-derived dendritic cells (BMDC) [105]. It is unclear which subpopulation contributes to the secretion of IL-1β and IL-18 in these cultures. Using FLT3 to replace GM-CSF generates pure BMDCs with a more cDC-like phenotype [105]. cDC1 derived from Flt3-treated BMDC showed a low level of NLRP3 expression, while the cDC2 population showed a much higher level of inflammasome components [106].

Whether NLRP3 inflammasome has a role in primary cDC1 dendritic cells is still under debate. Chakraborty and colleagues reported that the activation of NLRP3 inflammasome in conventional dendritic cells is an adjuvant to induce cytotoxic CD8+ T cell responses, indicating

that DC inflammasome activation has a physiological role [107]. On the other hand, it has been reported that both cDC1 and cDC2 conventional dendritic cells acquire a mechanism in which transcription factors IRF8 and IRF4 suppress the inflammasome-related genes. By doing this, conventional dendritic cells can surpass inflammasome-induced cell pyroptosis, preventing them from dying and maintaining their ability to keep priming T cells [108]. Therefore, whether or not NLRP3 inflammasome activation has a vital role in DC immune function still requires further investigation.

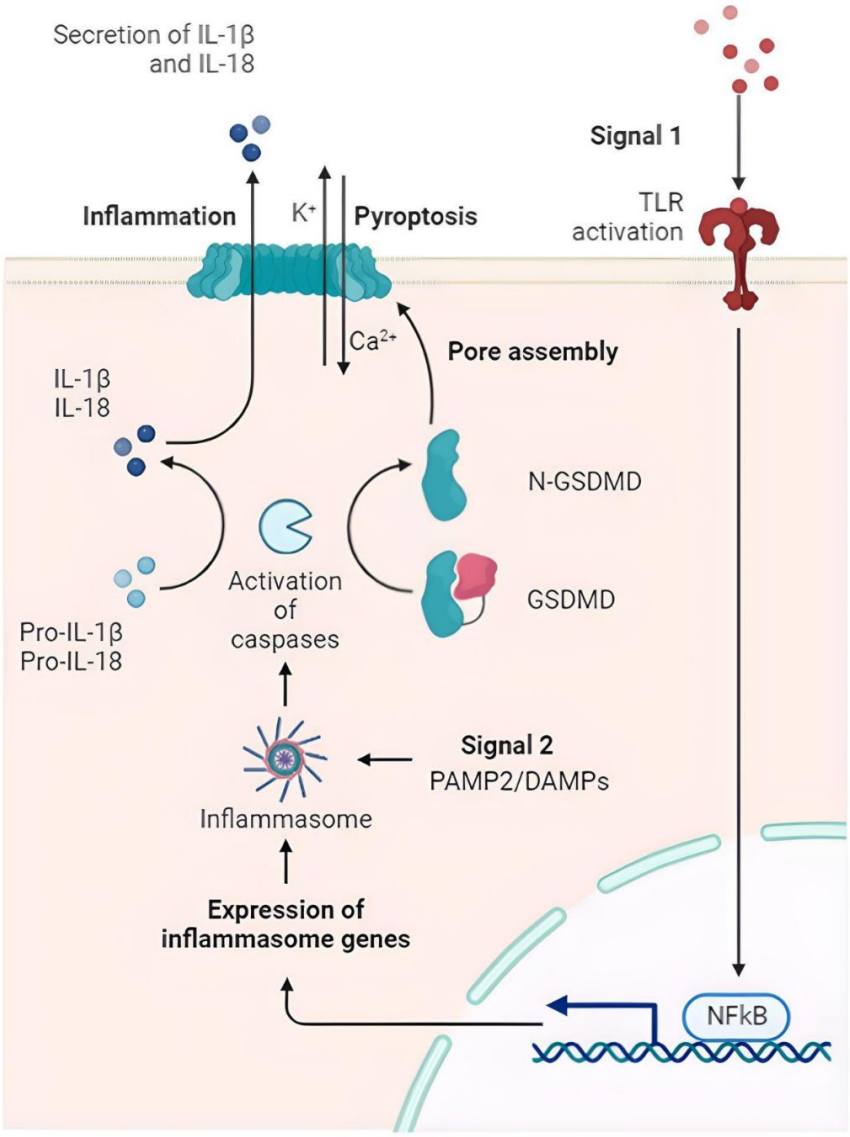

Figure 1.5 Overview of NLRP3 inflammasome activation. The NLRP3 inflammasome activation first requires the priming signal, TLR activation, which leads to NF-κB activation and upregulation of inflammasome genes. Inflammasome platforms are assembled and sense the second signal derived from exogenous PAMPs or endogenous DAMPs. The activated NLRP3 inflammasome leads to activation of caspase-1, which performs two major functions: 1. Cleavage of pro-IL-1β and pro-IL-18 to promote their secretion; 2. Cleavage and activation of GSDMD to drive pyroptosis. NLRP3 inflammasome activation is also regulated by ion flux. Potassium efflux and calcium influx both play vital roles in NLRP3 inflammasome activation. Modified from McDaniel et al. 2020 [108]. Created with BioRender.com

1.3.6 Antigen presentation:

Upon maturation by TLR agonists, one primary function of APCs is to present antigens to effector T lymphocytes. Antigens are engulfed by cells and processed into antigenic peptides by lysosomal proteases. The antigenic peptides are then coupled to major histocompatibility protein complexes (MHC), and the MHC-antigen complex is subsequently transported to the plasma membrane for antigen presentation. There are two subsets of MHCs, MHC-I and MHC-II, each with unique functions (**Figure 1.6**).

The MHC-II protein complex presents exogenous antigens. The pathway starts when exogenous substances are engulfed by APCs, processed into antigenic peptides by lysosomal proteases and loaded onto MHC-II molecules [9]. The antigens are then presented to $CD4^+$ T helper cells (**Figure 1.6A**), which subsequently differentiate into diverse subtypes of $CD4^+$ T cells, including Th1, Th2, Th9, Th17, $CD4^+$ cytotoxic T lymphocytes, T follicular helper (Tfh) cells, and induced regulatory T cell (Treg). Each subtype secretes different cytokines and serves a specific role within immune responses.

MHC-I usually presents self-antigens. Full-length proteins undergo degradation in the cytoplasm by the proteasome and aminopeptidases. The degraded peptides are then translocated to the endoplasmic reticulum, loaded onto the MHC-I complex [109], and presented to $CD8^+$ T cytotoxic cells to eliminate cancer cells or damaged cells (**Figure 1.6B**).

In some cases, exogenous antigen peptides can escape from endolysosomes and couple to MHC-I, a process referred to as cross-presentation [110]. Conventional $CD8^+$ ($CD141^+$ in humans) DCs comprise one of the two dendritic cell subtypes that can cross-present antigens [111]. Cross-presentation transforms naïve $CD8^+$ T cells into cytotoxic T lymphocytes (**Figure 1.6C**). The antigen-cross presentation has an important role in the treatment of cancers and viral infections, where we require a cytotoxic T cell immune response towards tumour cells and infected cells.

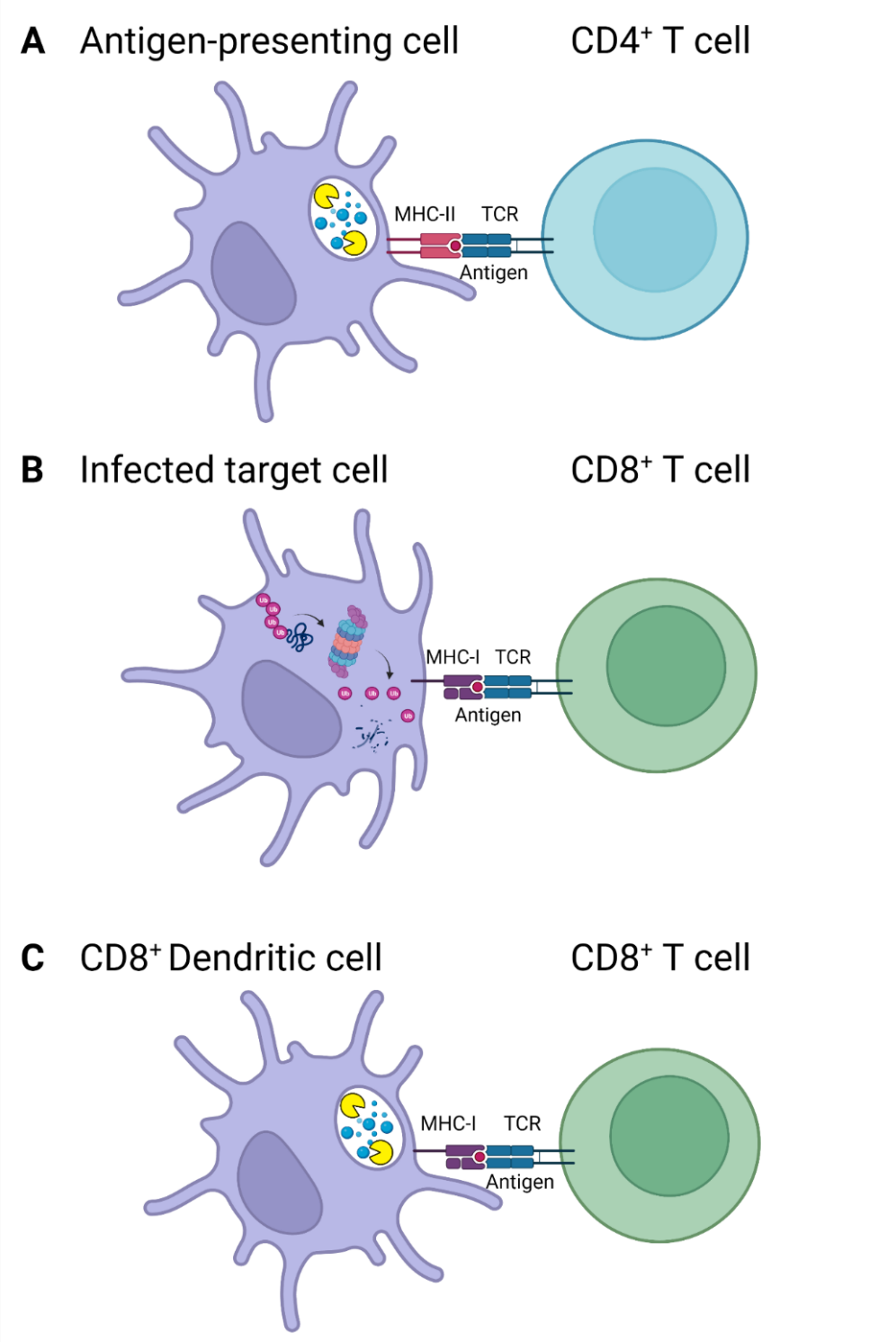

Figure 1.6 Antigen presentation and antigen-cross presentation. **A.** Antigen presentation through MHC-II. **B.** Presentation of self-antigen through MHC-I. **C.** Antigen cross-presentation through MHC-I. Created with BioRender.com

1.4 Proteases and immunity

1.4.1 Proteases and antigen uptake.

Proteases contribute to many aspects of immune function, including antigen presentation, antigen processing, cytokine maturation, and cytokine trafficking. Immune cells like dendritic cells and macrophages scavenge for pathogens and subsequently engulf them to provoke immune responses.

Lysosomal proteases mainly contribute to the processing and degradation of endocytosed substances. However, some reports indicate that lysosomal proteases may regulate the endocytosis mechanism. Cathepsin B and L are reportedly involved in the endocytosis of iota-toxin from *Clostridium perfringens* type E [112]. Briefly, the extracellular lysosomal enzyme acid sphingomyelinase (ASMase) induces ceramide accumulation on cell membranes and subsequently causes membrane invagination and hence endocytosis. Cathepsin B and L activate ASMase in kidney epithelial cells, further affecting endocytosis [112].

Cathepsin X has also been reported to be a negative regulator of clathrin-mediated endocytosis in human prostate cancer cells [53]. Cathepsin X cleaves off the C-terminal Tyr139 from profilin 1 and makes it unable to bind to clathrin. Clathrin and profilin 1 binding mediates endocytic uptake [113]. Cleavage by cathepsin X perturbates their interaction and negatively regulates clathrin-mediated endocytosis [53]. It needs to be noted that profilin is localised in the cytosol. Even though more evidence suggests that lysosomal proteases can escape to the cytosol during lysosomal rupture, it needs to be validated that cathepsin X can cleave a cytosolic protein at neutral pH.

The two examples above revealed that lysosomal proteases regulate cellular components and modulate endocytosis. Another report indicates that cathepsin L cleaves exogenous viral protein to facilitate viral entry into the host cells. The S-spike protein on the COVID-19 viral envelope can be cleaved by cathepsin L. This cleavage is crucial for the fusion of the endosomal membrane and the viral envelope, which enables viral entry into the host cells [114].

To conclude, there was scarce evidence about lysosomal modulating endocytosis. Lysosomal proteases may affect endocytosis by either modulating self-components or modifying exogenous substances.

Table 1.6 Proteases and endocytosis

Protease	Function	Reference
Cathepsin B and L	Endocytosis of *Clostridium perfringens* iota-Toxin	[112]
Cathepsin L	Cleavage of the SARS-CoV-2 spike protein to facilitate virus entry.	[114]
Cathepsin X	Cleavage of Profilin 1 C-Terminal Tyr139 and regulation of Cathryn-mediated endocytosis	[53]

1.4.2 Proteases and TLR signalling and maturation.

As discussed above, TLR receptors are PRRs that recognise PAMPs derived from exogenous pathogens. When TLR receptors interact with their designated agonists, the subsequent signalling pathway leads to DC maturation by expressing inflammatory genes.

TLR 3, 7, 8, and 9 are localised on endolysosomes **(Figure 1.4)**. They possess a C-terminal leucine-rich repeat in an extracellular loop, a transmembrane domain, and an N-terminal endolysosomal domain that recognises viral and bacterial nucleic acids such as double/single-stranded RNA or double-stranded DNA.

Several reports have suggested that the full activation of those TLR receptors requires a partial cleavage in the endolysosomal compartments. Cathepsin B and H, but not cathepsin L and legumain, cleaves TLR3 between 252 and 346 amino acids, resulting in a functional receptor for downstream signalling [115].

TLR9 is also processed by lysosomal proteases. TLR9 has a total molecular weight of ~130 kDa and can be processed into an active smaller fragment with a molecular weight of 72 kDa. Sepulveda et al. reported that pDCs lacking legumain failed to facilitate cleavage and secreted significantly less pro-inflammatory cytokines. They re-expressed the active 72 kDa TLR9 in legumain-deficient cells and showed that the active 72 kDa TLR9 restored the signalling [116]. In a different study, macrophages (RAW264.7) and DCs (DC2.4) showed that the cathepsins and legumain were involved in processing TLR9 receptors. They discovered that the loss of legumain activity did not entirely abolish TLR9 processing, while cathepsins could compensate for the loss of legumain and facilitate the processing. When a chemical inhibitor blocked both legumain and cathepsin activities, the signalling of TLR9 was significantly impaired [117]. The two studies shown above used two different cell models. Sepulveda et al. used plasmacytoid dendritic cells, while Ewald et al. mostly used macrophages and DC2.4. The DC2.4 cells constitutively express GM-CSF and may make the DCs phenotypically more macrophage-like [105, 118]. Therefore, it is likely that the processing of TLR9 differs across cell types.

Another protease-cell maturation mechanism was found not to be related to TLR cleavage. Cathepsin X is reported to cleave the integrin β2 receptor to modulate pDC maturation. The absence of such cleavage impaired surface marker expression, cytokine secretion and cell adhesion [3].

Table 1.7 Protease and TLR signalling/ cell maturation.

Proteases	Mechanism	References
Cathepsin B and H	Cleavage of TLR3 for immune function	[115]
Legumain and cathepsins	TLR9 processing and function in DCs	[116, 117]
Legumain and cathepsins	TLR3 and TLR7 processing and function in macrophages	[117]
Cathepsin X	Cleavage of integrin receptor to modulate pDC maturation.	[119]

1.4.3 Proteases in antigen processing and presentation:

The adaptive immune response depends on processing exogenous antigenic peptides and appropriate coupling between these peptides and MHC-II complexes. Lysosomal proteases perform two critical roles: proteolytic processing of foreign peptides into antigens and maturation of MHC-II complex that precedes successful coupling with antigens.

Exogenous antigens need to be processed by endolysosomal proteases into antigenic peptides before coupling to the MHC-II complex. The lysosomal proteolytic system is redundant, and the exact proteases responsible for antigenic peptide processing remain unknown [11]. It has been reported that cathepsin D, an aspartyl protease, can process antigens and activate T cells in vitro [120]. However, antigen presentation by APCs derived from cathepsin D knockout mice showed no significant differences [121]. Cathepsin E is another aspartyl protease reported to have a role in the proteolytic processing of antigens: inhibiting cathepsin E impairs the ability of antigen-presenting cells to present antigens [122]. Recent reports also suggested the roles of cysteine cathepsins such as cathepsin L and cathepsin S in antigen processing. Cathepsin L is found to directly influence the generation of cortical thymic epithelial cell antigenic peptides [123], while cathepsin S contributes to processing some B cell peptides in the spleen [124].

Moreover, legumain, a lysosomal cysteine protease, has been reported to have a defined role in the initial cleavage of tetanus toxin. Other proteases then process the protein into antigen after the initial cleavage [125]. Antigen processing reflects a redundancy of proteases within the endolysosomal network, making it difficult to study the relationship between antigenic peptides and specific lysosomal proteases.

Antigen presentation also requires the maturation of the MHC-II complex by endolysosomal proteases. MHC-II is assembled in the endoplasmic reticulum with a chaperone protein – the invariant chain (Ii cap). The Ii-MHC-II complex is then transported to the endosome, where lysosomal proteases degrade the invariant chain to prepare the complex for antigen loading. Legumain has been reported to initiate cleavage of the invariant chain. While inhibiting legumain or mutating legumain cleavage sites delayed the processing of the invariant chain, it did not entirely prevent it, indicating that other proteases can also process it [126]. Cathepsin L and S are critical lysosomal proteases regulating MHC-II maturation [11]. Cathepsin L and S have different tissue-specific localisation; thus, they regulate MHC-II maturation in a tissue-specific manner. Cathepsin L is primarily active in the thymus but not in

the spleen [127], whereas cathepsin S is mostly active in the spleen [128]. Accordingly, cathepsin L is responsible for the late-stage degradation of the invariant chain in cortical thymic endothelial cells, while cathepsin S degrades the invariant chain in splenic B cells [69].

1.4.4 Proteases in cytokine regulation:

Apart from antigen processing and presentation, proteases govern immune function by regulating cytokine activation, inactivation/degradation, and trafficking. Interleukins are secreted from immune cells in response to inflammation. The regulation of interleukin 1 family inflammatory cytokines by proteases has been well-characterised in the field.

Pro-IL-β and pro-IL-18 are converted to active IL-β and IL-18 by caspase-1 downstream of inflammasome activation [129-131]. However, bioactive IL-18 was also found in caspase-1-deficient mice, indicating that caspase-1 is not the only activator [132]. Neutrophil elastase and cathepsin G were also reported to cleave pro-IL-1β, although the resultant products had less bioactivity than the caspase-1-processed product [133, 134]. IL-1α also belongs to the interleukin 1 family and is released during tissue damage and necrotic cell death [135]. The processing of IL-1α into the mature form is regulated by multiple proteases, including elastase, granzyme B, and mast cell chymase [136]. Another interleukin 1 family member is IL-33, which proteases can activate or inactivate. IL-33 has some basal bioactivity before protease activation. The principal activator of IL-33 is caspase-1 [137]. Alternatively, its bioactivity can be abolished by caspase-3 and -7 [138].

IL-37 is an anti-inflammatory cytokine in the interleukin 1 family. IL-37 exerts its anti-inflammatory role by translocating to the nucleus, which depends on its proteolytic activation. Caspase-1 and caspase-4 can process IL-37 into bioactive form [139, 140]. A mutation of the cleavage site makes the cytokine unable to be translocated to the nucleus, indicating that proteases are involved with activating cytokines and regulating cytokine trafficking [141].

Cathepsin B, a cysteine protease like cathepsin X, is involved in TNFα secretion by macrophages. Secretion of TNFα is reduced upon treatment of cells with cathepsin B inhibitors or cathepsin B knockdown. Upon inhibition of cathepsin B, pro-TNFα accumulated in TNFα-containing vesicles, and the TNFα-containing vesicles were not transported to the plasma membrane, suggesting that cathepsin B mediates this transport or the shedding of pro-TNFα [70].

There are other cathepsins involved in the secretion of cytokines. However, these mechanisms are likely indirect. As described above, legumain and lysosomal cathepsins contribute to TLR3, 7, and 9 activations. Therefore, chemical inhibition of both legumain and cathepsins impaired

macrophage maturation and reduced TNFα secretion [117]. In addition, cathepsin X is responsible for TLR4 agonist-induced plasmacytoid dendritic cell maturation through the cleavage of β2-integrin. As a result, the inhibition of cathepsin X impaired pDC maturation and reduced the production of several cytokines, including TNFα, IL-10 and IL-12 [119].

1.4.5 Proteases and inflammasome activation.

As described earlier, inflammasome activation serves a critical role in innate immune function, and the process is heavily regulated by proteases, especially caspases and cathepsins. Caspase-1 is considered the central player of all other caspases in most inflammasomes, and caspase-11 (caspase-4/5 in humans) is involved in non-canonical inflammasome activation [131, 142]. Apart from the role in converting pro-IL-1β and pro-IL-18 as described earlier, both caspase-1 and caspase-11 can cleave GSDMD, generating a functional N-terminal fragment required for the secretion of IL-1β and cell pyroptosis [143]. Caspase-8 is reported to play a role in apoptosis in addition to caspase-1 in various inflammasome activation pathways [144-146]. This caspase-8-mediated cell death pathway is potentially important in cells lacking caspase-1 expression.

In addition to caspases, lysosomal cathepsins have been increasingly reported contributing to inflammasome activation. Upon NLRP3 activation, cathepsin B-deficient bone marrow-derived macrophages showed reduced IL-1β secretion and caspase-1 activation, indicating that cathepsin B somehow regulates NLRP3 inflammasome activation [147]. Cheviraux et al. reported that NLRP3 does not interact with cathepsin B in the lysosomes but in the ER. However, cathepsins in the ER stage are inactive pro-forms [16]. The co-localisation of cathepsin B and NLRP3 in the ER likely goes through similar protein translocation mechanisms post-protein synthesis. Cathepsin B has been reported to escape into the cytosol by the action of trypsin [148]. Investigating whether mature cathepsin B escapes the lysosomes to interact with NLRP3 in the cytosol will be necessary. Cathepsin G is a lysosomal serine protease reported to cleavage and activate GSDMD in addition to caspase-1/11 [149].

Cathepsin X has also been reported to have a role in inflammasome activation. Cathepsin X-deficient bone marrow-derived macrophages and dendritic cells exhibited a reduction in the secretion of IL-1β and IL-18 [30]. Its proposed mechanism is unexpected: the secreted inactive pro-cathepsin X contains an RGD motif that can bind to α5 integrin receptors. This interaction subsequently regulates inflammasome activation [64]. Multiple studies reported that α5β1 integrin engagement facilitates inflammasome activation; however, the exact mechanism remains to be elucidated [150-152]. The Syk tyrosine kinase is a critical component in the signalling of multiple integrin receptors, and thus, it could be a potential player in modulating inflammasome activation, but this needs further validation [153, 154].

Table 1.8 Proteases and inflammasome activation

Proteases	Function	Reference
Cathepsin B	Interaction with NLRP3 inflammasome	[147]
Cathepsin G	Cleavage and activation of GSDMD	[149]
Cathepsin X	Secretion of IL-1β and IL-18	[30, 64]
Caspase-1	Maturation of IL-1β and IL-18	[131]
Mouse Caspase-11 (Human Caspase-4/5)	Non-canonical inflammasome activation	[155]
Mouse Caspase-1/11 (Human Caspase-1/4/5)	Cleavage and activation of GSDMD	[97, 98]
Caspase-8	AIM2, NLRP3, and NAIP–NLRC4 inflammasomes activated apoptosis.	[144-146]

1.4.6 Cathepsin X and dendritic cell function:

Cathepsin X is highly expressed by antigen-presenting cells such as DCs. We hypothesise that, like other cathepsins, cathepsin X may be necessary for dendritic cell function. The activity of cathepsin X is required to activate plasmacytoid dendritic cells through proteolytic cleavage of integrin receptors [3]. However, cathepsin X is a lysosomal protease, and the carboxy cytosolic tail of the integrin receptor is not accessible by a lysosomal protease. Even though cathepsin X may escape from the lysosome into the cytosol, there is insufficient evidence about the existence of active cathepsin X in the cytosol as it needs a slightly acidic environment to become active. Therefore, how cathepsin X may cleave a cytosolic substrate needs further validation. The same report also indicated that inhibiting cathepsin X significantly impaired the ability of human plasmacytoid dendritic cells to secrete inflammatory cytokines, including TNFα, IL-10, and IL-12 [3]. These altered immunological phenotypes are most likely directly related to the impaired maturation of dendritic cells rather than the deficiency of cathepsin X.

Another group showed IL-1β and IL-18 secretion was impaired in bone marrow-derived dendritic cells from cathepsin X-deficient mice, as discussed above in the neuroinflammation model [30]. The IL-1β-dependant Th17 cell response was also attenuated. The precise roles of cathepsin X in these pathways have been further elucidated more recently. The regulatory function of cathepsin X in IL-1β depends on the RGD motif of secreted pro-cathepsin X through the α5 integrin signalling pathway [64].

Cathepsin X was shown to be expendable for Myelin oligodendrocyte glycoprotein (MOG)-related antigen presentation [30]. As discussed above, cathepsin X has broad substrate specificity and functions as a mono-carboxypeptidase. While not required for MOG degradation, cathepsin X may contribute to other aspects of antigen presentation, though this remains to be elucidated.

Table 1.9 Summary of proteases with known function in immunity.

Protease	Immune function	Reference
General lysosomal proteases	General antigen processing	[9]
Legumain	Processing of tetanus toxin for MHC-II presentation	[156]
Legumain and cathepsins	TLR9 processing and function in DCs TLR3 and TLR7 processing and function in macrophages	[116, 117] [117]
Cathepsin S	Maturation of the Invariant chain in B cells	[69]
Cathepsin L	Maturation of the Invariant chain in cortical thymic endothelial cells Toll-like receptor-related dendritic cell activation	[123] [68]
Cathepsin B	Regulation of TNFα containing vesicles Activation of NLRP3	[70] [147]
Cathepsin G	Cleavage of GSDMD and promotion of inflammasome activation	[149]
Cathepsin X	DC maturation through integrin cleavage Endocytosis through profilin cleavage Regulation of IL-1β secretion through RGD motif	[119] [53] [30, 64]

Caspase-1	Converting Pro-IL-1β into mature IL-1β Converting Pro-IL-18 into mature IL-18 Activates IL-33 Process IL-37 and facilitate nuclear translocation.	[129] [130] [137] [139, 141]
Mouse Caspase-1/11 (Human Caspase-1/4/5)	Cleavage and activation of GSDMD	[97, 98]
Caspase-3 and Caspase-7	Deactivate IL-33	[138]
Caspase-4	Activates IL-37	[140]
Mouse Caspase-11 (Human Caspase-4/5)	Non-canonical inflammasome activation	[155]
Neutrophil elastase and cathepsin G	Generating bio-active IL-1β	[133, 134]
Elastase, granzyme B, mast cell chymase	Activate IL-1α	[136]

1.5 Hypotheses and aims of the thesis.

Due to the high involvement of general proteases and lysosomal cathepsins in immune function, we believe that cathepsin X may have a role in DC immunity. We hypothesise that cathepsin X activity is critical to DC immunity. Therefore, the loss of cathepsin X activity may result in an impaired DC immune response and may also result in a changed lysosomal proteolytic environment that causes biological consequences.

To address this hypothesis, this thesis aims to achieve the following:

1. To characterise the regulation of cathepsin X activity, total level, and other related lysosomal proteases during dendritic cell maturation.
2. To investigate the impact of cathepsin X deficiency on dendritic cell immune functions, including cell maturation, antigen uptake, antigen presentation, and cytokine regulation.
3. To investigate the impact of cathepsin X deficiency on the lysosomal proteolytic network and to analyse the consequences of altered lysosomal proteolytic environment.

In **Chapter 3,** I characterised the active and total levels of both the intracellular lysosomal cathepsin X and secreted cathepsin X from dendritic cells during TLR-mediated cell maturation. In addition, the active and total levels of other related lysosomal proteases and intrinsic inhibitors were also investigated during DC maturation. We eventually proposed a mechanistic explanation of cathepsin X regulation during DC maturation.

In **Chapter 4,** I generated a cathepsin X deficient DC cell line using CRISPR-Cas9 to investigate the impact of cathepsin X on DC immunity. I subsequently analysed the ability of DCs to endocytose, present antigens, and secrete cytokines. I also conducted shotgun proteomics to broadly investigate the impact of cathepsin X deficiency on DC immune function.

In **Chapter 5,** I investigated the impact of cathepsin X deficiency on the lysosomal proteolytic network and its biological consequences.

Overall, I characterised the regulation of cathepsin X during TLR-mediated DC maturation and investigated the role of cathepsin X in DC immune function and the lysosomal proteolytic environment. The findings of my work will help to understand the relationship between lysosomal proteases and immunity with an ultimate goal of understanding the role of cathepsin X during disease progression.

Chapter 2. Materials and methods:

2.1 Cell culture

Cell lines and the medium used are described in **Table 2.1**. When passaging, DC1940 cells were lifted from the flask using Ethylenediaminetetraacetic acid-balanced salt solution (EDTA-BSS) (150 mM sodium chloride, 4 mM potassium chloride, 24 µM disodium hydrogen orthophosphate, 12 µM sodium dihydrogen orthophosphate, 15 mM HEPES, and 5 mM EDTA (The Peter Doherty Institute for Infection and Immunity media preparation unit (MPU)) supplemented with 2%(v/v) FBS). Raw cells were lifted from the flasks using a rubber policeman. All other cell lines were lifted using trypsin (0.125% for HSC-3 and HEK 293T, 0.25% for SCC-9 cells.) Cells were maintained in humidified incubators at 37 °C and 5% CO_2.

2.2 Mice

All experiments involving animals were conducted under the guidelines for using laboratory animals in research and approved protocols. All experiments were approved by the University of Melbourne Animal Ethics Committee. C57BL/6 mice were obtained from the Melbourne Bioresources Platform at Bio21 Molecular Science and Biotechnology Institute.

2.3 Harvesting primary splenic dendritic cells.

Splenic dendritic cells were harvested as described by Vremec [157]. Briefly, spleens were digested with 1 mg/mL DNase I (Boehringer Mannheim) and 7 mg/mL Collagenase Type III (Worthington) for 20 minutes at room temperature in KDS-RPMI-FBS (potassium dodecyl sulphate Roswell Park Memorial Institute; RPMI 1640 containing 33.6 mM HEPES, 1 mM sodium pyruvate, 24 mM $NaHCO_3$, 2% (v/v) FBS). Cell clumps were separated with 100 mM EDTA treatment for 5 minutes at room temperature. DCs were purified from blood cells with density gradient centrifugation in 1.977 g/cm^3 Nycodenz (Nycomed Pharma). DC populations were selected using a negative selection method by anti-rat-IgG-coupled magnetic beads (BioRad) and surface molecule antibodies (**Table 2.2**). DC purity was measured by flow cytometry for $CD11c^+$ surface marker expression. Briefly, cells were stained with CD11c antibody (PE561, 1:400, **Table 2.9**) in the dark on ice for 20 minutes. Cells were washed with

EDTA-BSS twice to remove excessive antibodies, followed by Propidium Iodide (PI) staining (0.5 µg/mL) to distinguish live/dead cells. Sample acquisition was carried out on LSR Fortessa (BD Bioscience). Cell populations were identified based on their forward and side scatter, with cell viability determined by negative staining with PI. DC purity was determined by positive staining with CD11c antibody PE561 against all live cells. The cDC purity was above 90%. Primary cells were cultured at 37 °C and 10% CO_2 in RPMI 1640 supplied with 33.6 mM HEPES, 24 mM sodium bicarbonate (NaHCO3), 60 µg/mL penicillin, 100 µg/mL streptomycin and 100 µM β-mercaptoethanol.

2.4 Harvesting T lymphocytes

Total lymph node lymphocytes were isolated by forcing mashed tissues through a 40 µm cell strainer (BD) with KDS-RPMI-FBS. For $CD4^+$ and $CD8^+$ cell enrichment, unwanted cells were negatively depleted by surface molecule cocktails (**Table 2.2**) and incubation with anti-rat-IgG-coupled magnetic beads (BioRad). Purity was assessed by flow cytometry as mentioned above (CD4, TCRVα2 for $CD4^+$ T cells, CD8, TCRVα2 for $CD8^+$ T cells, **Table 2.9**).

Table 2.1 Description of cells.

Cell line	Cell type	Media	Supplements	Origin
Mutu DC1940	Mouse dendritic cells	Iscove's Modified Dulbecco's Medium (IMDM)(Gibco)	10% (v/v) FBS. 60 µg/mL penicillin 100 µg/mL streptomycin 100 µM β-mercaptoethanol	[81]
Mutu DC1940 Cas9	Mouse dendritic cells	Iscove's Modified Dulbecco's Medium (IMDM)(Gibco)	10% (v/v) FBS. 60 µg/mL penicillin 100 µg/mL streptomycin 100 µM β-mercaptoethanol	[158]
Splenic $CD11c^+$ Dendritic cells	Mouse primary dendritic cells	RPMI 1640 (ThermoFisher)	33.6 mM HEPES 24 mM sodium bicarbonate ($NaHCO_{3)}$ 60 µg/mL penicillin 100 µg/mL streptomycin 100 µM β-mercaptoethanol	Harvested as described below.
RAW 264.7	Mouse macrophage	Dulbecco's Modified Eagle Medium (DMEM)(Gibco)	10% (v/v) FBS. 1% (v/v) antibiotic-antimycotic	[159]
HSC-3	Human oral squamous cell carcinoma	DMEM(Gibco)	10% (v/v) FBS. 1% (v/v) antibiotic-antimycotic	Derived from metastatic lymph nodes in the tongue [160]
HEK 293T	Human embryonic kidney cells	DMEM(Gibco)	10% (v/v) FBS. 1% (v/v) antibiotic-antimycotic	[161]

Table 2.2 Antibody depletion cocktails.

Cell type	Antigen	Host	Clone	Dilution	Supplier
CD11c$^+$ DCs	Anti-mouse CD3	Rat	KT3-1.1	1:100	WEHI antibody factory facility
	Anti-mouse CD90	Rat	T24/31.7	1:50	
	Anti-mouse erythroid lineage	Rat	TER119	1:10	
	Anti-mouse Ly6G & Ly6C	Rat	RB68C5	1:50	
	Anti-mouse CD45R/B220	Rat	RA36B2	1:100	
OT-1 CD8$^+$ T cells	Anti-mouse anti-CD4	Rat	GK1.5	1:10	
	Anti-mouse anti-CD11b	Rat	M1/70	1:50	
	Anti-mouse erythroid lineage	Rat	TER/119	1:10	
	Anti-mouse CD45R/B220	Rat	RA3-6B2	1:100	
	Anti-mouse Ly6G	Rat	1A8	1:10	
	Anti-mouse MHCII	Rat	M5/114	1:20	
OT-II CD4 T$^+$ cells	Anti-mouse CD8	Rat	YTS169.4	1:25	
	Anti-mouse CD11b	Rat	M1/70	1:50	
	Anti-mouse erythroid lineage	Rat	TER/119	1:10	
	Anti-mouse CD45R/B220	Rat	RA3-6B2	1:100	
	Anti-mouse Ly6G	Rat	1A8	1:10	
	Anti-mouse MHCII	Rat	M5/114	1:20	

2.5 Dendritic cell stimulation

1 x 10^6 DC1940 cells were plated in 6-well plates overnight for cell attachment. DC stimulants were added after cells were attached for 24 hours, as shown in the table below. Primary splenic DCs were harvested as described above. Primary cells were subsequently plated in 6-well plates at a 1 x 10^6 cells/mL density, followed by stimulation with TLR agonists and cytokines, as described below **(Table 2.3)**, for 24 hours.

Table 2.3 Dendritic cell stimulation.

Stimulants	Concentration	Product Number	Supplier
CpG	0.500 µM	-	Bioneer
LPS	1.00 µg/mL	14011	Cell Signaling
Poly I:C	100 µg/mL	INV-tlrl-pic	Invivogen
Pam3CSK4	500 ng/mL	tlrl-pms	Invivogen
FSL-1	0.500 µg/mL	tlrl-fsl	Invivogen
R848	2.00 µg/mL	tlrl-r848	Invivogen
IL-4	20.0 ng/mL	214-14-20	Peprotech
IL-6	20.0 ng/mL	406-ML-005	R&D Systems
IL-10	20.0 ng/mL	RMIL105	Invitrogen
IFNγ	50.0 ng/mL	315-05-100	Peprotech

2.6 Activity-based probes:

Live cell labelling: Referring to **Table 2.4**, probes were dissolved in DMSO, diluted from a 1 mM DMSO stock, and added to the cell culture 4 hours before harvesting (final concentration 1 µM, 0.1% DMSO). Cells were collected and centrifuged, and the supernatant was removed, followed by washing with PBS to eliminate excess probe and serum. PBS was removed by centrifugation and pipetting. Cells were lysed with PBS containing 0.1% Triton X-100. Cell lysates were cleared of debris by centrifugation at max speed for 7 minutes, and supernatants were transferred to a new tube. BCA assay (Thermo Fisher) was then used to determine the total protein concentration using Fluorostar® (GE). Sample buffer (10% glycerol, 40 mM Tris-Cl, pH 6.8, 2% SDS, 0.01% bromophenol blue, 1.25% beta-mercaptoethanol) was added to each sample, followed by a 5-minute boiling at 95 °C. Equal protein amounts (in general 80 µg) were resolved on homemade 15% SDS-PAGE gels. The gels were scanned for Cy5 fluorescence using a Typhoon flatbed laser scanner (GE Healthcare).

Lysate labelling: Cells were collected and pelleted by centrifugation. Media was removed, and cells were washed with PBS. PBS was removed by pipetting after centrifugation. For measuring proteases that require an acidic pH for activity, cells were lysed using citrate buffer (50 mM citrate, pH 5.5, 0.5% 3-[(3-cholamidopropyl) dimethylammonio]-1-propanesulfonic acid (CHAPS), 0.1% Triton X-100, 4 mM dithiothreitol (DTT)). Alternatively, cells were lysed with PBS containing 0.1% Triton X-100 for neutral pH proteases. Cell lysates were then cleared of debris by centrifugation, and supernatants were transferred to a new tube. BCA assay was used to determine the total protein concentration using Fluorostar® (GE). A total of ~80 µg protein was aliquoted into 20 µl lysis buffer, and ABPs were added from a 1:100 dilution of a 100 µM DMSO stock (final concentration 1 µM, 1% DMSO). Samples were incubated at 37 °C for 20 minutes. Sample buffer (10% glycerol, 40 mM Tris-Cl, pH 6.8, 2% SDS, 0.01% bromophenol blue, 1.25% beta-mercaptoethanol) was added to each sample, followed by a 5-minute boiling at 95 °C. Proteins were resolved on homemade 15% SDS-PAGE gels. The gels were scanned for Cy5 fluorescence using a Typhoon flatbed laser scanner (GE Healthcare).

Table 2.4 Activity-based probes.

Activity-based probes	Targets	Reference
sCy5-Nle-SY	Cathepsin X/S	[162]
BMV109	Pan cathepsin probe	[163]
FY01	Cathepsin C	[164]
LE28	Legumain	[165]
PK105b	Neutrophil elastase	[166]
PK-DPP	Trypsin-like serine protease	[167]
FP-Biotin	Pan serine protease probe	[168]

2.7 Small molecule protease inhibitors

Small molecule protease inhibitors were diluted from 1000x DMSO stock and administered directly into cell culture (0.1% final DMSO) with an incubation time of 24 hours. The concentration and target of each protease inhibitor are summarised in the table below (**Table 2.5)**.

Table 2.5 Small molecule protease inhibitors.

Inhibitors	Target	Concentration	Reference
MDV-590	Cathepsin S	50 µM	[169]
Biotin-Hex-Nle-SY	Cathepsin X/S	50 µM	Modified from sCy5-Nle-SY [162]
SD134	Legumain	100 µM	[170]

2.8 Inhibition of NF-κB activation

NF-κB Activation Inhibitor, 6-Amino-4-(4-phenoxyphenylethylamino) quinazoline (Calbiochem®, 481406) was reconstituted in DMSO with an initial concentration of 50 mM. NF-κB Activation Inhibitor was diluted from 1000x DMSO stock and administered directly into cell culture (0.1% final DMSO) 4 hours before the administration of CpG. The final concentration used was indicated in the relevant section.

2.9 Analysis of conditioned media

For conditioned media (CM) analysis, cells were washed with serum-free media when passaging to remove all serum. Cells were then plated at $1x10^6$ cells/well in 6-well plates for 24 hours. CM was collected after incubation and spun at 300 xg for five minutes to remove cell debris. The media was then concentrated using Amicon® Ultra 0.5 mL 3kDa Centrifugal Filters by centrifugation at 14,000 xg for 20 minutes at 4°C. Concentrated media was centrifuged from filters into a new collection tube at 1,000 xg for 2 minutes at 4°C. BCA assay was used to determine the total protein concentration using Fluorostar® (GE). A total of ~80 µg protein was aliquoted into 20 µl lysis buffer, and ABPs were added from a 1:100 dilution of a 100 µM DMSO stock (final concentration 1 µM, 1% DMSO). Samples were incubated at 37 °C for 20 minutes. Sample buffer (10% glycerol, 40 mM Tris-Cl, pH 6.8, 2% SDS, 0.01% bromophenol blue, 1.25% beta-mercaptoethanol) was added to each sample, followed by a 5-minute boiling at 95 °C. Proteins were resolved on homemade 15% SDS-PAGE gels. The gels were scanned for Cy5 fluorescence using a Typhoon flatbed laser scanner (GE Healthcare).

2.10 Immunoblotting

Proteins on gels were transferred onto nitrocellulose membranes using a Trans-Blot Turbo Transfer System (BioRad) in transfer buffer (1x Trans-Blot® Turbo™ Transfer Buffer (BioRad) containing 20% ethanol). Membranes were incubated in primary antibodies overnight in a cold room (4 °C) **(Table 2.6)**. The membranes were washed with PBS containing 0.05% Tween-20 (PBST) three times. Membranes were then incubated in the secondary antibody on an orbital shaker for one hour at room temperature **(Table 2.6)** and then washed three times using PBST and once with PBS. IR800 immunoblots were scanned using Typhoon. HRP labelling was visualised on a ChemiDoc® MP imager (BioRad) using Amersham ECL Western blotting reagents (GE).

2.11 Immunoprecipitation

Lysates were previously labelled with probes, boiled, and solubilised with sample buffer (SB). The lysates were divided into input and pulldown samples, each containing an equal amount of total protein (generally 40 µg). 500 µL immunoprecipitation (IP) buffer (PBS, pH7.4, 0.5% NP-40, 1 mM EDTA) was added to the pulldown sample. Protein A/G agarose beads (Santa Cruz Biotechnology; 40 µL slurry) were washed using IP buffer and then added to the pulldown sample along with antibody (**Table 2.6,** 1:100) on ice. The mixture was rotated overnight at 4 °C. The beads were washed using IP buffer four times and a final wash with 0.9% NaCl. The remaining NaCl was removed using an insulin syringe, and 20 µl 2X sample buffer was added. The beads were boiled before running on the gel to elute immunoprecipitated proteins. Samples were resolved on homemade 15% SDS-PAGE gels. The gels were scanned for Cy5 fluorescence using a Typhoon flatbed laser scanner (GE Healthcare).

Table 2.6 Western blotting and immunoprecipitation antibodies.

Antigen	Host	Concentration	Product Number	Supplier
Cathepsin X	Goat	1:1,000 1:100 for IP	AF1033	R&D Systems
Cathepsin S	Goat	1:500	AF1183	R&D Systems
Cathepsin B	Goat	1:1,000	AF965	R&D Systems
Cathepsin L	Goat	1:1,000	AF1515	R&D Systems
Cathepsin H	Goat	1:1,000	AF1013	R&D Systems
Legumain	Goat	1:1,000	AF2058	R&D Systems
Caspase-1	Rabbit	1:1,000	A0964-100	Gene Search
Stefin A	Rabbit	1:1,000	AB61223	Abcam
Stefin B	Rabbit	1:1,000	AB92449	Abcam
Cystatin C	Goat	1:1,000	AF1238	R&D Systems
Cystatin E/M	Rat	1:1,000	MAB1284	R&D Systems
β Actin	Rabbit	1:10,000	MA5-15739	Life Technologies
Tubulin	Rabbit	1:10,000	A5060	Sigma Aldrich
Lamin A (C-terminal)	Rabbit	1:10,000	L1293	Sigma Aldrich
Lamin B1	Rabbit	1:10,000	33-2000	Invitrogen
Anti-Goat 800	Donkey	1:10,000	92632214	Licor
Anti-goat HRP	Donkey	1:10,000	A15999	Invitrogen
Anti-rabbit 800	Donkey	1:10,000	92632213	Licor

2.12 Immunofluorescence

Immunofluorescence for lysosomal cathepsin X:

1 cm round coverslips were coated with 10 µg/mL anti-MHC class II N22 antibody (WEHI antibody factory facility) and incubated for 2 hours at 37°C in a humid incubator. The coverslips were washed twice with PBS containing 2% FBS and once with the DC culture media.

1 x 10^5 cells were placed on the coverslip in 20 µL culture media and incubated for 10 minutes at room temperature, followed by 20 minutes at 37°C. 1 mL culture media with or without 0.5 µM CpG was added to each well, and cells were incubated for 24 hours at 37 °C. The coverslips were washed twice with PBS, fixed and permeabilised with ice-cold methanol, and placed at -20°C for 5 minutes. The coverslips were washed with PBS 3 times and blocked with PBS containing 10% Normal Horse Serum (NHS) for 30 minutes at room temperature.

Anti-cathepsin X antibody was diluted in blocking buffer (1:200) and applied to coverslips at 4 °C overnight. The primary antibody was washed away with PBS, and the secondary antibody (anti-goat 568; 1:1,000 in blocking buffer, ThermoFisher) was applied to coverslips for 1 hour at room temperature in the dark. The secondary antibody was then washed away using PBS. DAPI (1 µg/mL) was added to the coverslip for 5 minutes at room temperature and then washed with PBS.

Coverslips were mounted on glass slides with the Prolong Diamond mounting solution (ThermoFisher). The coverslips were left on the slides in the dark at room temperature for 24 hours and then stored at 4 °C. Samples were imaged using the Leica SP8 Confocal Microscope (Leica) with a 63x/1.40 oil objective.

Immunofluorescence for nuclear cathepsin L/X:

Ibidi slide chambers (Ibidi 80826) were washed with 250 µL PBS twice and 250 µL IMDM media once. 25,000 cells were added to each chamber with 250 µL media and were incubated overnight. The attached cells were washed with 150 µL PBS twice and were fixed with 150 µL 4% PFA in PBS at room temperature for 10 minutes. The cells were then permeablised with 150 µL 0.1% Triton X-100 at room temperature for 3 minutes. The cells were subsequently washed with PBS, followed by blocking with blocking buffer (10% NHS in PBS) at room temperature for 30 minutes. 150 µL primary antibody diluted in blocking buffer (1:200) was added to each chamber, followed by incubation at 4 °C overnight. The cells were washed with 150 µL 0.1 Triton X-100 in PBS twice. The secondary antibody was diluted in the blocking buffer (1:1,000) and added to each chamber, followed by an incubation at room temperature for 1 hour. The cells were washed with 150 µL 0.1 Triton X-100 in PBS twice. The nuclei were stained with DAPI in PBS (1:1,000) at room temperature for 5 minutes. After washing with PBS 3 times, the cells were stored in the mounting buffer (90% Glycerol in PBS) and imaged using the Leica SP8 Confocal Microscope (Leica) with a 63x/1.40 oil objective.

The nuclear cathepsin L was quantified using ImageJ. Briefly, the area of nuclear (region of interest) was selected using the “Analyse Particles” function. The staining of nuclear cathepsin L was subsequently measured within the region of interest.

Table 2.7 Immunofluorescence antibodies.

Antigen	Host	Dilution	Product Number	Supplier
Cathepsin X	Goat	1:200	AF1033	R&D Systems
Cathepsin L	Goat	1:200	AF1515	R&D Systems
Anti-goat 568	Donkey	1:1,000	A-11057	ThermoFisher

2.13 CRISPR-Cas9 Knockout

Cathepsin X knockdown cell lines were generated using the CRISPR/Cas9 system. The FgH1tUTGCFP backbone vector (provided by Marco Herald, WEHI) was first linearised by mixing the backbone vector with 10X buffer 3.1 (NEB) and BsmB1. 100 µM of guide RNA was annealed by combining 3 M NaCl, 1 M MgCl2, 1 M Tris-HCl (pH7.5), and 1 M TE buffer. The mixture was incubated at 96 °C for 5 minutes and at 80 °C for one hour. Annealed oligonucleotides were then phosphorylated at the 5' end by incubating with 10X T4 DNA ligase buffer (Promega, containing 1 mM ATP) and 0.5 U/µL T4 polynucleotide kinase (Promega) at 20 minutes at 37 °C and then 10 minutes at 70 °C. The phosphorylated oligonucleotides were ligated with FgH1tUTGCFP vector with 10X T4 ligase buffer (Promega) and T4 ligase (Promega) overnight at room temperature.

Stbl3 competent *E. coli* cells were transformed with the vector by heat shock. Briefly, *E. coli* cells were mixed with the vector for 30 minutes on ice, followed by a 45-second heat shock (42 °C). *E. coli* cells were incubated in SOC media (2% (w/v) tryptone, 0.5% (w/v) yeast extract, 8.56 mM sodium chloride, 10 mM magnesium chloride, 10 mM magnesium sulphate, 2.5 mM potassium chloride and 20 mM glucose (ThermoFisher)) for one hour at 37 °C with constant shaking. The *E. coli* was spread on separate LB/100Amp Agar plates and incubated overnight at 37 °C. The plasmid was extracted using a PureYield Plasmid Miniprep Kit (Promega) and was sequenced at the Australian Genome Research Facility (AGRF, PeterMac). The colony with successful insert was grown in LB (1% (w/v) Peptone 140, 0.5% (w/v) yeast extract and 0.5% (w/v) sodium chloride (ThermoFisher)) to amplify the plasmid DNA. DNA was extracted using a PureYield Plasmid Miniprep (Promega) for further transfection.

HEK293T cells were used for plasmid transfection and packing lentivirus. HEK293T cells were cultured in DMEM (Gibco) media at 37 °C and 10% CO_2 until 70% confluent. Lentivirus was formed by mixing 10 µg/mL plasmid DNA, 1 mg/mL PEI, 5 µg pDML, 2.5 µg RSV-REV, 3 µg VSV and 10 µg sgRNA vector with HEK293T cells overnight (37 °C, 5% CO_2). The media was exchanged to IMDM DC media the next day, and HEK293T cells were permitted to produce the virus in fresh media overnight (37 °C, 5% CO_2). The supernatant containing the virus was filtered with a 0.45 µm filter and collected before adding it to target cells (DC1940/Cas 9 cells). The target cells and the viral supernatant were added with 8 µg/mL polybrene (Sigma-Aldrich) and centrifuged at 2200 rpm for 2 hours at 32 °C. Cells were grown in DC1940 media, and the

transduction efficiency was checked by gating for Cyan Fluorescent Protein (CFP)-positive cells on an L.S.R. Fortessa flow cytometer (BD Bioscience). CFP-positive cells were sorted at Murdoch Children's Research Institute (MCRI) using BD Influx to obtain a pure population. The knockout was induced by adding 1 μg/mL doxycycline (Sigma-Aldrich). In addition to bulk-sorted cells, some CFP-positive cells were sorted to make single-cell clones.

hBIM cells were adopted as the wild-type negative control and produced with the abovementioned technique. The hBIM cells were transduced with guide RNA targeting the human BCL2-like gene, which is not found in the mouse genome. Therefore, hBIM cells should not have genome editing but have undergone the same procedure as the cathepsin X knockout cells.

Table 2.8 CRISPR-Cas9 oligos.

Name	Target gene	Sequence	Target Exon
Guide RNA	Cathepsin X (*Ctsz*)	TTGCTACCATCCCATTCGCG	Exon 1
Guide RNA	Human Bcl-2-like protein-11 (hBIM)	GCCCAAGAGTTGCGGCGTAT	Exon 3
Primers for sequencing	Cathepsin X (*Ctsz*)	Forward: GTCAAGAGGTCGAAGGTGCT Reverse: CCAGCAGAACCCAGGACTA	Exon 1

2.14 Cathepsin X rescue

Three constructs of murine cathepsin X cDNA cloned into the puc57 vector were purchased from Biomatik. The three constructs include the WT cathepsin X, inactive cathepsin X, whose active cysteine was switched to a serine (C94S), and cathepsin X, whose RGD motif was mutated into an HGD motif (R40H). Without changing the amino acid sequence, the EcoRI restriction site was mutated within all three constructs from GAATTC to GAGTTC; the PAM sequence following the guide RNA target site was mutated from GGG to GTG. Subsequently, the three cathepsin X variants were amplified by PCR with primers generating Gibson Assembly overhangs:

5' overhang = 5'CCTTCTCTAGGCGCCGGCCGGATCC

3' overhang = 5'GTCGACCCTGTGGAATGTGTGTCAG

According to the manufacturer's protocol, the purified PCR products were cloned into the retroviral pBABE-puro vector with the Gibson Assembly kit (NEB). Sanger sequencing was subsequently conducted to ensure the correct insertion of cDNA. According to the manufacturer's protocol, pBABE vectors were transfected into HEK293T cells along with pGag-pol and pVSV-G vectors with Lipofectamine 3000 (Thermofisher). After 24 hours, the supernatant was replaced with fresh DC media. The cells were incubated further overnight to produce the virus. The resulting supernatant was then used to infect DC1940 cells by adding 8 µg/mL polybrene for 24 hours. A negative control in which no virus was added was implemented. The transduction mixture was replaced with fresh media the next day. The infected cells were then selected with 1 µg/mL puromycin until all the negative control cells died.

2.15 Cytokine quantification:

1 x 10^6 DC1940 cells were plated in a 6-well plate and cultured overnight for attaching. Cells were then treated with CpG for the indicated time. Conditioned media was then collected and briefly centrifuged to remove cell debris. The conditioned media was subsequently analysed with Proteome Profiler Mouse XL Cytokine Array (R&D Systems, ARY028) or BD™ Cytometric Bead Array (CBA). Mouse Inflammation Kit (BD cat 552364) and Mouse IL-1β Flex Set (BD cat 560232) were used according to the manufacturer's manual.

2.16 Antigen uptake assay:

1 cm round coverslips were coated with 10 µg/mL anti-MHC class II N22 antibody (WEHI antibody factory facility) and incubated for 2 hours at 37°C in a humid incubator. The coverslips were washed twice with PBS containing 2% FBS and once with the DC culture media. 1 x 10^5 cells were placed on the coverslip in 20 µL culture media and incubated for 10 minutes at room temperature, followed by 20 minutes at 37°C. 1 mL culture media with or without Lucifer yellow (Invitrogen, 1 mg/mL) was added to each well. Cells were incubated at 37°C 5% CO_2 for 15 minutes or one hour. Control cells were placed on ice for the indicated time. Cells were then fixed with ice-cold methanol for 10 minutes and analysed using an SP8 microscope.

DC1940 cells were resuspended at 1 million cells/mL in IMDM media. 200uL of cell suspension was added into each well in a 96-well plate. To make Cy5-OVA, 5 mg of OVA (A5503, Sigma) was dissolved into 500 µL PBS, followed by 45.3 µL of 2 mg/mL Cy5-NHS (Lumiprobe). The mixture was stored at 4°C overnight. An empty 1.5 mL 7k Zeba column (Thermo Scientific) was centrifuged at 1,500 g for 1 minute and flow-through discarded. The column was washed twice with 300 µL PBS each time, followed by centrifugation at 1,500 g for 1 minute. The OVA-Cy5-NHS mixture was added to the column and centrifuged at 1,500 g for 2 minutes. The concentration of the OVA-Cy5 was determined by the following formula:

$$Protein\ (M) = \frac{A280 - (Amax_{dye} \times 0.13)}{31775}$$

Cy5-OVA (300 µg/mL) was added into cell media and incubated with target cells for 4 minutes on ice or at 37°C 5% CO_2. Cells were washed using EDTA-BSS (2%FCS) before flow cytometry analysis on L.S.R. Fortessa (BD Bioscience).

2.17 Antigen presentation assay:

As described above, $CD8^+$ or $CD4^+$ T cells were harvested from OT-I or OT-II mouse lymph [171, 172]. T cells were then labelled with Cell Tracer Violet (CTV, 1.67 µM; Sigma-Aldrich) to quantify proliferation. Target DCs were pulsed with OVA (1 mg/ml) and 0.5 µM CpG for 45 minutes at 37°C. T cells and pulsed DCs were co-cultured for three days before analysing. Cells were stained with antibodies for CD4/8 and TCRVα2. 25,000 counting beads were added to each well and analysed using flow cytometry. $CD4^+$, $TCRV\alpha2^+$, and alive cells (PI^-) were gated, and a histogram of the CTV signal was created, separating the proliferated T cells (differently strong CTV-stained cells in the histogram) from the non-proliferated cells. The number of proliferated cells was determined using the following formula:

$$\frac{Added\ bead\ (\boldsymbol{BA})}{Gated\ beads\ (\boldsymbol{GB})\ )} \times proliferated\ cells\ (\boldsymbol{PC})$$

2.18 Flow cytometry:

DC1940 cell surface molecules were stained with fluorescent antibodies, as listed in the table below (**Table 2.9**). Briefly, around 200,000 cells were seeded in 96-well plates. The cells were stained with specific antibodies diluted in BSS-EDTA 2% FBS) in the dark at 4 °C for 20 minutes. Cells were centrifuged at 1,700 rpm for 2 minutes to remove the staining buffer. Cells were washed with BSS-EDTA 2% FBS followed by centrifugation at 1,700 rpm for 2 minutes twice. Propidium Iodide (PI) (0.5 µg/mL) was diluted in BSS-EDTA 2% FBS and resuspended the cell pellet to differentiate live/dead cells. CBA cytometric beads were examined by flow cytometry according to the manufacturer's protocol. Sample acquisition was conducted on L.S.R. Fortessa (BD Bioscience). Data analysis was performed using FlowJo V10.0.7 (TreeStar Inc.) or FCAP Array V3.0.1 (BD).

Cell sorting was conducted using BD. Influx (Murdoch Children Research Institute).

Table 2.9 Antibodies for flow-cytometry.

Antigen	Host	Fluorophore	Concentration	Clone	Catalogue	Supplier
CD11b	Rat	PE-Cy7	1:200	M1/70	101216	BioLegend
CD11c	Hamster	PE561	1:400	N418	117308	BioLegend
CD4	Rat	FITC	1:200	GK1.5	100406	BioLegend
CD8	Rat FITC	BV421 FITC	1:200 1:200	53-6.7	100738	BioLegend WEHI antibody factory facility
CD40	Rat	APC	1:200	FGK45.5	157505	BioLegend
CD86	Rat Rat	PE APC	1:200 1:400	GL-1	105007 105011	BioLegend BioLegend
MHC-I	Mouse	APC	1:200	AF6-88.5.5.3	CABT-L4417	BioLegend
MHC-II	Rat	AF700	1:200	M5/114	107621	BioLegend
TCV Vα2	Rat	APC	1:400	B20.1		WEHI antibody factory facility

2.19 RNA isolation, cDNA synthesis and quantitative real-time PCR

Cells were plated on 35 mm dishes. When confluent, cells were collected and lysed with 1 mL Trizol. 200 µL of chloroform was added. The samples were mixed by inverting the tubes and incubated at room temperature for 3 minutes. The samples were centrifuged at 12,000 g at 4°C for 15 minutes. The resulting top clear phase contained RNA was collected, and the rest was discarded. 500 µL isopropanol was added to the collected clear phase, followed by a 10-minute incubation at room temperature. The mixture was centrifuged at 12,000 g, 4°C for 15 minutes. Supernatamt was removed. The RNA pellets were washed twice with 75% ethanol, followed by centrifugation at 12,000 g for 10 minutes to remove ethanol. The washed RNA pellets were dissolved with nanofiltered (NF) water.

Before cDNA synthesis, we removed genomic DNA using DNase (Therscientific, EN0521). Briefly, 1 µg of RNA was mixed with 1 µL 10x reaction buffer with $MgCl_2$, 1 µL of DNase I, RNase-free (#EN0521), and NF water to a final volume of 10 µL. The mixture was incubated at 37°C for 30 minutes. 1 µL of 50 mM EDTA was added to the mixture and incubated at 65°C for 10 minutes.

9 µL of the mixture was mixed with 1 µL of Random Primer from the cDNA synthesis kit (Promega, A5001). The mixture was heated at 70°C for 5 minutes in a PCR machine. The samples were chilled on ice for 5 minutes, followed by the addition of 5 µL GoScript 5X Reaction Buffer, 1.5 µL $MgCl_2$, 1 µL PCR Nucleotide Mix, 0.5 µL Recombinant RNasin, 5 µL NF water, and 1 µL GoScript Reverse Transcriptase. The mixture was incubated at 25 °C for 5 minutes, 42°C for 1 hour, and 70°C for 15 minutes for cDNA synthesis.

For each qPCR reaction, 5 µL GoTaq® qPCR Master Mix (Promega, A6001), 0.5 µL of both forward primer and reverse primer **(Table 2.10)**, and 3 µL of NF water were added to 1 µL of cDNA sample. Gene expression was determined relative to the housekeeping gene GAPDH using the QuantStudio™ 6 system (ThermoFisher).

Table 2.10 Primers for quantitave PCR.

Target	Sequence
Cathepsin X	F: GGATTGTCCGAAATTCATGG R: ACTCTCGATGGCAAGGTTGT
Cathepsin L	F: AGAGTAGCACCAGTGGAAGT R: CCGTTGTGTAGCTGGATCATT
GAPDH	F: GGTGCTGAGTATGTCGTGGA R: CGGAGATGATGACCCTTTTG

2.20 Nuclear fractionation

Cells were seeded in 10 cm dishes. When confluent, cells were collected and lysed with 200 µL buffer A **(Table 2.11)**, followed by centrifugation at 4 °C, 3000 rpm for 10 minutes. The supernatant was collected and contained cytosolic fraction. The remaining cell pellets contained nuclear fraction and were dissolved with 50 µL buffer B **(Table 2.11)**, followed by sonicating for 10 seconds 2 times at 40% amp (QSONICA Q500). The homogenate was left on ice for 30 minutes, followed by centrifugation at max speed for 20 minutes at 4 °C. The supernatant contained the nuclear fraction, and the debris was discarded. For cytosolic proteins, an equal protein amount (in general 80 µg) was resolved on homemade 15% SDS-PAGE gels. The nuclear protein samples were loaded at the same volume as their corresponding cytosolic samples and, therefore, were 4 times more concentrated. The purity of the cytosolic fraction and the nuclear fraction was assessed with cytosolic marker tubulin antibody and nuclear marker Lamin A antibody **(Table 2.6)**.

Table 2.11 Nuclear fractionation buffer recipe.

Buffer name	**Buffer A pH 7.9**	**Buffer B pH 7.9**
Components	10 mM HEPES 1.5 mM $MgCl_2$ 10 mM KCL 0.5 mM DTT 0.05 % NP40	5 mM HEPES 1.5 mM $MgCl_2$ 0.2 mM EDTA 0.5 mM DTT 26% glycerol (v/v) 300 mM NaCl

2.21 Shotgun proteomics

DC1940 cells were plated in 6-well plates (triplicates) and treated with CpG as described above. Samples were prepared according to S-Trap™ mini spin column digestion protocol, except as stated below. Briefly, cells were lysed with 46 µL 1x lysis buffer (5% SDS, 50 mM TEAB pH 8.5). Genomic DNA was digested by benzonase (100 units per 50 µg protein sample), followed by a 10-minute room temperature incubation. Samples were reduced by adding 1 µL 120 mM tris(2-carboxyethyl) phosphine (TCEP) at room temperature for 10 minutes. Disulphide bonds were alkylated by adding 4 µL Chloroacetic acid (CAA, final concentration 40 mM), followed by a 15-minute incubation at 55°C with shaking. 1 µg trypsin (dissolved in 40 uL acetic acid, 50 mM Tetraethylammonium bromide (TEAB)) was used for each sample. Dried protein was stored at -80 °C until analysis. For analysis, 80 µL loading buffer (2% Acetonitrile (ACN), 0.1% Trifluoroacetic acid (TFA)) was added to the dried protein. The proteins were dissolved with vortexing and sonication for 15 minutes in a water bath sonicator. Samples were centrifuged at 21,000 xg for 10 minutes, and the supernatant's protein concentration was measured using nanodrop (Thermo Scientific). Samples were diluted at 0.17 mg/mL with loading buffer (2% ACN, 0.1% TFA) and submitted for data-independent acquisition (DIA) method on the Bruker TIMS-TOF Pro mass spectrometer machine at the Mass Spectrometry and Proteomics Facility at Bio21 Molecular Science and Biotechnology Institute. Raw files were analysed using Spectronaut software (Ver 15.2.21089, Biognosys). The search was against Murine's unreviewed and reviewed proteins from UniProt sequence databases (March 2021). Post-analysis and volcano plots were conducted using Perseus (1.6.15.0). MS2Quantity parameter was used to determine the relative amount of proteins detected and to calculate log2(x)-ratios of each protein in WT/*Ctsz*$^{-/-}$ DC1940 cells. Three replicate groups were averaged, and only proteins quantified based on >2 unique peptides were considered for analysis. Missing values were imputed in Perseus with the default setting. A volcano plot was generated as *Ctsz*$^{-/-}$ versus WT DC1940 cell.

2.22 Recombinant protease cleavage assay

Recombinant proteases were dissolved in 50 mM Sodium Acetate and 500 mM Sodium Chloride. 500ng of each protease **(Table 2.12)** was used in the cleavage assay. Proteases (proteins) were incubated as indicated at 37 °C. Sample buffer (5X: 10% glycerol, 40 mM Tris-Cl, pH 6.8, 2% SDS, 0.01% bromophenol blue, 1.25% beta-mercaptoethanol) was added to each sample, followed by a 5-minute boiling at 95 °C. Samples were resolved on homemade 15% SDS-PAGE gels. The gels were scanned for Cy5 fluorescence using a Typhoon flatbed laser scanner (GE Healthcare).

Table 2.12 Recombinant proteins

Name	Host	Supplier	Catalogue
Legumain	Human	Kind gift from H. Brandstetter	-
Cathepsin X	Human	R&D Systems	934-CY
Cathepsin L	Human	R&D Systems	952-CY
Trypsinogen	Bovine	Sigma	T1143-250mg

2.23 Coomassie Stain

The SDS-PAGE gel was stained with 0.5% Brilliant Blue (Sigma), 50% Methanol, and 10% Acetic acid for 30 minutes. The gel was washed with Destain buffer three times (30% Ethanol, 10% Acetic acid) on an orbital shaker for 10 minutes each time. The gel was left in the water on an orbital shaker overnight.

2.24 Statistical analysis

Statistical analyses were performed using GraphPad Prism 8. Unpaired t-tests were performed to analyse the differences between the two groups. Ordinary one-way ANOVA followed by Dunnett's multiple comparisons test was used to compare more than two groups where indicated. Mean data points were expressed as mean ± SEM. $P < 0.05$ was considered significant.

Chapter 3. Characterising the regulation of cathepsin X during dendritic cell maturation

3.1 Introduction:

Cathepsin X is a lysosomal cysteine protease with strict carboxyl-mono-exopeptidase activity; it cleaves one amino acid from the C-terminus of its substrates. It is synthesised as an inactive zymogen with a short pro-peptide sequence (40 aa in mice and 38 aa in humans) and trafficked through the mannose-6-phosphate pathway. When reaching the acidic environment in lysosomes, pro-cathepsin X is activated by other lysosomal proteases by removing the pro-peptide sequence. A cysteine residue at the pro-peptide region forms a disulphide bridge with the active cysteine, making pro-cathepsin X inactive and unable to autoactivate.

Cathepsin X is primarily active and located in the lysosome and requires an acidic pH for its proteolytic activity. Despite its intracellular lysosomal distribution, it has also been reported to be secreted. Secreted cathepsin X is mostly in its inactive zymogen form [21, 48]. Whether or not active cathepsin X can be secreted and cleave extracellular substrates is currently unknown. When secreted, however, the RGD motif on the pro-peptide sequence can bind to β3 integrins to promote cancer cell proliferation in pancreatic cancer and bind to α5 integrins to affect inflammasome activation [48, 64].

Cathepsin X has been associated with various diseases, including cancer and inflammation. However, its roles in normal physiological conditions are poorly understood. More information about the function of cathepsin X in normal physiology needs to be investigated to understand its role in disease progression and ultimately use it as a therapeutic target.

Cathepsin X is predominantly expressed by immune cells, such as antigen-presenting cells, including dendritic cells. Naïve dendritic cells have high phagocytic activity. They scavenge and capture exogenous pathogens and are subsequently activated by pathogen-associated molecular patterns (PAMPs) through Toll-like receptors (TLRs). They undergo functional changes and exert their immune functions upon activation, including presenting antigens to T cells and secreting cytokines. Due to the temporal functional changes of dendritic cells throughout the infection process, we speculate that protease regulation is also constantly alternating.

In this chapter, we characterised the change of active and total levels of cathepsin X and other related proteases in the context of DC maturation. We showed the characterisation of intracellular lysosomal and secreted cathepsin X during DC maturation. In addition, we proposed a potential regulatory mechanism of cathepsin X upregulation in the context of TLR-9 agonist (CpG)-mediated DC maturation.

3.2 Results

3.2.1 The activity-based probe sCy5-Nle-SY labels active cathepsin X in dendritic cells

To study cathepsin X activity in dendritic cells, we used an activity-based probe, sCy5-Nle-SY, which was developed in our lab [162]. We first characterised the specificity of this probe in an immortalised mouse dendritic cell line, DC1940 (**Table 2.1**). We incubated sCy5-Nle-SY with living cells or cell lysates prepared in an acidic citrate buffer to achieve an optimal acidic pH to maintain cathepsin X activity. Proteins were resolved by SDS-PAGE, and probe labelling was analysed with a flatbed laser scanner using a Cy5 filter.

As previously observed in macrophages, sCy5-Nle-SY exhibited differential labelling profiles in living dendritic cells and lysates. In lysates, sCy5 specifically labelled cathepsin X. We confirmed the identity of this band by immunoprecipitation of the probe-labelled lysate with a cathepsin X-specific antibody (**Figure 3.1A**). In living cells, however, sCy5-Nle-SY labelled both cathepsin X (35 kDa) and cathepsin S (25 kDa) to similar extents (**Figure 3.1BC**). When cells were pre-treated with a cathepsin S-specific inhibitor, MDV590 [169], sCy5-Nle-SY exclusively labelled cathepsin X (**Figure 3.1D**). We opted to use live cell labelling for most experiments to reflect the state of cathepsin X activity in situ without disruptions to compartmentalisation, pH levels, and protein interactions. As cathepsin X and S are clearly resolved by SDS-PAGE, the activity of both proteases could be monitored simultaneously.

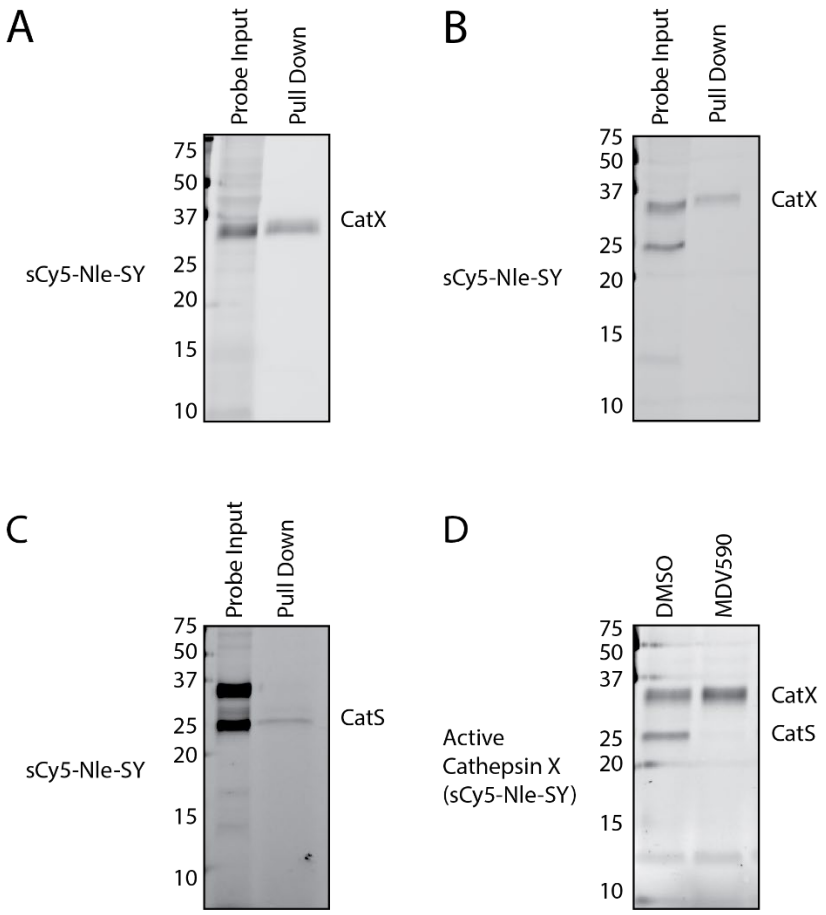

Figure 3.1 Application of activity-based probe sCy5-Nle-SY in Mutu DC1940 cells. A. sCy5-Nle-SY labelling of DC1940 cell lysates (input) and immunoprecipitation with a cathepsin X-specific antibody (Pull Down), as shown by in-gel fluorescence. **B.C.** sCy5-Nle-SY labelling of live DC1940 cells and cathepsin X/S immunoprecipitation, as shown by in-gel fluorescence. **D.** sCy5-Nle-SY labelling of live DC1940 cells after overnight pre-treatment with MDV590 (50 µM), as shown by in-gel fluorescence.

3.2.2 Cathepsin X is differentially regulated by TLR agonists

To investigate whether cathepsin X is activated during dendritic cell maturation, we stimulated DC1940 cells with six different TLR agonists, including Pam3 (TLR1/2), FSL-1 (TLR2/6), Poly I:C (TLR3), LPS (TLR4), R848 (TLR7/8), and CpG (TLR9). Using flow cytometry, we measured the cell surface expression of CD86 in naïve and stimulated cells to determine the extent of maturation (**Figure 3.2A**). The cells strongly responded to Pam3 (TLR1/2), FSL-1 (TLR2/6), Poly I:C (TLR3), and CpG (TLR9). In response to LPS, there was only a partial increase in CD86 surface expression, indicating only a subset of the DCs matured upon treatment. The DCs did not respond to R848.

We then incubated sCy5-Nle-SY with live DCs to compare the levels of active cathepsin X in naïve and mature DCs. CpG treatment strongly induced cathepsin X activity (11.15-fold, p=0.0391), while Pam3 and FSL-1 increased cathepsin X activity to a lesser extent (4.694-fold, p=0.0009 and 7.008-fold, p=0.0255, respectively). Although Poly I:C treatment induced DC maturation to a similar extent as CpG, Pam3, and FS-1, it did not significantly impact cathepsin X activity. In agreement with LPS only partially inducing DC maturation, this agonist slightly increased cathepsin X activity (2.335-fold, p=0.007) (**Figure 3.2BC**). We next measured total cathepsin X levels by immunoblotting with a cathepsin X-specific antibody, which showed a similar pattern as cathepsin X activity (**Figure 3.2BD**). These results suggest that cathepsin X is differentially regulated at the expression level upon TLR-induced DC maturation. Accordingly, mRNA expression of cathepsin X was significantly increased after CpG treatment, as measured by RT-PCR (4.214-fold, p=0.0007; **Figure 3.2E**). CpG treatment of primary $CD11c^+$ DCs isolated from mice spleen also provoked a 2.216-fold increase (p=0.001) in total cathepsin X protein, mirroring the effect in the DC1940 cell line (**Figure 3.2FG**).

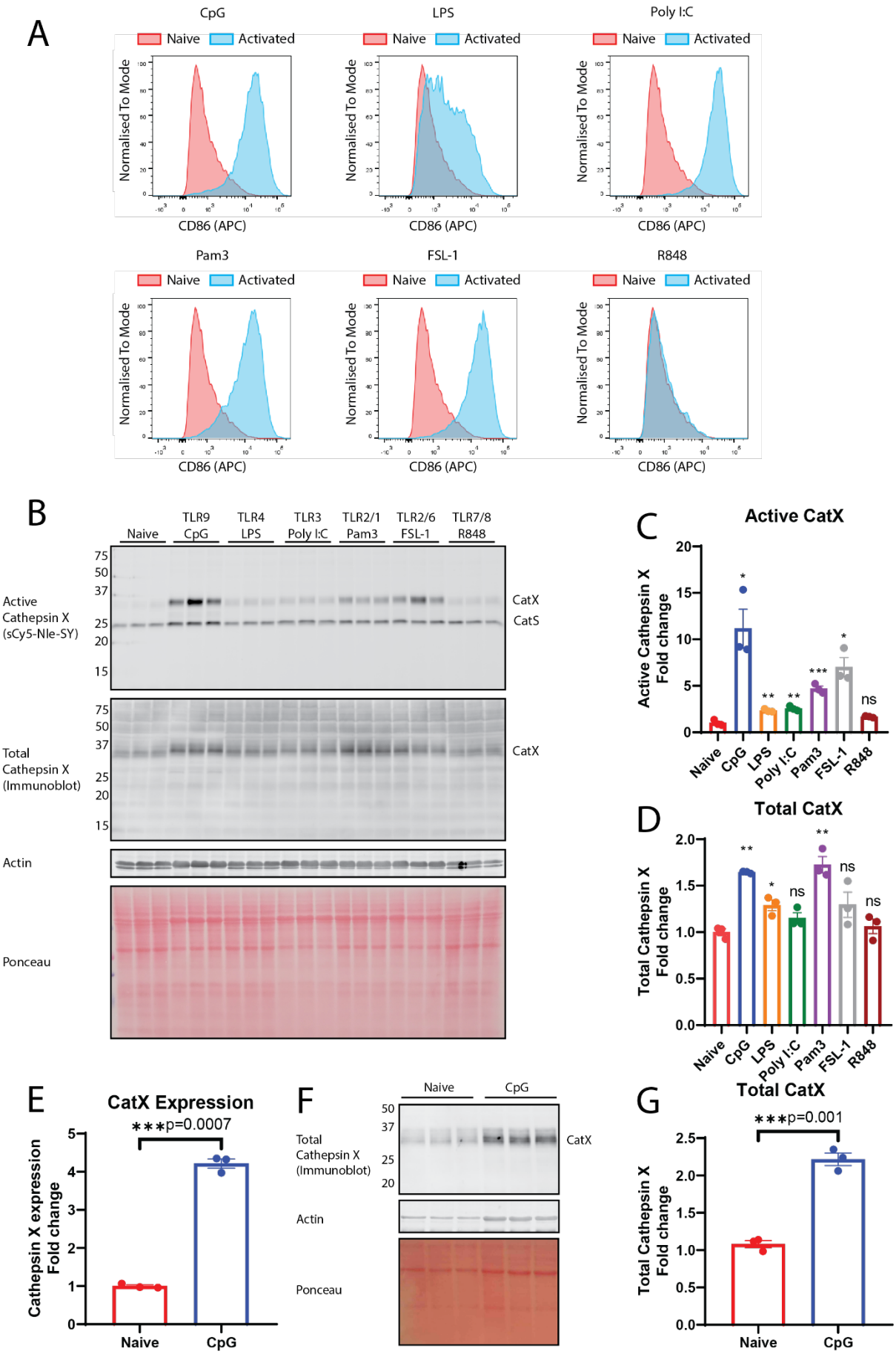
A
CpG
LPS
Poly I:C
Pam3
FSL-1
R848
Naive
Activated
Normalised To Mode
CD86 (APC)
B
Naive
TLR9 CpG
TLR4 LPS
TLR3 Poly I:C
TLR2/1 Pam3
TLR2/6 FSL-1
TLR7/8 R848
Active Cathepsin X (sCy5-Nle-SY)
Total Cathepsin X (Immunoblot)
Actin
Ponceau
CatX
CatS
75
50
37
25
20
15
C
Active CatX
Active Cathepsin X Fold change
Naive
CpG
LPS
Poly I:C
Pam3
FSL-1
R848
ns
D
Total CatX
Total Cathepsin X Fold change
E
CatX Expression
***p=0.0007
Cathepsin X expression Fold change
F
Naive
CpG
Total Cathepsin X (Immunoblot)
Actin
Ponceau
CatX
G
Total CatX
***p=0.001
Total Cathepsin X Fold change

Figure 3.2 Cathepsin X is differently regulated by TLR agonists. A. Maturation of DC1940 cells pre-treated with TLR agonists for 24 hours as shown by surface CD86 expression. **B.** Dendritic cells were pre-treated with TLR agonists for 24 hours, followed by sCy5-Nle-SY as shown by in-gel fluorescence. Cathepsin X total expression was examined by immunoblot using cathepsin X antibodies. Actin expression and ponceau stain were used as loading controls. **C. D.** Densitometry of active (35 kDa) and total cathepsin X (35 kDa) bands displayed the average intensity normalised to the naïve state (fold change). Statistics were performed using the Brown–Forsythe and Welch ANOVA tests. n=3. **E.** Quantitative PCR analysis of cathepsin X mRNA normalised to mouse GAPDH in naïve and CpG-treated DC1940 cells, reported as fold-change compared to naïve state. Statistics were performed using the unpaired Student's t-test. n=3. **F.** Primary $CD11c^+$ cells were pre-treated with CpG for 24 hours, followed by immunoblotting. Actin and ponceau stain were used as a loading control. n=3. **G.** Densitometry of total cathepsin X (35 kDa) bands displayed the average intensity normalised to the naïve state (fold change). Statistics were performed using the unpaired Student's t-test. n=3. Error bars represent SEM. ns $P > 0.05$, *$P \leqslant 0.05$, **$P \leqslant 0.01$, ***$P \leqslant 0.001$, **** $P \leqslant 0.0001$.

3.2.3 CpG treatment increased intracellular and secreted cathepsin X.

By immunofluorescence, we examined the localisation of cathepsin X in naïve and CpG-activated DCs. In agreement with the immunoblot, total cathepsin X levels were increased after maturation. In both naïve and CpG-treated cells, cathepsin X exhibited a punctate cytoplasmic distribution consistent with lysosomal localisation (**Figure 3.3A)**. We also demonstrated that cathepsin X secretion is increased upon CpG treatment (3.213-fold, p=0.0011). In both naïve and mature DCs, however, cathepsin X was secreted primarily in the zymogen form, and thus, no labelling by sCy5-Nle-SY was detected (**Figure 3.3B**). Cathepsin X remained inactive in its pro-form as it contained a disulfide bridge connecting the cysteine residue in its pro-peptide and mature peptide [49]. We subsequently acidified the conditioned media supplied with DTT to disrupt the disulphide bridge of pro-cathepsin X. The pro-cathepsin X thus became active (**Figure 3.3C**). Cathepsin S is also active in neutral pH and thus could be labelled by BMV109 at both pH (**Figure 3.3C**)[173].

We next demonstrated that the effect of CpG on active and total cathepsin X in DC1940 cells is concentration-dependent, with significant increases occurring as low as 0.04 µM and plateauing by 0.2 µM (**Figure 3.3D)**. We also investigated the timing of cathepsin X regulation by CpG. Cathepsin X was not significantly increased after 8 hours, reached maximal levels at 24 and 32 hours, and declined by 48 hours (**Figure 3.3E**).

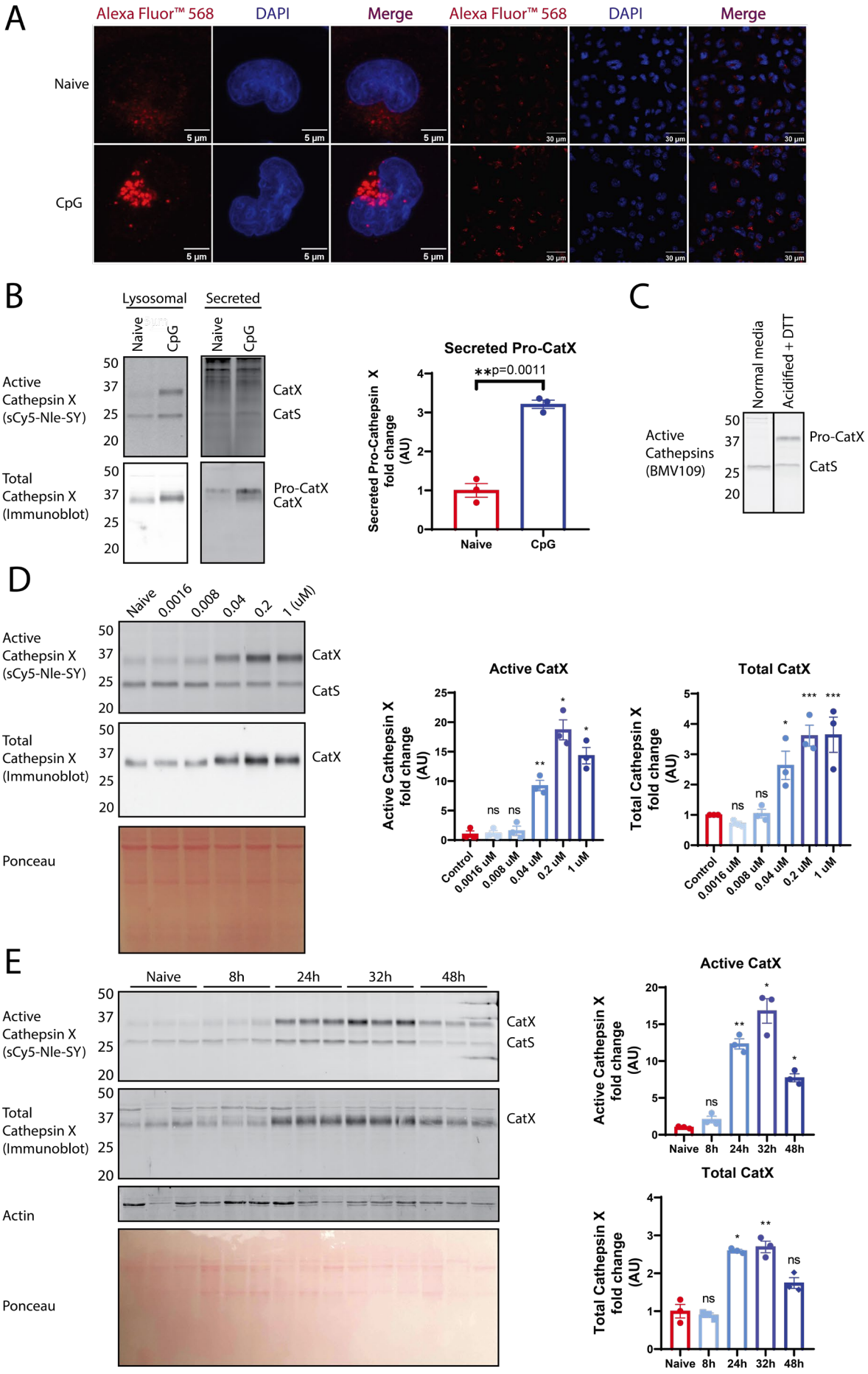
A
Alexa Fluor™ 568
DAPI
Merge
Alexa Fluor™ 568
DAPI
Merge
Naive
CpG
5 µm
30 µm
B
Lysosomal
Secreted
Naive
CpG
Naive
CpG
Active Cathepsin X (sCy5-Nle-SY)
Total Cathepsin X (Immunoblot)
50
37
25
20
CatX
CatS
Pro-CatX
CatX
Secreted Pro-CatX
**p=0.0011
Secreted Pro-Cathepsin X fold change (AU)
Naive
CpG
C
Normal media
Acidified + DTT
Active Cathepsins (BMV109)
Pro-CatX
CatS
D
Naive
0.0016
0.008
0.04
0.2
1 (uM)
Active Cathepsin X (sCy5-Nle-SY)
Total Cathepsin X (Immunoblot)
Ponceau
CatX
CatS
CatX
Active CatX
Active Cathepsin X fold change (AU)
ns
Control
0.0016 uM
0.008 uM
0.04 uM
0.2 uM
1 uM
Total CatX
Total Cathepsin X fold change (AU)
E
Naive
8h
24h
32h
48h
Active Cathepsin X (sCy5-Nle-SY)
Total Cathepsin X (Immunoblot)
Actin
Ponceau
CatX
CatS
CatX
Active CatX
Active Cathepsin X fold change (AU)
Total CatX
Total Cathepsin X fold change (AU)

Figure 3.3 Intracellular and secreted cathepsin X were increased upon CpG activation. A. Intracellular cathepsin X in naïve and CpG-treated DCs as shown by immunofluorescence. Scale bar (single cell)=5μm. Scale bar (wideview) =30μm. **B.** Comparison of intracellular and secreted cathepsin X in naïve and CpG-treated DCs as shown by in-gel fluorescence and immunoblot. Densitometry of secreted pro-cathepsin X (37 kDa) bands displayed the average intensity relative to the naïve state (fold change). Statistics were performed using unpaired Student's t-tests. n=3. **C.** Comparison of activity-labelling of normal conditioned media and acidified conditioned media (acidified with 10x citrate buffer containing 40 mM DTT) labelled by BMV109. **D.** DC1940 cells were stimulated with increasing concentrations of CpG for 24 hours, followed by sCy5-Nle-SY labelling and immunoblotting. Ponceau stain was used as a loading control**.** Densitometry of active cathepsin X (35 kDa) and total cathepsin X (35 kDa) bands displayed the average intensity relative to the naïve state (fold change). Statistics were performed using the Brown–Forsythe and Welch ANOVA tests. n=3. **E.** DC1940 cells were stimulated with CpG at different time points, followed by sCy5-Nle-SY labelling and immunoblotting. Actin expression and Ponceau stain were used as loading controls. Densitometry of active cathepsin X (35 kDa) and total cathepsin X (35 kDa) bands displayed the average intensity relative to the naïve state (fold change). Statistics were performed using the Brown–Forsythe and Welch ANOVA tests. n=3. Error bars represent SEM. ns $P > 0.05$, *$P \leqslant 0.05$, **$P \leqslant 0.01$, ***$P \leqslant 0.001$, **** $P \leqslant 0.0001$.

3.2.4 Lysosomal cysteine proteases and inhibitor cystatin C are differentially regulated in response to TLR9 activation.

We next aimed to examine whether upregulation by CpG was specific to cathepsin X or a general feature of cysteine proteases. Using a pan-cathepsin ABP BMV109, which targets cathepsin B, L, S, and X, we again observed increased levels of cathepsin X upon CpG treatment. Cathepsin S activity was significantly decreased (0.4791-fold, p=0.0001) upon maturation, and this correlated with a decrease in total cathepsin S levels (0.4143-fold, p=0.0004) (**Figure 3.4A)**. The 25 kDa band labelled by sCy5-Nle-SY was conversely increased upon CpG treatment (**Figure 3.2B**), suggesting that there may be another protease labelled by this probe that both co-migrates with cathepsin S and binds to the cathepsin S-specific inhibitor. We have not yet successfully purified this species, which has precluded definitive proteomic identification. The activities of cathepsin B and cathepsin L were lower than cathepsin X and S in DCs and were not consistently labelled by BMV109 (**Figure 3.4AB)**. By immunoblot, mature DCs showed increased pro-form (~37 kDa) and single-chain forms of cathepsin B (~30 kDa) (1.826-fold, p=0.0009 and 2.163-fold, p=0.0014, respectively) upon CpG treatment. Pro-cathepsin L (~35 kDa) and single chain cathepsin L (~27 kDa) also increased after CpG treatment (2.914-fold, p=0.0026 and =5.411-fold, p=0.0011, respectively). However, the heavy chain forms of both cathepsin B and L remained unchanged **(Figure 3.4B)**. FY01, a cathepsin C-selective probe, labelled multiple species in DCs, but we did not observe significant changes between naïve- and CpG-treated cells. Total cathepsin C levels were also unchanged (**Figure 3.4C)**. Using LE28, we measured the activity of another lysosomal cysteine protease legumain (asparaginyl endopeptidase). While legumain activity and total mature legumain remained unchanged, we observed increased pro-legumain (3.322-fold, p=0.0002, **Figure 3.4D**). Finally, we examined levels of cystatin C, an endogenous inhibitor of both cathepsins and legumain. In agreement with previous reports, cystatin C expression was strongly downregulated upon DC maturation (0.169-fold, p=0.0158, **Figure 3.4E**) [174]. Collectively, these data suggest that lysosomal cysteine proteases are differentially regulated by TLR9 agonism, with cathepsin X being the only protease exhibiting strong upregulation in both total and active levels.

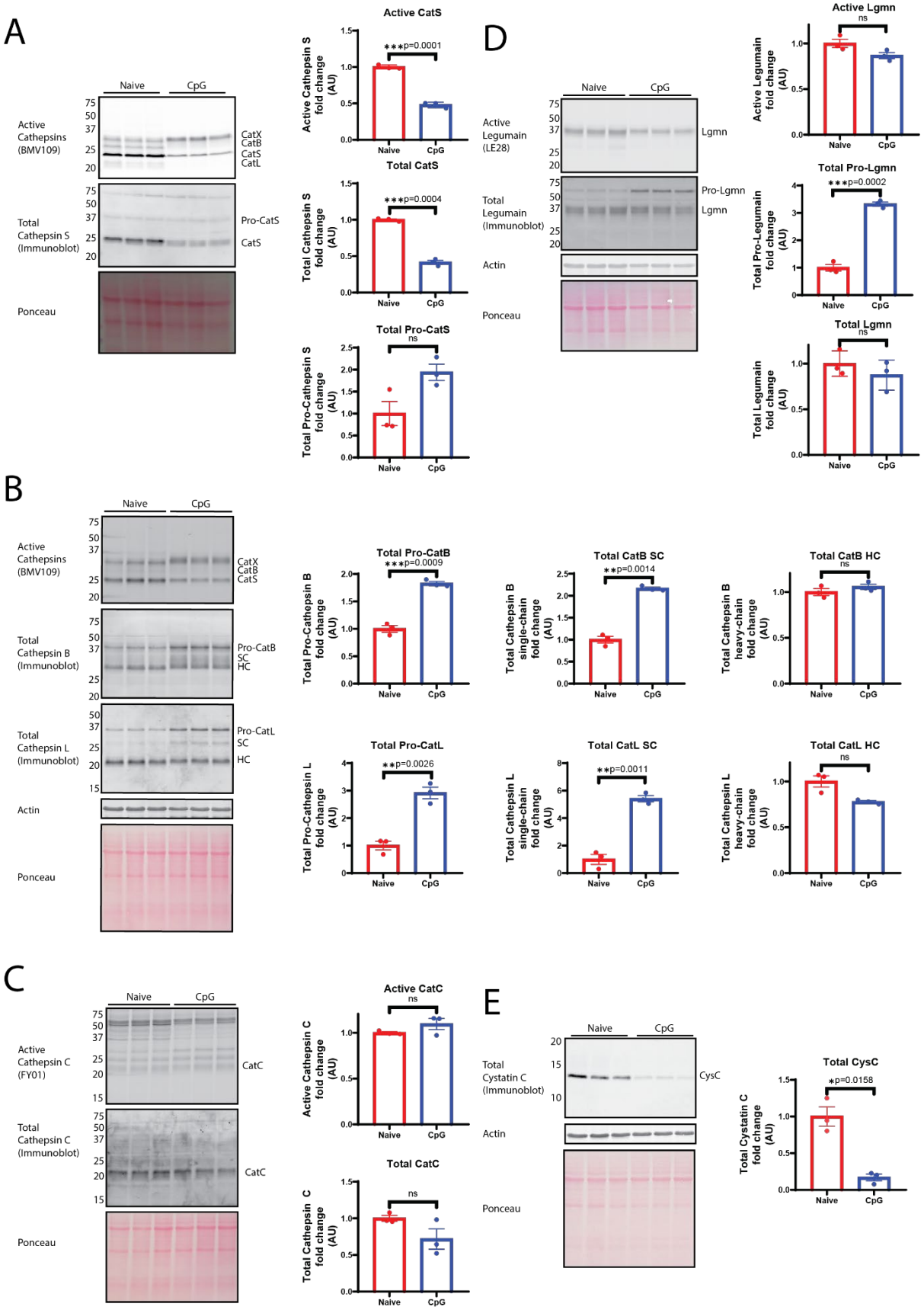
A
Naive
CpG
Active Cathepsins (BMV109)
CatX
CatB
CatS
CatL
Total Cathepsin S (Immunoblot)
Pro-CatS
CatS
Ponceau
Active CatS
***p=0.0001
Active Cathepsin S fold change (AU)
Total CatS
***p=0.0004
Total Cathepsin S fold change (AU)
Total Pro-CatS
ns
Total Pro-Cathepsin S fold change (AU)
B
Total Cathepsin B (Immunoblot)
Pro-CatB
SC
HC
Total Cathepsin L (Immunoblot)
Pro-CatL
SC
HC
Actin
Total Pro-CatB
***p=0.0009
Total Pro-Cathepsin B fold change (AU)
Total CatB SC
**p=0.0014
Total Cathepsin B single-chain fold change (AU)
Total CatB HC
ns
Total Cathepsin B heavy-chain fold change (AU)
Total Pro-CatL
**p=0.0026
Total Pro-Cathepsin L fold change (AU)
Total CatL SC
**p=0.0011
Total Cathepsin L single-chain fold change (AU)
Total CatL HC
ns
Total Cathepsin L heavy-chain fold change (AU)
C
Active Cathepsin C (FY01)
CatC
Total Cathepsin C (Immunoblot)
CatC
Ponceau
Active CatC
ns
Active Cathepsin C fold change (AU)
Total CatC
ns
Total Cathepsin C fold change (AU)
D
Active Legumain (LE28)
Lgmn
Total Legumain (Immunoblot)
Pro-Lgmn
Lgmn
Actin
Ponceau
Active Lgmn
ns
Active Legumain fold change (AU)
Total Pro-Lgmn
***p=0.0002
Total Pro-Legumain fold change (AU)
Total Lgmn
ns
Total Legumain fold change (AU)
E
Total Cystatin C (Immunoblot)
CysC
Actin
Ponceau
Total CysC
*p=0.0158
Total Cystatin C fold change (AU)

Figure 3.4. Lysosomal cysteine proteases and inhibitor cystatin C are differentially regulated in response to TLR9 activation. A. DC1940 cells were stimulated with CpG for 24 hours, followed by BMV109 labelling and cathepsin S immunoblotting. Ponceau stain was used as a loading control. Densitometry of active cathepsin S (25 kDa), pro-cathepsin S (37 kDa), and total cathepsin S (25 kDa) bands displayed the average intensity relative to the naïve state (fold change). Statistics were performed using unpaired Student's t-tests. n=3. **B.** DC1940 cells were stimulated with CpG for 24 hours, followed by BMV109 labelling and cathepsin B/L immunoblotting. Actin expression and Ponceau stain were used as loading controls. Densitometry of pro-cathepsin B/L, cathepsin B/L single chain, and cathepsin B/L heavy chain bands displayed the average intensity relative to the naïve state (fold change). Statistics were performed using unpaired Student's t-tests. n=3. **C.** DC1940 cells were stimulated with CpG for 24 hours, followed by FY01 labelling and cathepsin C immunoblotting. Ponceau stain was used as a loading control. Densitometry of active cathepsin C (21 kDa) and total cathepsin C (21 kDa) bands displayed the average intensity relative to the naïve state (fold change). Statistics were performed using unpaired Student's t-tests. n=3. **D.** DC1940 cells were stimulated with CpG for 24 hours, followed by LE28 labelling and legumain immunoblotting. Actin expression and ponceau stain were used as loading controls. Densitometry of active legumain (37 kDa), pro-legumain (60 kDa), and total legumain (37 kDa) bands displayed the average intensity relative to the naïve state (fold change). Statistics were performed using unpaired Student's t-tests. n=3. **E.** DC1940 cells were stimulated with CpG for 24 hours, followed by cystatin C immunoblotting. Actin expression and ponceau stain were used as loading controls. Densitometry of total cystatin C (13 kDa) bands displayed the average intensity relative to the naïve state (fold change). Statistics were performed using unpaired Student's t-tests. n=3. Error bars represent SEM. ns $P > 0.05$, *$P \leqslant 0.05$, **$P \leqslant 0.01$, ***$P \leqslant 0.001$, **** $P \leqslant 0.0001$.

3.2.5 Cathepsin X upregulation by CpG is IL-6 dependent.

Having demonstrated that CpG treatment leads to robust upregulation of cathepsin X transcription in dendritic cells, we next sought to determine the mechanisms that govern its expression.

Activation of TLR9 leads to the translocation of NF-κB into the nucleus, where it acts as a transcription factor to promote the expression of inflammatory genes **(Figure 1.4)**. As the cathepsin X gene promoter contains a putative NF-κB binding site [175], we queried whether cathepsin X transcription in DCs was NF-κB-dependent. We used 6-Amino-4-(4-phenoxyphenylethylamino) quinazoline to inhibit the NF-κB activation at different concentrations [176]. The NF-κB activation inhibitor reduced the secretion of IL-6 (0.71-fold, $p=0.0123$), IL-10 (0.38-fold, $p=0<0.0001$), and TNFα (0.41-fold, $p=0.0001$), indicating effective reduction in NF-κB activity **(Figure 3.5A)**.

Treatment with this inhibitor, however, did not prevent the upregulation of cathepsin X in response to CpG treatment **(Figure 3.5B)**. This suggests that NF-κB is not likely to be responsible for directly promoting cathepsin X transcription. This is in agreement with the observation that cathepsin X expression is induced at late time points (24 h; **Figure 3.3D**).

TLR9 signalling also leads to the activation of interferon regulatory factors (IRFs) and expression of Type I interferons, including IFNα and IFNβ (**Figure 1.4)**. To investigate whether type I interferons could induce upregulation of cathepsin X, we stimulated DCs with both IFNα and IFNβ. We did not, however, observe significant changes between naïve cells and cells treated with IFNα or IFNβ **(Figure 3.5C)**. Interestingly, we found that type II interferon IFNϒ prevented the upregulation of cathepsin X by CpG **(Figure 3.5D)**.

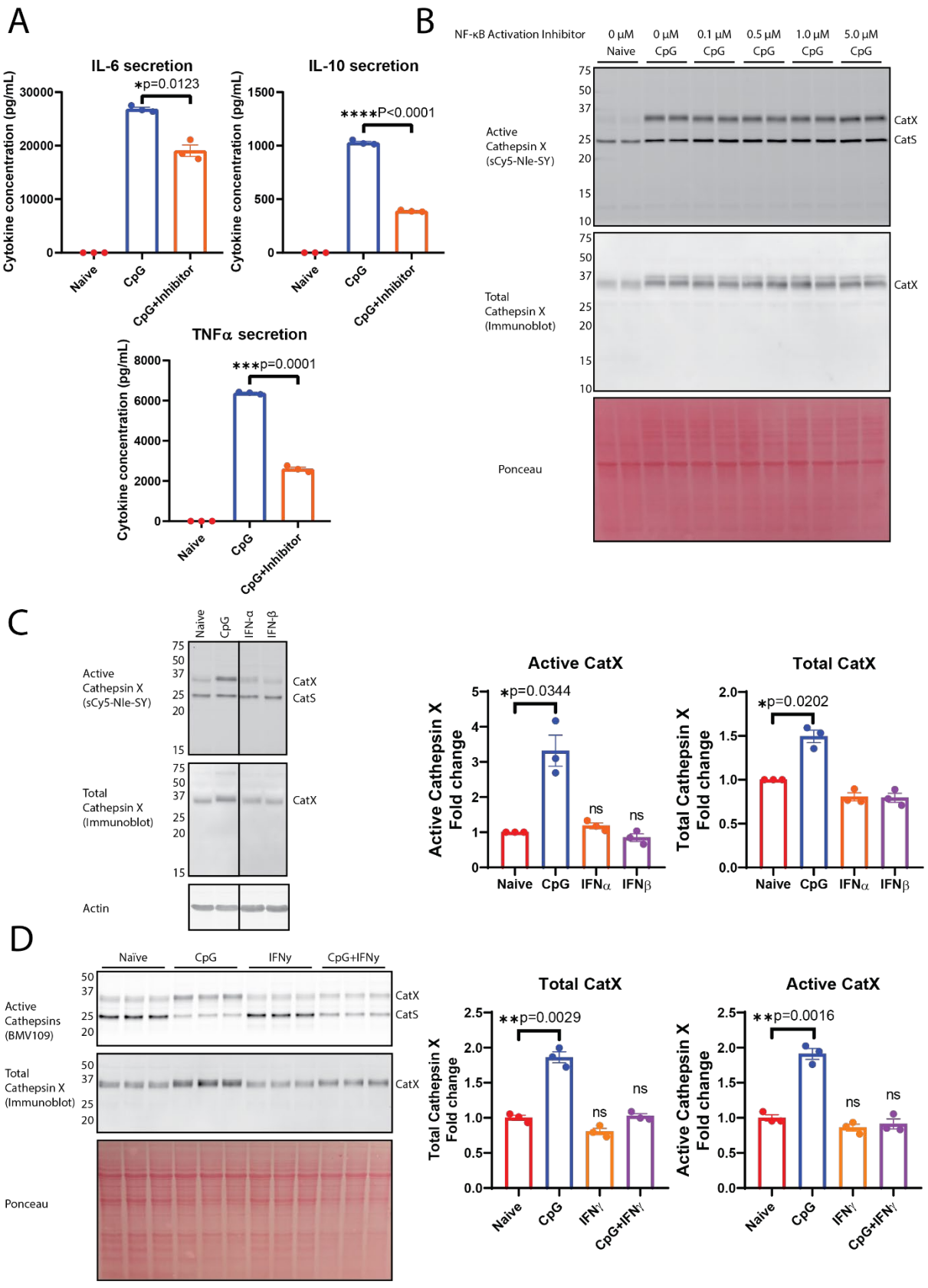
A
IL-6 secretion
*p=0.0123
Cytokine concentration (pg/mL)
30000
20000
10000
0
Naive
CpG
CpG+Inhibitor
IL-10 secretion
****P<0.0001
1500
1000
500
TNFα secretion
***p=0.0001
8000
6000
4000
2000
B
NF-κB Activation Inhibitor
0 μM Naive
0 μM CpG
0.1 μM CpG
0.5 μM CpG
1.0 μM CpG
5.0 μM CpG
Active Cathepsin X (sCy5-Nle-SY)
CatX
CatS
Total Cathepsin X (Immunoblot)
Ponceau
C
Naive
CpG
IFN-α
IFN-β
Actin
Active CatX
Total CatX
*p=0.0344
*p=0.0202
Active Cathepsin X Fold change
Total Cathepsin X Fold change
ns
IFNα
IFNβ
D
Naïve
CpG
IFNγ
CpG+IFNγ
Active Cathepsins (BMV109)
Total Cathepsin X (Immunoblot)
Ponceau
Total CatX
Active CatX
**p=0.0029
**p=0.0016
IFNγ
CpG+IFNγ

Figure 3.5 Cathepsin X upregulation was not directly governed by NF-κB activation. A. Secretion of IL-6, IL-10, and TNFα by DC1940 treated with NFκB activation inhibitor (5μM) for 4 hours cells and stimulated with CpG (0.5μM) for 24 hours. Statistics were performed using unpaired Student's t-tests. n=3. **B.** DC1940 cells were pre-treated with NFκB activation inhibitor for 4 hours, CpG (0.5μM) activation for 24 hours, and sCy5-Nle-SY labelling and cathepsin X immunoblotting. Ponceau stain was used as a loading control. **C.** DC1940 cells were pre-treated with CpG, IFN-α, or IFN-β for 24 hours, followed by sCy5-Nle-SY labelling and cathepsin X immunoblotting. Densitometry of active cathepsin X (35 kDa) and total cathepsin X (35 kDa) bands displayed as the average intensity relative to the naïve state (fold change). Statistics were performed using unpaired Student's t-tests. n=3 **D.** DC1940 cells were pre-treated with CpG, IFN-ϒ, or a combination treatment of CpG and IFN-ϒ for 24 hours, followed by sCy5-Nle-SY labelling and cathepsin X immunoblotting. Ponceau stain was used as a loading control. Densitometry of active cathepsin X (35 kDa) and total cathepsin X (35 kDa) bands displayed the average intensity relative to the naïve state (fold change). Statistics were performed using unpaired Student's t-tests. n=3. Error bars represent SEM. ns $P > 0.05$, *$P \leqslant 0.05$, **$P \leqslant 0.01$, ***$P \leqslant 0.001$, **** $P \leqslant 0.0001$.

We next hypothesised that the factors secreted by DCs during CpG-mediated maturation could be responsible for promoting cathepsin X expression. To test this hypothesis, we pulsed DCs with CpG for 3 hours and then changed the media to wash out CpG. After 24 hours, we collected the conditioned media containing secreted factors and applied it to naïve DCs for 24 hours **(Figure 3.6A)**. Active and total cathepsin X levels were significantly elevated in the cells treated with conditioned media compared to naïve cells (3.170-fold, p=0.0009 and 1.447-fold, p=0.0457, respectively) **(Figure 3.6B)**. This suggests that factors secreted from DCs downstream of CpG activation may be responsible for inducing cathepsin X expression.

Using a cytometric bead array, we quantified the major cytokines secreted by DCs during CpG-induced maturation. Upon CpG treatment for 24 hours, the conditioned media contained high levels of TNFα and IL-6 and a detectable level of IL-10 **(Figure 3.6C)**. Secretion of IFNϒ, MCP-1 and IL-12 was negligible. According to the literature, IL-10 and IL-6, as well as IL-4 and IL-13, can activate the STAT3/6 signalling pathways to upregulate the expression of several cathepsins in macrophages [21]. We tested whether IL-4, IL-6, and IL-10 could similarly affect cathepsin X expression in DCs. Treatment with IL-6, but not IL-4 or IL-10, significantly increased the active and total level of cathepsin X (2.439-fold, p=0.0002 and 1.736-fold, p=0.0383) (**Figure 3.6DE)**. We further validated this by quantitative PCR, demonstrating that IL-6 could provoke cathepsin X mRNA expression in a time-dependent manner, with a significant increase observed starting from the 8-hour time point (1.451-fold, p=0.0014) through to 24-hour post-treatment (2.285-fold, p=0.0002) **(Figure 3.6F)**. Secretion of IL-6 post-CpG stimulation was increased at 4 hours post-CpG administration and peaked at 8 hours post-CpG administration **(Figure 3.6G)**, suggesting that IL-6 secretion precedes cathepsin X upregulation. As Poly I:C treatment did not elicit a robust increase in cathepsin X level (**Figure 3.2B**), we compared the level of IL-6 secretion between CpG-treated DCs and Poly I:C treated DCs and found that CpG-activated DCs secreted significantly more IL-6 compared to Poly I:C treated DCs (20.120-fold, p=0.0080) **(Figure 3.6H)**.

CpG activation also increased the level of pro-cathepsin B and cathepsin B single chain but decreased the level of cathepsin S and cystatin C. We further questioned whether IL-6 is responsible for mediating these. We found that treating DCs with IL-6 increased the level of cathepsin S, pro-cathepsin B, cathepsin B single chain, and cathepsin B heavy chain. The level of cystatin C remained unchanged upon IL-6 treatment (**Figure 3.6I**). In addition, IL-6 and IL-

10 co-treatment further increased the level of total cathepsin S (1.45-fold, p=0.0147). However, IL-10 treatment alone did not significantly change the level of cathepsin B, S, or cystatin C (**Figure 3.6I**).

Overall, these results suggest that IL-6 is at least partially responsible for mediating the increase in cathepsin X expression during TLR9-induced DC maturation.

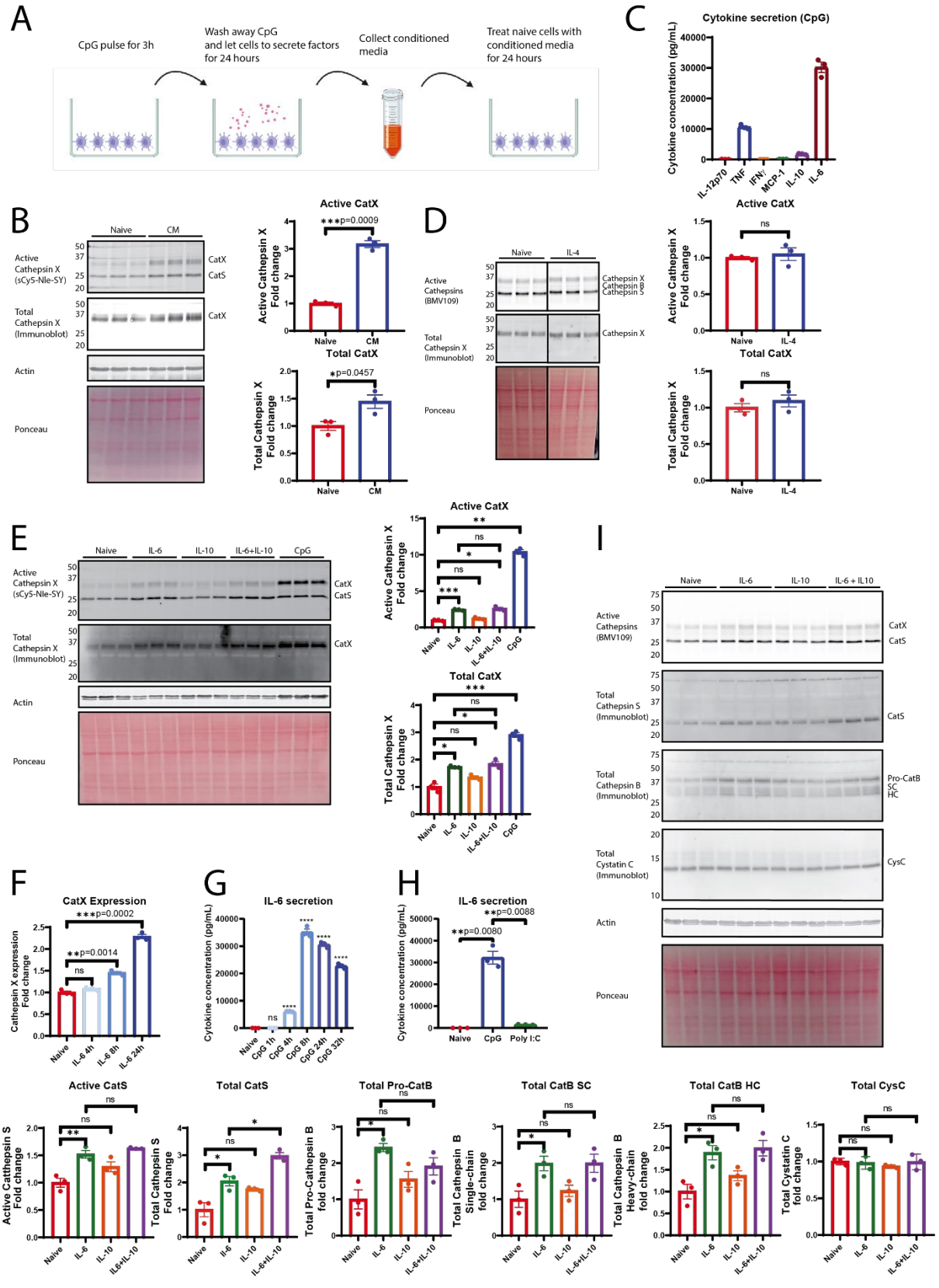
A
CpG pulse for 3h
Wash away CpG and let cells to secrete factors for 24 hours
Collect conditioned media
Treat naive cells with conditioned media for 24 hours
C
Cytokine secretion (CpG)
Cytokine concentration (pg/mL)
IL-12p70
TNF
IFNγ
MCP-1
IL-10
IL-6
B
Naive
CM
Active Cathepsin X (sCy5-Nle-SY)
Total Cathepsin X (Immunoblot)
Actin
Ponceau
CatX
CatS
Active CatX
***p=0.0009
Active Cathepsin X Fold change
Total CatX
*p=0.0457
Total Cathepsin X Fold change
D
Naive
IL-4
Active Cathepsins (BMV109)
Cathepsin X
Cathepsin B
Cathepsin S
Total Cathepsin X (Immunoblot)
Ponceau
ns
E
Naive
IL-6
IL-10
IL-6+IL-10
CpG
I
IL-6 + IL10
Total Cathepsin S (Immunoblot)
Total Cathepsin B (Immunoblot)
Pro-CatB
SC
HC
Total Cystatin C (Immunoblot)
CysC
F
CatX Expression
***p=0.0002
**p=0.0014
Cathepsin X expression Fold change
IL-6 4h
IL-6 8h
IL-6 24h
G
IL-6 secretion
Cytokine concentration (pg/mL)
CpG 1h
CpG 4h
CpG 8h
CpG 24h
CpG 32h
H
IL-6 secretion
**p=0.0088
**p=0.0080
Poly I:C
Active CatS
Total CatS
Total Pro-CatB
Total CatB SC
Total CatB HC
Total CysC
Active Cathepsin S Fold change
Total Cathepsin S Fold change
Total Pro-Cathepsin B fold change
Total Cathepsin B Single-chain fold change
Total Cathepsin B Heavy-chain fold change
Total Cystatin C fold change

Figure 3.6 Cathepsin X upregulation by CpG is IL-6 dependent. A. Naïve DC1940 cells were treated with CpG for 3 hours, and the CpG was subsequently washed away. Cells were left in fresh media to secrete factors for 24 hours. Conditioned media was collected and applied to new naïve DC1940 cells for a further 24 hours. **B.** DC1940 cells were pre-treated with conditioned media for 24 hours, followed by sCy5-Nle-SY and cathepsin X immunoblotting. Actin expression and Ponceau stain were used as loading controls. Densitometry of active and total cathepsin X bands displayed the average intensity relative to the naïve state (fold change). Statistics were performed using unpaired Student's t-tests. n=3. **C.** DC1940 cells were pre-treated with CpG for 24 hours. The concentration of IL-12 p70, TNFα, IFN-ϒ, MCP-1, IL-10, and IL-6 in the conditioned media was analysed with the BD® Cytometric Bead Array. **D.** DC1940 cells were pre-treated with IL-4 for 24 hours, followed by sCy5-Nle-SY and cathepsin X immunoblotting. Ponceau stain was used as a loading control. Densitometry of active and total cathepsin X bands displayed the average intensity relative to the naïve state (fold change). Statistics were performed using unpaired Student's t-tests. n=3. **E.** DC1940 cells pre-treated with IL-6, IL-10, CpG, or a combination treatment of IL-6 and IL-10 for 24 hours, followed by sCy5-Nle-SY and cathepsin X immunoblotting. Actin expression and Ponceau stain were used as loading controls. Densitometry of active and total cathepsin X (35 kDa) bands displayed the average intensity relative to the naïve state (fold change). Statistics were performed using unpaired Student's t-tests. n=3. **F.** Quantitative PCR analysis of cathepsin X mRNA normalised to mouse GAPDH in naïve, and IL-6 treated DC1940 cells at different time points, reported as fold-change compared to the naïve state. Statistics were performed using unpaired Student's t-tests. n=3. **G.** Secretion of IL-6 by DC1940 cells stimulated with CpG at different lengths. Statistics were performed using the Brown–Forsythe and Welch ANOVA tests. n=3. **H.** Secretion of IL-6 by DC1940 cells stimulated with CpG or Poly I:C for 24 hours. Statistics were performed using the unpaired Student's t-test. n=3. **I.** DC1940 cells were pre-treated with IL-6, IL-10, or a combination treatment of IL-6 and IL-10 for 24 hours, followed by BMV109 labelling, cathepsin B, S and cystatin C immunoblotting. Actin expression and Ponceau stain were used as loading controls. Densitometry of active and total cathepsin S (25 kDa), pro-cathepsin B (38 kDa), single-chain (32 kDa), heavy chain (29 kDa), and cystatin C (13 kDa) bands displayed the average intensity relative to the naïve state (fold change). Statistics were performed using unpaired Student's t-tests. n=3. The error bar represents SEM. ns $P > 0.05$, *$P \leqslant 0.05$, **$P \leqslant 0.01$, ***$P \leqslant 0.001$, **** $P \leqslant 0.0001$.

3.3 Discussion

In this chapter, we applied the cathepsin X-specific activity-based probe sCy5-Nle-SY to DC1940 dendritic cells. When applying the probe in acidified cell lysate, we showed that the sCy5-Nle-SY had a high specificity towards cathepsin X. By live cell labelling, we confirmed that sCy5-Nle-SY labels both cathepsin X and cathepsin S. The identity of the band representing cathepsin S was validated with immunoprecipitation and a cathepsin S inhibitor MDV590. It remained a question of why the probe labels cathepsin S in the live cell condition. Our current hypothesis is due to cell compartmentalisation. Some evidence suggests that different lysosomal cathepsins are located in different lysosomes [177]. Therefore, the probe may first enter the cells' compartments with a higher level of cathepsin S and lower cathepsin X. As a result, the probe was forced to bind with cathepsin S. This needs further investigation with cell compartment markers and confocal microscopy.

Next, we stimulated DC1940 cells with multiple TLR agonists. DC1940 cells were readily activated by Poly I:C, CpG, Pam3 and FSL-1, partially activated by LPS and did not respond to R848. Cathepsin X active and total levels were significantly elevated when DC matured, especially upon CpG activation. In primary splenic cD11c^{+} dendritic cells, we also observed a significant increase in cathepsin X total level post-CpG treatment. However, the sCy5-Nle-SY probe did not label active cathepsin X well in living primary cells. We speculated that the primary cells were stressed when culturing in vitro and were not actively taking up the probe (data not shown).

We subsequently conducted confocal microscopy looking at the intracellular staining of cathepsin X. Cathepsin X exhibited a typical lysosomal punctate staining, indicating its potential localisation. However, this needs to be further confirmed with co-stain with lysosomal markers (e.g., LysoTracker) in future experiments. Similarly, we observed an increased cathepsin X staining intensity in cells treated with CpG. However, we did not see a noticeable difference in localisation in Naïve and CpG-treated cells. It would be interesting to incorporate the sCy5-Nle-SY into microscopy to investigate the localisation of active cathepsin X. The specificity of the probe can be improved by applying a cathepsin S inhibitor MDV590. Applying an endolysosomal marker may give us more insight into the trafficking and activation of cathepsin X in general or CpG-mediated DC maturation.

Our data also showed that the secreted cathepsin X was significantly increased in CpG-matured DCs. The secreted cathepsin X could not be labelled with activity-based probes in neutral pH. By immunoblot, the secreted cathepsin X had a higher molecular weight than the intracellular lysosomal cathepsin X. We proposed that cathepsin X was mainly secreted in its proform which is in agreement with the study from Dongyao et al. [21]. Pro-cathepsin X contains a pro-peptide sequence, and a disulphide bridge links a cysteine in the pro-peptide sequence to the active site cysteine. We tried to add DTT to acidified conditioned media to disrupt the disulphide linkage and make an optimal pH environment for cathepsin X activity, followed by administering pan cathepsin probe BMV109. In this condition, we could make the secreted cathepsin X active and able to be labelled by the probe (**Figure 3.3C**). This further validated that the secreted cathepsin X was in its proform. Whether secreted cathepsin X has extracellular substrates is not fully elucidated. Cathepsin X requires an acidic environment to be active and may not cleave its substrates in normal physiological conditions. However, in the context of an acidic cancer microenvironment, other secreted lysosomal proteases may autoactivate and activate pro-cathepsin X. Subsequently, cathepsin X may cleave some extracellular substrates and play a role in disease progression. Alternatively, the pro-peptide sequence of cathepsin X contains an RGD motif that may be more relevant in normal physiological conditions. The RGD motif can bind to β2 integrin receptors to promote cell proliferation and to α5 integrin receptors to facilitate NLRP3 inflammasome activation [48, 64]. Whether or not the RGD motif has a role in the DC function needs further validation.

Another critical question is how cathepsin X was secreted. Cathepsin X contains two glycosylation sites, which may play a role in its mannose 6-dependent trafficking. A disruption of the mannose 6-phosphate tagging may result in the mislocalisation of lysosomal proteases, making them secreted instead of transported to the lysosomes [23]. Investigating and comparing intracellular and secreted cathepsin X glycosylation status using mass spectrometry techniques will be necessary.

We were surprised that the extent of cathepsin upregulation was not proportional to DC maturation status. CpG, Pam3, FSL-1 and Poly I:C all stimulated DC1940 cells to a similar extent; however, we only detected a minor increase in cathepsin X active level and total level in Poly I:C treated cells. We hypothesise that the discrepancy in cathepsin X expression was due to differences in downstream signalling nodes in different TLR agonists. In TLR1/2 (Pam3), TLR

2/6 (FSL-1), and TLR 9 (CpG) receptors, upon engaging with their specific TLR agonists, MyD88 adaptor protein was recruited in the signalling pathway. By contrast, in TLR 3 (Poly I:C) mediated signalling, a different adaptor protein, TRIF, was recruited [82]. MyD88 and TRIF-dependent signalling pathways ultimately activate two transcription factors: the NF-κB and the interferon regulatory factors (IRFs). MyD88-dependent signalling cascade is inclined to NF-κB activation and, subsequently, the induction of pro-inflammatory genes such as interleukins. Interleukins activate the STAT3 transcription factor to induce cathepsin expression. On the other hand, the TRIF-dependent pathway is more closely related to the IRF activation and triggers the expression of type I interferons (e.g., IFNβ) [178]. We speculated that the differences between the two signalling cascades might cause the differences in cathepsin X regulation and may infer their biological relevance.

TLR3 and TLR9 recognise different types of pathogen-related patterns. TLR3 primarily detects viral dsRNA, often resulting from intermediate viral replication in infected host cells [179]. On the other hand, TLR9 recognises CpG motifs commonly found in bacterial and viral DNA. When DCs encounter bacterial or viral DNA recognised by TLR9, it may signify the presence of an invading pathogen-like bacteria. In response, DCs may upregulate lysosomal proteases, including cathepsin X, to facilitate the degradation of the invading pathogen and the presentation of antigens to the T cells. TLR3, on the other hand, recognises viral dsRNA, which is generated during viral replication [179]. Some evidence suggests that mRNA released by infected/necrotic cells can be endocytosed to activate TLR3 signalling [180, 181]. In this case, the host cells do not require the same upregulation of lysosomal proteases. The immune response is finely tuned to differentiate different infection situations to avoid excessive protease expression, which may cause further damage to cellular biology.

We next proposed a potential mechanism that explains the upregulation of cathepsin X during CpG-mediated DC maturation. We noticed that the upregulation of cathepsin X occurred late, starting from 24 hours-post CpG stimulation. The actin levels were variable across the samples as the morphology of DCs would change during maturation. Therefore, the measuring of protein loading was best to be accompanied by the ponceau stain. The second naïve sample showed a low actin level, and we believed this was probably due to insufficient antibody staining during western blot incubation, as the ponceau stain showed a similar total protein level compared to other related samples.

The secretion of cytokines happened at a much earlier time point. We demonstrated that IL-6 secretion occurred as early as 4 hours post-CpG treatment (**Figure 3.6G**). IL-6 expression is directly governed by the NF-κB activation. If the same NF-κB activation also controlled cathepsin X upregulation, we would expect to see increased expression at earlier time points. As a result, we speculated that the upregulation of cathepsin X was not directly related to CpG-mediated NF-κB activation but to other post-maturation mechanisms. We validated this hypothesis using an NF-κB inhibitor. When treating the DC1940 cells with the NF-κB inhibitor and CpG, we found the DCs still upregulate cathepsin X active/total level to the same extent as CpG-only treated cells. Inspired by Dongyao et al., who showed that inflammatory cytokines led to increased expression of multiple lysosomal proteases through STAT3 and STAT6-dependent pathways, we hypothesised that the inflammatory cytokines secreted during DC maturation might play a role in regulating the expression of cathepsin X [21].

We first designed an experiment and showed that cathepsin X activity/total expression could be increased independently of direct CpG activation: we first treated DCs with CpG for a short period and washed away all the residue CpG with fresh DC media. The activated cells were left in fresh media overnight to secrete inflammatory factors. Using conditioned media containing secreted factors (cytokines/chemokines) from CpG-activated cells to treat naïve cells, we were able to increase the active/total level of cathepsin X. This indicates that the increased expression of cathepsin X was at least partially promoted by secreted factors. We subsequently treated naïve DC1940 cells with various inflammatory cytokines, including IL-4, IL-6, and IL-10, which have been reported to activate the STAT3 and STAT6 transcription factors to increase the expression of several lysosomal proteases. Cathepsin X active/total level was only increased by IL-6 but not IL-4 or IL-10. We further validated this by quantitative PCR and showed IL-6 treatment increased the mRNA level of cathepsin X, showing the IL-6-STAT3 pathway regulated the expression of cathepsin X. We also stimulated the naïve cells with type I interferons, including IFNα and IFNβ which were induced by the other TRIF-IRFs dependent arm of TLR signalling and showed the level of active/total cathepsin X remained unchanged.

The results supported our hypothesis that cathepsin X upregulation was not due to a direct CpG-mediated signalling pathway but rather the subsequent IL-6 secreted by CpG-activated DCs. This may also explain why we did not see a robust increase in cathepsin X active/total level in Poly I:C treated DCs. DCs stimulated with TLR3 (Poly I:C) had a distinct TLR signalling

pathway favouring Type I interferon expression [178]. We quantified IL-6 secretion in the context of Poly I:C induction, and we found that the level of IL-6 secretion was significantly lower than CpG-activated DCs.

In an in vivo context, it is essential to note that IL-6 can be secreted by various cell types when they encounter infections. This includes immune cells, which respond to pathogen components by activating TLRs [82]. Stromal cells, in addition to immune cells, can also produce IL-6 by activating TLR2, TLR4, or NOD2 [182]. The secretion of IL-6 by this diverse range of cells may have a pivotal role in orchestrating the regulation of lysosomal proteases, which may have further critical roles in processes like antigen processing and presentation in immune cells.

In addition to cathepsin X, we investigated the active and total levels of other lysosomal proteases in CpG-mediated DC maturation. We used a pan-cysteine cathepsin probe BMV109 to look at the active level of cathepsin B, L, S, and X. We observed inconsistencies in the labelling of cathepsin B and L between experiments; however, when they were observed, they were always labelled at much lower levels than cathepsin X and S. By immunoblotting, we found that the proform and the intermediate (single chain) forms of cathepsin B and L were significantly elevated. In contrast, the mature double chain forms of cathepsin B and L were unchanged. Using BMV109, we found that the activity level of cathepsin S was reduced while sCy5-Nle-SY showed a slight increase in the activity level. We further investigated this using cathepsin S immunoblot and showed that the level of mature cathepsin S was decreased. We still could not explain why active cathepsin S was increased using sCy5-Nle-SY labelling. We speculate that the 25 kDa labelled by sCy5-Nle-SY was not solely cathepsin S but also a different protease with a similar molecular weight and could be inhibited by the cathepsin S inhibitor MDV590. Alternatively, the two probes may traffic to different compartments within the cells. This needs further investigation by pulling down the labelled proteases and analysis with mass spectrometry.

Similarly, the legumain proform significantly increased while its mature form remained constant. This result indicated that cathepsin X was not the only lysosomal protease increasingly expressed in CpG activation. Cathepsin B/L and legumain were upregulated mainly in their proforms and intermediate forms. We may see more mature forms when leaving cells long enough in culture as the proform and intermediate forms get processed into

the final form. IL-6 24-hour treatment increased the heavy-chain form of cathepsin B (**Figure 3.6I**), while CpG 24-hour treatment did not (**Figure 3.4B**). We hypothesise that the cells needed time to respond to CpG to secrete IL-6. While direct IL-6 treatment readily activated the STAT3 signalling, the cells had more time to process pro-cathepsin B and cathepsin B single chain to the heavy chain.

We also notice a reduction in the level of cathepsin S and cystatin C during CpG activation. IL-10 is an inhibitory cytokine secreted during DC maturation and has been reported to induce the downregulation of cathepsin S and cystatin C [174, 183]. Therefore, we questioned if IL-10 was responsible for the reduction of cathepsin S and cystatin C in DC1940 cells during CpG activation. Chan and colleagues showed that the administration of IL-10 blunted the IFN-ϒ induced cathepsin S upregulation in macrophages [183]. Our results suggested that IL-10 treatment alone did not change the basal level of cathepsin S. However, co-treating cells with IL-10 and IL-6 further increased the level of mature cathepsin S (**Figure 3.6I**). Indicating IL-10 may have some synergistic role in increasing cathepsin S expression with IL-6. This discrepancy may be due to different cell types (macrophages vs dendritic cells) and stimuli (IFN-ϒ vs CpG).

In addition, treating DC1940 cells with IL-10 did not reduce the level of cystatin C, which was inconsistent with the work from Xu and colleagues [174]. Xu and colleagues treated cells with IL-10 at a concentration of 50 ng/mL, which is higher than we did (20 ng/mL) and may explain the discrepancy. However, the DC1940 cells only secreted IL-10 at a concentration of ~1,000 pg/mL after CpG activation (**Figure 3.6C**). Therefore, we doubt if such a high concentration was biologically relevant in DC1940 cells. Thus, the downregulation of cathepsin S and cystatin C during CpG activation seemed not related to IL-6 or IL-10 in DC1940 cells.

Overall, the increased level of multiple proteases in DC maturation suggests that these proteases may have a role in DC function.

Chapter 4. Investigating the function of cathepsin X in dendritic cell immunity

4.1 Introduction

The previous chapter showed that intracellular and secreted cathepsin X were significantly upregulated during DC maturation, especially upon CpG activation. Most related lysosomal proteases/cathepsins also showed an increased level of their pro-forms upon CpG activation except cathepsin S. We further found that the upregulation of cathepsin X was not due to direct CpG-mediated TLR9 signalling. We proposed that upon CpG-mediated maturation, dendritic cells started to secrete IL-6, activating the STAT3 signalling pathway and causing the upregulation of cathepsin X. In contrast, Poly I:C mediated DC maturation did not elicit a profound secretion of IL-6 and, therefore, did not increase the level of cathepsin X.

As cathepsin X was significantly upregulated during CpG-mediated DC maturation, we hypothesised that cathepsin X was needed for DC function.

Lysosomal proteases are reported to be involved with immune cell maturation. Legumain, cathepsin B, and cathepsin L are all involved with TLR9-mediated cell maturation [184, 185]. Legumain cleaves the TLR9 receptor in mDCs and pDCs to activate the TLR receptor. Cathepsin B and L inhibition resulted in a downregulation of cell maturation in B cells under TLR9 stimulation. However, inhibiting one lysosomal protease does not entirely block the TLR9 signalling, indicating that the activation of the TLR9 receptor is highly redundant. There might be multiple proteases able to cleave and activate TLR9 receptor signalling. Cathepsin X is also linked to pDC maturation by cleaving and subsequently activating Mac-1 [3]. Inhibition of cathepsin X decreased pDC surface marker expression, cell migration/adhesion, and cytokine secretion.

Dendritic cells are antigen-presenting cells. They serve as the bridge between the innate and the adaptive immune system. Naïve dendritic cells scavenge exogenous antigens and engulf them. Cathepsin X was thought to play a role in clathrin-mediated endocytosis through cleaving profilin 1 in human prostate cancer cells [53]. Upon endocytosing exogenous antigens, lysosomal proteases participate in the degradation of antigens [11]. The resulting peptides are presented to T cells for further immune activities. Lysosomal proteases are heavily involved in

antigen-presentation. Cathepsin L, S and legumain all have been reported to mature the MHC-II complex [69, 126].

Activated DCs also exhibited increased expression and secretion of inflammatory cytokines to regulate immunity. Proteases are well-known for their regulation of cytokines. Some proteases are involved in the activation of cytokines. For example, caspase-1 cleaves and activates IL-1β in the context of inflammasome activation [129, 130]. Cathepsin X also has a role in inflammatory cytokine regulation. As mentioned above, cathepsin X regulates pDC maturation; hence, lack of cathepsin X impairs the secretion of TNFα, IL-10 and IL-12 [3]. In addition, secreted cathepsin X regulates the secretion of IL-1β that is irrelevant to cell maturation through RGD/α5-integrin interaction [30, 64].

In this chapter, we analysed the impact of cathepsin X deficiency on DC maturation, antigen uptake, antigen presentation and cytokine secretion. Furthermore, shotgun proteomics was implemented to broadly investigate the impact of cathepsin X deficiency on DC biology.

4.2 Results

4.2.1 Generating cathepsin X deficient cells using CRISPR-Cas9

Having demonstrated that cathepsin X was upregulated during DC maturation, we aimed to interrogate its contribution to DC function, including maturation, antigen uptake, antigen presentation and cytokine secretion.

We generated cathepsin X-deficient cells with CRISPR-Cas9. DC1940 cells stably expressing Cas9 were transduced with an inducible CFP-FGH1t lentiviral vector containing a guide RNA targeted to the first exon of *Ctsz*. Successfully transduced cells expressing CFP were sorted, and knockout of cathepsin X was induced by the administration of doxycycline (**Figure 4.1A**). Control cells were similarly transduced with a vector containing the human hBIM (Bcl-2-like 11) specific guide RNA, which does not target the murine genome.

Knockout efficiency was assessed by analysing cathepsin X activity with the sCy5-Nle-SY ABP and immunoblotting with a cathepsin X-specific antibody. Compared to hBIM control cells, the Ctsz-targeted cells exhibited a significant loss of cathepsin activity and expression, while the cathepsin S activity was unchanged (**Figure 4.1B)**.

A

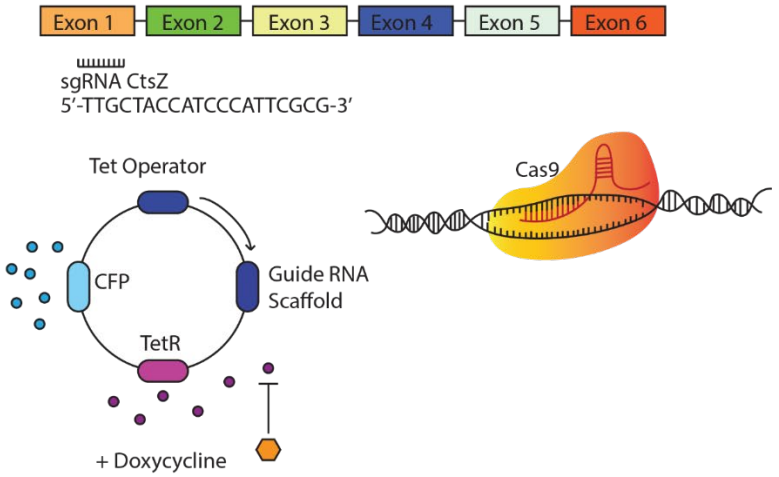

B

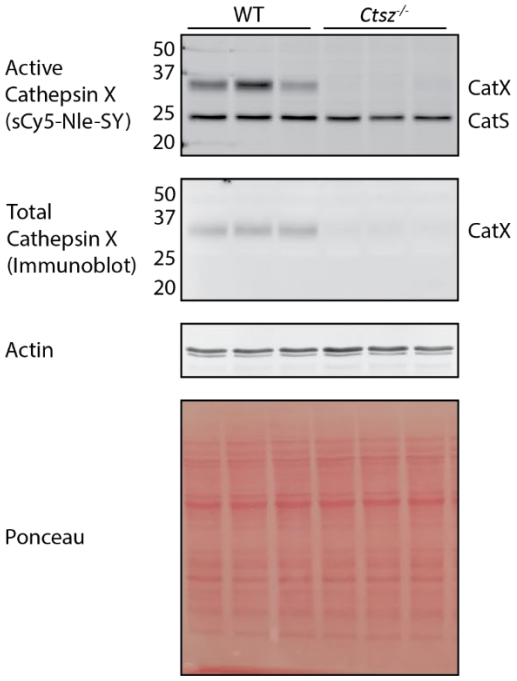

Figure 4.1 Generating cathepsin X deficient DCs with CRISPR-Cas9. A. Schematic diagram of CRISPR-Cas9 design. The guide RNA was designed to target the first exon of *Ctsz*. Successfully transfected cells expressed CFP fluorophore and were sorted and selected by flow cytometry. The expression of the guide RNA was induced by adding doxycycline. **B.** WT and cathepsin X-deficient Mutu DC1940 dendritic cells were labelled with sCy5-Nle-SY. Cells were then lysed and analysed by SDS-PAGE in-gel fluorescence. Total Intracellular cathepsin X was examined by immunoblot using cathepsin X antibody. Actin expression and Ponceau stain were used as loading controls.

4.2.2 Cathepsin X deficient cells mature normally upon CpG activation

Cathepsin X has previously been reported to have a role in pDC maturation [3], where maturation-related surface markers decreased upon cathepsin X inhibition, including CD86 and MHC-II.

To determine whether cathepsin X functions similarly in cDCs (DC1940 cells), we compared the surface expression of four receptors known to be elevated during DC maturation in wild-type and *Ctsz*$^{-/-}$ cells. Surface expression of CD40, CD86, MHC-I and MHC-II was identical between the two cell lines (**Figure 4.2A-D**), indicating the loss of cathepsin X did not impact DC maturation.

We further investigated the impact of cathepsin X deficiency on DC maturation on different TLR agonists. Consistent with **Figure 3.2A**, DC1940 cells responded well towards CpG, Poly I:C, Pam3 and FSL-1. DC1940 cells responded partially upon LPS activation and did not respond to the R848 agonist (**Figure 4.2 E-J)**. We found that cathepsin X deficiency did not alter DC maturation upon CpG, Poly I:C, Pam3 and FSL-1 agonists. However, cathepsin X deficient cells showed an impaired maturation upon LPS stimulation, which aligned with Obermajer et al. [3] (**Figure 4.2F**).

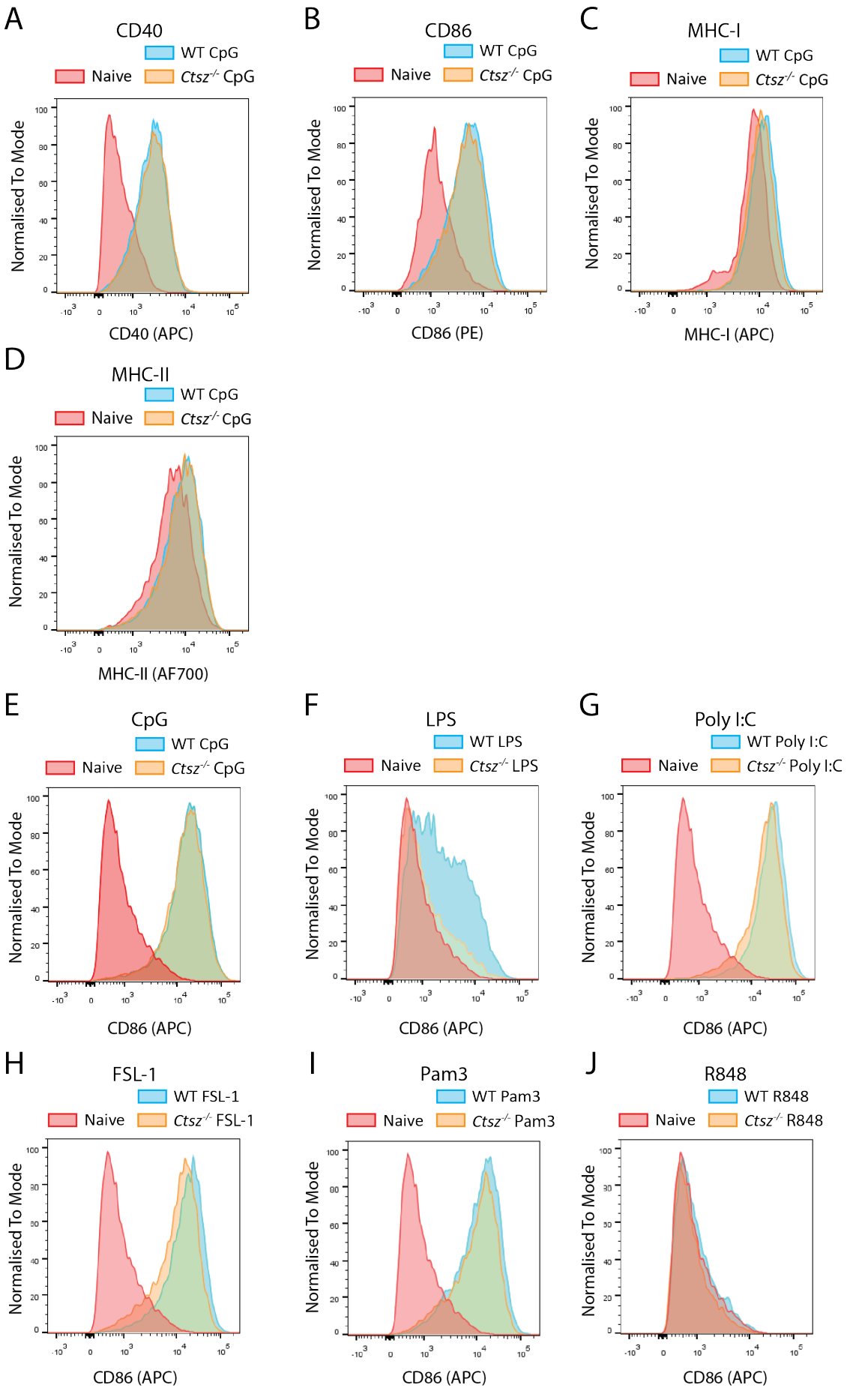
A
CD40
WT CpG
Naive
Ctsz-/- CpG
Normalised To Mode
CD40 (APC)
B
CD86
WT CpG
Naive
Ctsz-/- CpG
Normalised To Mode
CD86 (PE)
C
MHC-I
WT CpG
Naive
Ctsz-/- CpG
Normalised To Mode
MHC-I (APC)
D
MHC-II
WT CpG
Naive
Ctsz-/- CpG
Normalised To Mode
MHC-II (AF700)
E
CpG
WT CpG
Naive
Ctsz-/- CpG
Normalised To Mode
CD86 (APC)
F
LPS
WT LPS
Naive
Ctsz-/- LPS
Normalised To Mode
CD86 (APC)
G
Poly I:C
WT Poly I:C
Naive
Ctsz-/- Poly I:C
Normalised To Mode
CD86 (APC)
H
FSL-1
WT FSL-1
Naive
Ctsz-/- FSL-1
Normalised To Mode
CD86 (APC)
I
Pam3
WT Pam3
Naive
Ctsz-/- Pam3
Normalised To Mode
CD86 (APC)
J
R848
WT R848
Naive
Ctsz-/- R848
Normalised To Mode
CD86 (APC)

Figure 4.2 Surface expression of DC maturation markers of WT and cathepsin X deficient cells. A-D. DC1940 cells were treated with CpG for 24 hours, followed by the flow cytometry analysis of DC surface markers CD40, CD80, MHC-I and MHC-II, respectively. **E-J.** DC1940 cells were treated with CpG, LPS, Poly I:C, FSL-1, Pam3 or R848 for 24 hours, followed by the flow cytometry analysis of the CD86 surface marker.

4.2.3 Cathepsin X deficiency did not alter the endocytosis of exogenous antigens.

Cathepsin X has been previously described to cleave profilin and may have a role in modulating clathrin-mediated endocytosis [53]. Endocytosis of antigens is the first crucial step in DC immunity, as exogenous antigens need to be engulfed by DCs into the endolysosomal compartment and subsequently processed into antigenic fragments for antigen presentation. We, therefore, investigated the contribution of cathepsin X to the endocytosis of exogenous antigens.

We first used a small molecule dye, Lucifer Yellow, to examine its effects on liquid-phase endocytosis. Lucifer Yellow (LY) has a molecular weight of only 521.57 g/mol and is up taken by non-specific endocytosis. We incubated the dye with WT and *Ctsz*$^{-/-}$ DCs at 37°C or on ice as the control. At 37°C, the cells readily took up the dye, as indicated by punctate intracellular staining. No intracellular dye was observed after incubation on ice, reflecting suppression of endocytosis **(Figure 4.3A)**. When dye intensity was normalised to cell number, we observed no significant differences in dye uptake between WT and *Ctsz*$^{-/-}$ cells **(Figure 4.3B)**.

We also examined if cathepsin X deficiency had an impact on macropinocytosis. Fluorescently labelled OVA has been widely used as a standard tool for studying macropinocytosis, although OVA can also be endocytosed via mannose receptor-mediated endocytosis [186-188]. Macropinocytosis is often described as "cell drinking". DCs non-specifically uptake exogenous soluble proteins or antigens constitutively through this route and is a major mechanism of antigen uptake. We incubated OVA-Cy5 with WT and *Ctsz*$^{-/-}$ DCs at 37°C or on ice as a control. When incubated on ice, the uptake of OVA-Cy5 was negligible **(Figure 4.3CD)**. At physiological temperature, WT and *Ctsz*$^{-/-}$ cells exhibited no significant differences in fluorescence intensity **(Figure 4.3CD)**, suggesting that cathepsin X deficiency does not significantly impact macropinocytosis or antigen uptake.

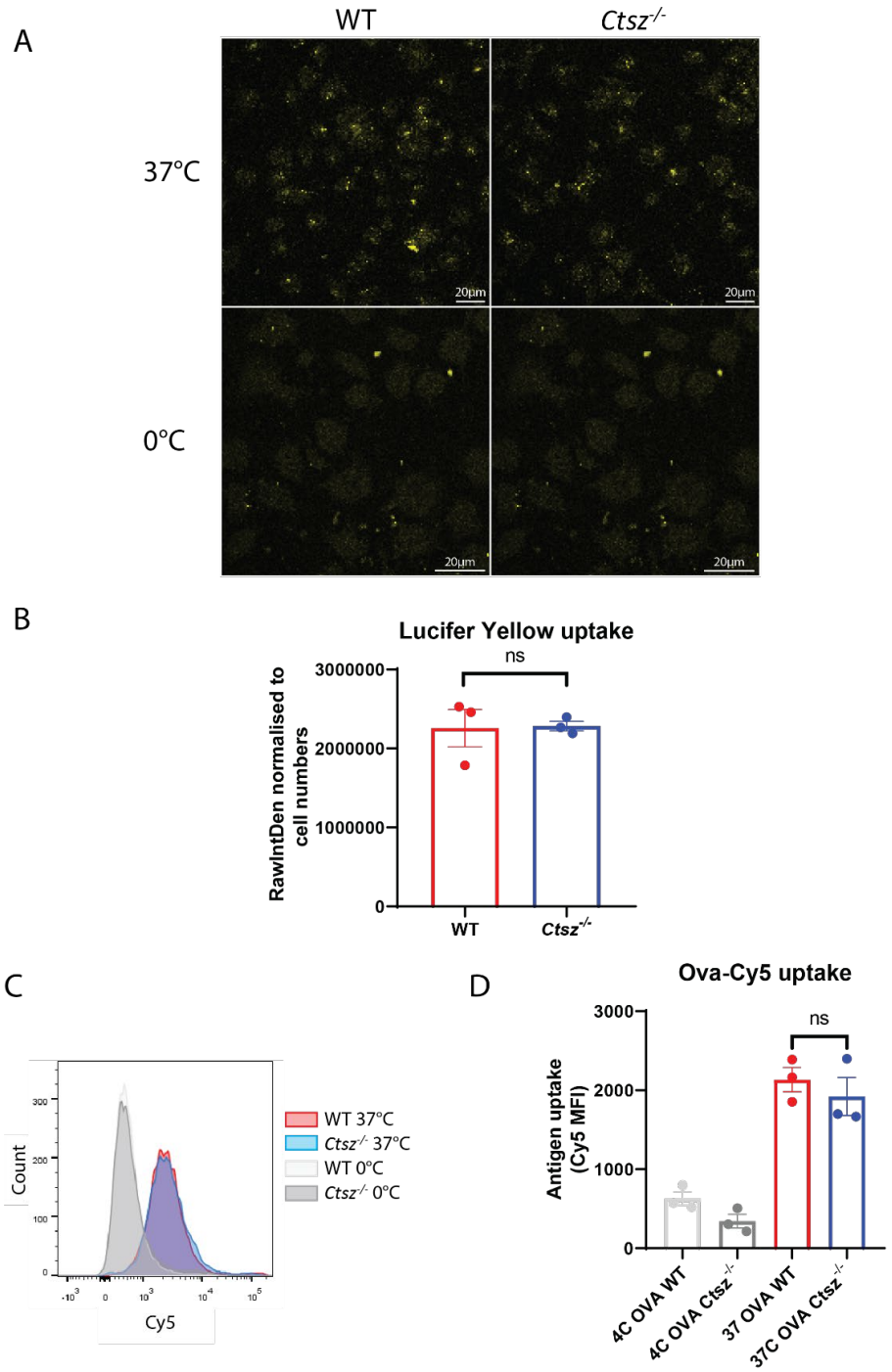

Figure 4.3 Endocytosis analysis of WT and cathepsin X-deficient cells. A. Immunofluorescence of Lucifer Yellow uptake by WT and *Ctz*$^{-/-}$ DCs. **B.** Quantification of Lucifer Yellow intensity normalised to cell numbers. Statistics were performed using unpaired Student's t-tests. n=3. **C.** Flow cytometry analysis of OVA-Cy5 uptake by WT and *Ctz*$^{-/-}$ DCs. **D.** Quantification of mean fluorescence intensity of Cy5. Statistics were performed using unpaired Student's t-tests. n=3. Error bars represent SEM. ns P > 0.05, *P ⩽ 0.05, **P ⩽ 0.01, ***P ⩽ 0.001, **** P ⩽ 0.0001.

4.2.4 Cathepsin X deficiency did not alter antigen presentation and cross-presentation.

Antigen presentation is the next important step in DC immunity. After exogenous antigens are engulfed, they are processed within endolysosomes and presented to T cells. The MHC-II complex mediates the canonical pathway of exogenous antigen presentation. $CD8^+$ dendritic cells can also conduct antigen cross-presentation where exogenous antigens are loaded onto MHC-I to present to T cells **(Figure 1.5C)**. Herein, we sought to investigate the impact of cathepsin X deficiency on both antigen presentation pathways.

We used two transgenic mouse strains, OT-I and OT-II mice, to investigate antigen presentation. $CD4^+$ T cells derived from OT-II mice can primarily recognise ovalbumin peptide residues 323-339 when presented by MHC-II. $CD8^+$ T cells isolated from OT-I mice have modified T cell receptors designed to recognise ovalbumin peptide residues 257-264 when presented by MHC-I and can be used to study antigen cross-presentation. Successful antigen presentation leads to the proliferation of the specific type of T cells, and the extent of cell proliferation reflects the ability of DC antigen proliferation. To quantify T cell proliferation, T cells were stained with Cell Tracer Violet (CTV). Each time T cells go through cell division, the CTV intensity will be halved, allowing us to differentiate the actively proliferating T cells from the inactive T cells.

The proliferation of $CD4^+$ and $CD8^+$ in response to specific ovalbumin peptides was unaltered in the absence of cathepsin X, suggesting this protease does not mediate canonical antigen presentation or cross-presentation **(Figure 4.4AB)**.

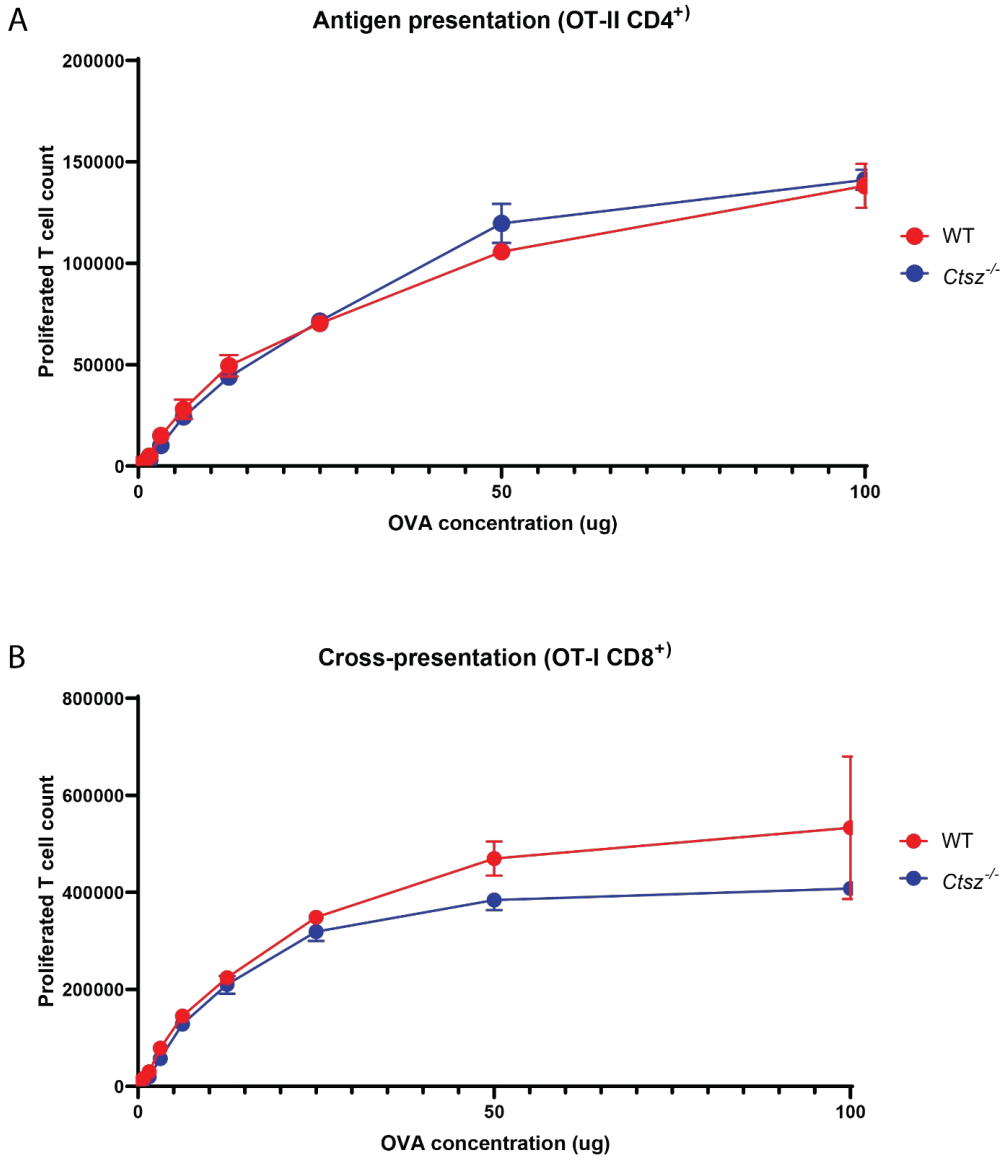

Figure 4.4 The comparison of antigen presentation and cross-presentation between WT and cathepsin X-deficient DCs. A. Antigen cross-presentation assay of OVA to $CD8^+$ T cells. **B.** Antigen presentation assay of OVA to $CD4^+$ T cells. Statistics were performed using unpaired Student's t-tests. n=3. Error bars represent SEM. ns $P > 0.05$, *$P \leqslant 0.05$, **$P \leqslant 0.01$, ***$P \leqslant 0.001$, **** $P \leqslant 0.0001$.

4.2.5 Cathepsin X deficiency did not alter the secretion of IL-6, IL-10, IL-12, TNFα and MCP-11

Secretion of inflammatory cytokines and chemokines is a crucial feature of DC maturation. Cathepsin X inhibition has been previously reported to hinder plasmacytoid DC maturation and, therefore, reduce the secretion of TNFα, IL-6, and IL-12 [3]. In addition, cathepsin B, a closely related lysosomal cysteine cathepsin of cathepsin X, has also been proven to have a role in the trafficking of TNFα and hence regulate secretion [70]. We, therefore, investigated the impact of cathepsin X on cytokine/chemokine secretion.

We first broadly examined the impact of cathepsin X deficiency on cytokine/chemokine secretion using a cytokine array kit that captured 111 soluble proteins. After CpG activation, WT and *Ctsz*$^{-/-}$ cells exhibited increased secretion of multiple soluble proteins (**Figure 4.5AB**). However, we did not observe apparent differences in any secreted proteins between WT and *Ctsz*$^{-/-}$ cells. Some secreted proteins were subtly different. The cathepsin X-deficient cells tended to secrete less CCL3/CCL4, CCL5, IL-6, and IL-12 (**Figure 4.5AB**); however, no statistical significance could not be obtained from the two replicates.

We, therefore, investigated a more focused set of cytokines using a BD™ Cytometric Bead Array (CBA). We did not observe significant differences in secreted MCP-1/CCL2, IL-6, IL-10, IL-12, and TNFα levels between WT and *Ctsz*$^{-/-}$ cells **(Figure 4.5 C-G)**. Secretion of IFNϒ was below the detection limit (data not shown).

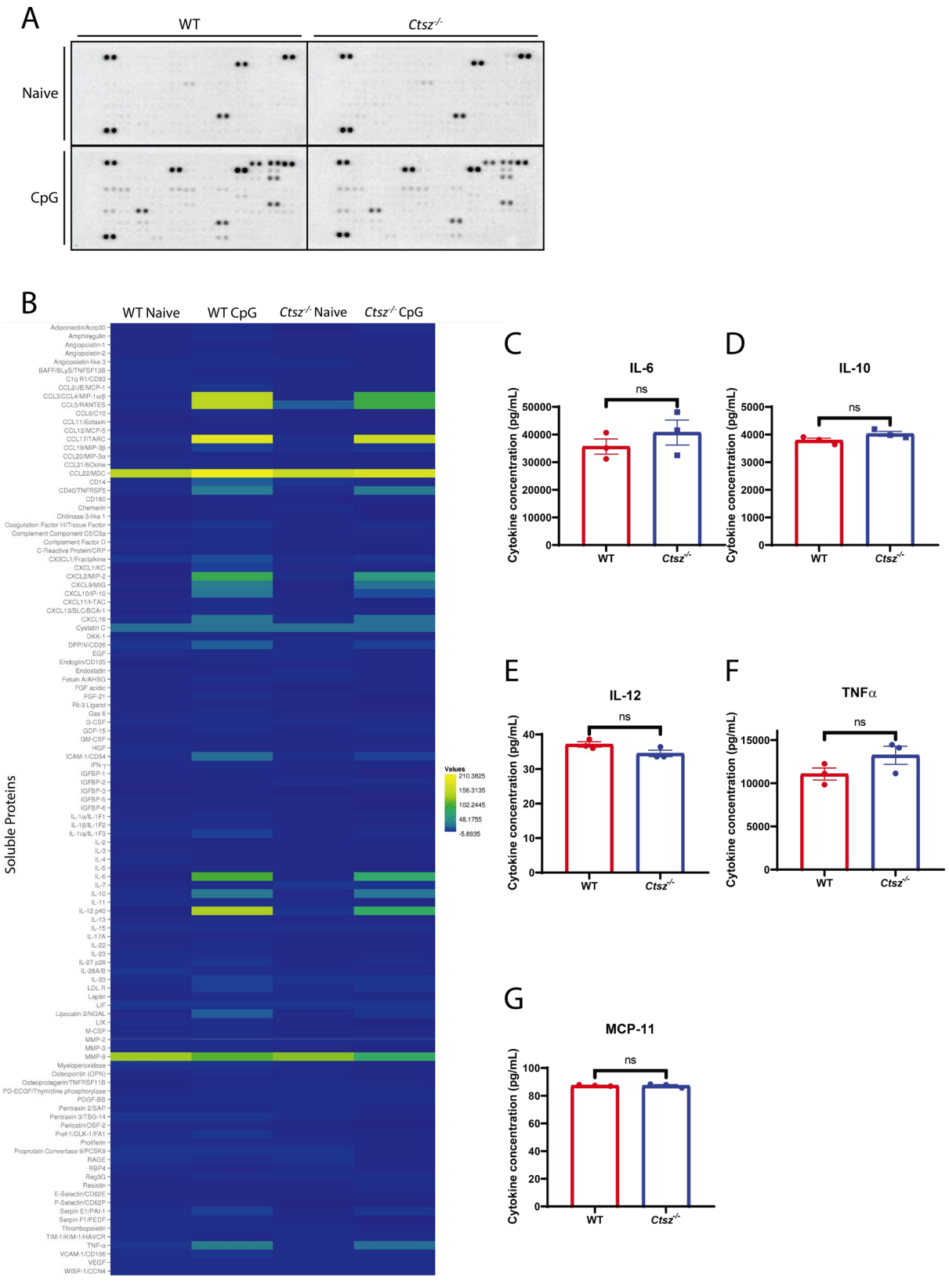
A
WT
Ctsz-/-
Naive
CpG
B
WT Naive
WT CpG
Ctsz-/- Naive
Ctsz-/- CpG
Soluble Proteins
Values
210.3825
156.3135
102.2445
48.1755
-5.8935
C
IL-6
ns
Cytokine concentration (pg/mL)
WT
Ctsz-/-
D
IL-10
ns
E
IL-12
ns
F
TNFα
ns
G
MCP-11
ns

Figure 4.5 Examination of cytokine secretion in cathepsin X-deficient cells. A. Cytokine array analysis of secreted proteins from WT and *Ctsz*$^{-/-}$ DC1940 cells before and after stimulation with CpG for 24 hours. **B.** Heatmap of a cytokine array depicting 111 soluble proteins secreted by WT and *Ctsz*$^{-/-}$ DC1940 cells before and after stimulation with CpG for 24 hours. **C-G.** Comparison of IL-12, MCP, TNFα, IL-6, and IL-10 secretion between WT and *Ctsz*$^{-/-}$ DCs stimulated with CpG for 24 hours. Statistics were performed using unpaired Student's t-tests. n=3. Error bars represent SEM. ns $P > 0.05$, *$P \leqslant 0.05$, **$P \leqslant 0.01$, ***$P \leqslant 0.001$, **** $P \leqslant 0.0001$.

4.2.6 Cathepsin X deficiency causes an increase in TMEM176B and results in lower secretion of IL-1β.

To study the impact of cathepsin X deficiency on DC function in a more systematic, unbiased manner, we applied shotgun proteomics. As expected, cathepsin X total protein level was significantly enriched in CpG-activated wild-type cells compared to *Ctsz*$^{-/-}$ cells. We observed an additional 39 proteins that were significantly enriched in wild-type cells and 17 proteins that were enriched in *Ctsz*$^{-/-}$ cells after CpG activation (log2(1.5) > 0.585, log10(0.05)> 1.301, n=3). Among the latter group was TMEM176B (a 3.693-fold increase compared to *Ctsz*$^{-/-}$, p=0.0130) **(Figure 4.6A)**.

TMEM176B, or transmembrane protein 176b, is a phagolysosomal resident protein and has been implicated in the regulation of IL-1β secretion [103]. TMEM176B can regulate inflammasome activation and IL-1β by modulating cytosolic calcium levels. Calcium influx into the cytosol is a prerequisite for inflammasome activation. Cytosolic calcium is essential in assembling the inflammasome and activating caspase-1, which converts pro-IL-1β to mature IL-1β. In this context, TMEM176B is a negative regulator of inflammasome activation. TMEM176B hinders the calcium influx and, therefore, halts the activation of caspase-1 **(Figure 4.6B)**.

To verify that TME176B expression was regulated by cathepsin X and not CRISPR-mediated off-target effects, we re-expressed cathepsin X in the *Ctsz*$^{-/-}$ cell line. As demonstrated by sCy5-Nle-SY labelling and cathepsin X immunoblot, the rescued cell line re-expressed functional cathepsin X **(Figure 4.6C)**. By shotgun proteomics, cathepsin X was significantly enriched in the rescued cell line. TMEM176B was rescued in the re-expressed cells (a 6.731-fold increase compared to *Ctsz*$^{-/-}$, p=0.0080) **(Figure 4.6D)**, suggesting its levels are influenced by cathepsin X. However, in naïve DCs, we did not see a significant change in TMEM176B. Conversely, its paralog TMEM176A was found to be significantly increased cathepsin X-deficient cells (**Figure 4.6E**). Treating DCs with CpG also increased the level of TMEM176B (**Figure 4.6F**).

We hypothesised that cathepsin X deficiency leads to increased TMEM176B and inhibited calcium influx, leaving Caspase-1 inactive and unable to convert pro-IL-1β to the mature, actively secreted form **(Figure 4.6B)**. To test this hypothesis, we aimed to investigate IL-1β secretion in WT and *Ctsz*$^{-/-}$ DC1940 cells. Inflammasome activation requires two signals. The first signal is the priming of the cells with TLR agonists. The TLR signalling upregulates

inflammatory genes, including inflammasome activation-associated genes. We found that CpG activation increased the level of NLRP3 and Caspase-1 (**Figure 4.6F**). The second signal activates the inflammasome. We used CpG or LPS and adenosine triphosphate (ATP) for the first and second signals, respectively. Co-administration of CpG and ATP did not elicit a boost in the secretion of IL-1β, nor did LPS/ATP co-treatment **(Figure 4.6G)**. This may be explained by the fact that $CD8^+$ DCs, modelled by DC1940 cells, are not the primary cell type that goes through inflammasome activation. CpG treatment alone, however, induced some IL-1β secretion compared to naïve cells **(Figure 4.6G)**. We also measured the secretion of IL-1β upon treatment with different TLR agonists and found that CpG treatment induced the most robust increase in IL-1β secretion **(Figure 4.6H)**. After pooling data from three independent experiments, we observed a ~20% reduction in the secretion of IL-1β from *Ctsz*$^{-/-}$ cells compared to WT ($p<0.0001$) **(Figure 4.6I)**.

In conclusion, our data suggest that cathepsin X deficiency might result in impaired secretion of IL-1β, possibly due to increased TMEM176B expression. The mechanism of TEM176B regulation by cathepsin X remains enigmatic; however, there may be a direct interaction as the two proteins are known to co-locate in endolysosomes. We looked at the TMEM176B peptides identified by mass spectrometry; however, this did not provide additional insight into the regulatory mechanism.

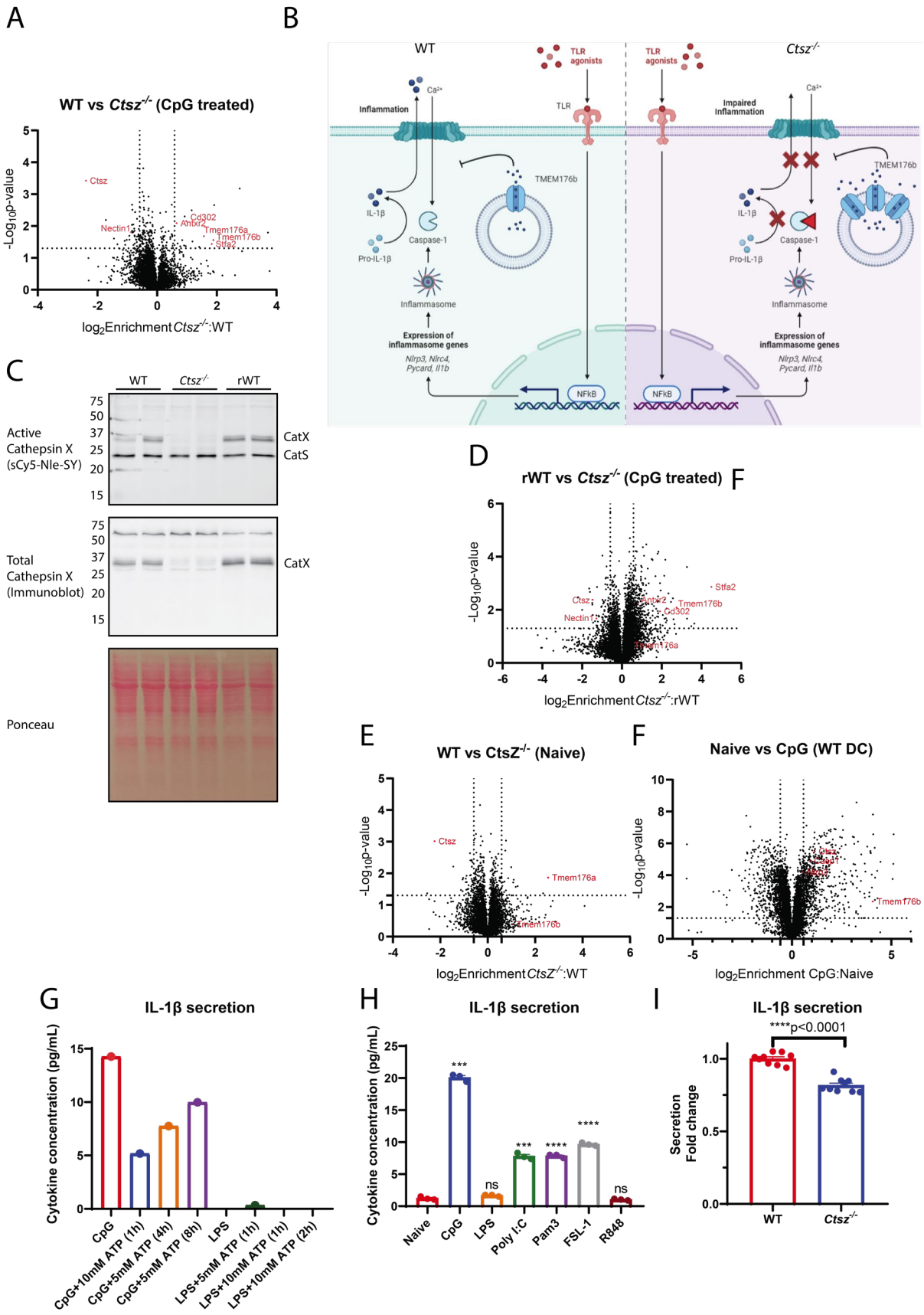
A
WT vs Ctsz-/- (CpG treated)
-Log10p-value
log2Enrichment Ctsz-/-:WT
Ctsz
Cd302
Anxr2
Tmem176a
Tmem176b
Stfa2
Nectin1
B
WT
Ctsz-/-
TLR agonists
TLR
Ca2+
Inflammation
Impaired Inflammation
TMEM176b
IL-1β
Pro-IL-1β
Caspase-1
Inflammasome
Expression of inflammasome genes
Nlrp3, Nlrc4, Pycard, Il1b
NFkB
C
WT
Ctsz-/-
rWT
Active Cathepsin X (sCy5-Nle-SY)
Total Cathepsin X (Immunoblot)
Ponceau
CatX
CatS
75
50
37
25
20
15
D
rWT vs Ctsz-/- (CpG treated)
log2Enrichment Ctsz-/-:rWT
E
WT vs CtsZ-/- (Naive)
log2Enrichment CtsZ-/-:WT
F
Naive vs CpG (WT DC)
log2Enrichment CpG:Naive
G
IL-1β secretion
Cytokine concentration (pg/mL)
CpG
CpG+10mM ATP (1h)
CpG+5mM ATP (4h)
CpG+5mM ATP (8h)
LPS
LPS+5mM ATP (1h)
LPS+10mM ATP (1h)
LPS+10mM ATP (2h)
H
IL-1β secretion
Cytokine concentration (pg/mL)
Naive
CpG
LPS
Poly I:C
Pam3
FSL-1
R848
ns
***
****
I
IL-1β secretion
****p<0.0001
Secretion Fold change
WT
Ctsz-/-

Figure 4.6 Secretion of IL-1β was impaired in *Ctsz*$^{-/-}$ cells and was potentially caused by the increased TMEM176B. A. Volcano plot from the shotgun proteomics analysis of CpG-treated WT vs *Ctsz*$^{-/-}$ DCs. **B.** Potential mechanistic role of cathepsin X regulating IL-1β through TMEM176B. Created with BioRender.com. **C.** WT, *Ctsz*$^{-/-}$, and *Ctsz*$^{-/-}$ cells with rescued expression of WT cathepsin X were labelled with sCy5-Nle-SY. Cells were then lysed and analysed by SDS-PAGE in-gel fluorescence. Intracellular cathepsin X total level was examined by immunoblot using cathepsin X antibody. Ponceau stain was used as a measure of protein loading. **D**. Volcano plot from the shotgun proteomics analysis of CpG-treated rescued WT vs *Ctsz*$^{-/-}$ DCs. **E.** Volcano plot from the shotgun proteomics analysis of naïve WT vs *Ctsz*$^{-/-}$ DCs. **F.** Volcano plot of the shotgun proteomics analysis of naïve WT DCs vs CpG activated WT DCs. **G.** Quantifying IL-1β secretion from Mutu DC1940 cells stimulated by CpG or LPS with ATP treatment for different lengths. **H.** Quantification of IL-1β secretion from Mutu DC1940 cells stimulated with TLR agonists. Statistics were performed using the Brown–Forsythe and Welch ANOVA tests. n=3 **I.** Secretion of IL-1β between WT and *Ctsz*$^{-/-}$ DCs stimulated with CpG for 24 hours relative to WT cells (fold-change). n=3. Statistics were performed using unpaired Student's t-tests. Error bars represent SEM. ns $P > 0.05$, *$P \leqslant 0.05$, **$P \leqslant 0.01$, ***$P \leqslant 0.001$, **** $P \leqslant 0.0001$.

4.3 Discussion:

In this chapter, we investigated the role of cathepsin X in dendritic cell immune function. We first generated a cathepsin X-deficient DC1940 cell line using CRISPR-Cas9. We used a DC1940 cell line constitutively expressing Cas9 protein [158]. The guide RNA of cathepsin X was designed to target the first exon of cathepsin X and was transduced with a doxycycline-inducible lentiviral system. Successfully transduced cells expressed a CFP protein for cell sorting. We also included a WT control cell line that underwent the same CRISPR-Cas9 process, while the guide RNA targeted the human BCL2-like gene (hBIM). The human BCL-2 gene does not exist in the murine genome, and there should be no genetic editing in the hBIM cells.

In this study, we did not conduct single-cell cloning for both WT and *Ctsz*$^{-/-}$. We previously observed significant clonal variations. *Ctsz*$^{-/-}$ single-cell clones exhibited different growth rates and cytokine secretion profiles. Therefore, we sorted successfully transduced cells based on CFP fluorescence. We collected all the CFP-positive cells and cultured them as a bulk population. We hypothesise that the bulk population would maintain heterogeneity of the cell population and minimise the impact of clonal variation.

As CpG activation induced the most robust increase in cathepsin X upregulation, we decided to investigate the role of cathepsin X in DC immunity upon CpG activation. We first investigated whether cathepsin X deficiency impairs DC1940 cell maturation. We stimulated DCs with TLR9 agonist (CpG) for 24 hours and analysed the level of several surface molecules, including CD40, CD86, MHC-I and MHC-II. We did not observe any differences in the levels of all the surface markers we investigated. Obermajer and colleagues reported that cathepsin X inhibition impairs the maturation of plasmacytoid dendritic cells stimulated with TLR4 agonist (LPS). It might be possible that cathepsin X does not regulate the TLR9 signalling pathway but other TLR receptors. We stimulated DC1940 cells with LPS for 24 hours and looked at the surface expression of CD86. We did notice a reduction in CD86 surface expression in cathepsin X-deficient cells (**Figure 4.2F**). However, DC1940 cells do not have a solid response to LPS, as shown in the previous result chapter. Investigating whether cathepsin X is crucial for TLR4-mediated maturation of primary cDCs would be essential.

We then investigated if cathepsin X deficiency would affect antigen uptake using two different agents, Lucifer Yellow and OVA-Cy5. A non-specific endocytic pathway endocytoses Lucifer

Yellow and reflects the impact of cathepsin X deficiency on general endocytosis. We did not observe any differences in LY uptake between wildtype and cathepsin X deficient cells. We repeated the experiment with a different agent, the OVA-Cy5, which is widely used to measure macropinocytosis and did not observe a difference either. However, OVA can also be endocytosed via the mannose receptor-mediated endocytosis [187, 188]. To validate if cathepsin X deficiency affects macropinocytosis specifically, the method needs to be improved by pre-treating cells with a mannose receptor agonist, mannan, to inhibit mannose receptor-mediated endocytosis before OVA-Cy5 addition.

We also questioned whether losing a lysosomal protease would reduce the proteolytic activity of the dendritic cells. As reported, cathepsin X deficiency did not alter the processing of Myelin oligodendrocyte glycoprotein antigen in bone marrow-derived dendritic cells [30]. Allan et al. differentiated progenitor cells into dendritic cells with GMCSF, and the resulting dendritic cells were more macrophage-like [189]. The proteolytic activity of the cells can be analysed with DQ™ Ovalbumin, a fluorogenic substrate for proteases. When intact, the DQ™ Ovalbumin is quenched. Lysosomal proteases remove the quenching effect upon cleavage, and green fluorescence will be emitted. However, the DC1940 cell line originally expressed GFP protein, making it unable to examine the lysosomal proteolysis with this method. To investigate if conventional dendritic cells require cathepsin X for lysosomal proteolysis, we will need to isolate splenic dendritic cells from cathepsin X-deficient mice and conduct DQ™ Ovalbumin analysis.

As we could not investigate the impact of cathepsin X deficiency on antigen processing, we sought to focus on the downstream effects of antigen processing antigen presentation. A reduced antigen processing ability would reflect an impaired ability to process antigens. We did not observe any differences in antigen presentation between WT DCs and cathepsin X-deficient DCs. This may reflect that cathepsin X deficiency did not alter antigen processing. Therefore, unlike cathepsin S and cathepsin L, cathepsin X may not have a role in antigen presentation [11].

Given the delayed upregulation of cathepsin X discussed in **Chapter 3**, cathepsin X may not play a role in the immediate immune function of DCs. In the same chapter, we demonstrated that the IL-6 signalling pathway induces the upregulation of cathepsin X. IL-6 is known for its versatile effects on various aspects of cellular behaviour, including growth, differentiation,

viability, and mobility, particularly within the context of immune responses, haematopoiesis, and inflammatory processes [190]. Notably, IL-6 has also been reported to act as an immunosuppressive cytokine, maintaining DCs in their naive state. IL-6 increases the expression of cathepsin S, which in turn degrades intracellular MHC-II αβ dimers, ultimately leading to reduced T cell activation [191, 192]. Consequently, similar to cathepsin S, cathepsin X may not be immediately involved in the immune function of DCs but could be more focused on maintaining their maturation status by degrading excess immune molecules. To validate this hypothesis, further investigation is required, specifically by comparing the maturation status of DCs over an extended period between wild-type and cathepsin X-deficient cells.

Allan et al. reported that cathepsin X deficiency impaired IL-1β secretion during NLRP3-mediated inflammasome activation. They further concluded that cathepsin X regulates IL-1β secretion post-translationally as there were no significant differences in pro-IL-1β mRNA levels between WT and cathepsin X-deficient BMDMs/BMDCs [30]. Further studies showed that the mechanism of cathepsin X regulation on IL-1β secretion was not dependent on its proteolytic activity. Secreted pro-cathepsin X containing an RGD motif could activate α5β1 and contribute to NLRP3 inflammasome activation [64].

Our results suggested an alternative way to explain the regulation of cathepsin X on IL-1β. We did shotgun proteomics to examine the broader impact of cathepsin X deficiency. TMEM176B was significantly increased in cells lacking cathepsin X. TMEM176B has been reported to inhibit NLRP3 inflammasome activation. Genetic depletion of TMEM176B enhanced the activation of caspase-1 and subsequently increased the secretion of IL-1β. The authors explained that TMEM176B inhibits calcium influx. The loss of TMEM176B increased the level of cytosolic Ca^{2+} and contributed to NLRP3 inflammasome activation [103]. To validate our hypothesis, our experimental approach will involve several key steps. First, we will assess and compare the cytosolic calcium levels in both wild-type and cathepsin X deficient dendritic cells as they undergo maturation. This will be accomplished by utilising a calcium probe, such as Fura-2. Given that TMEM176B governs calcium influx, our expectation is that cathepsin X-deficient cells will exhibit reduced cytosolic calcium level. Furthermore, we will examine the activation of caspase-1 through western blot. The reason for this investigation is that caspase-1 activation is downstream of calcium influx and plays a vital role in inflammasome activation/IL-1β secretion. Lastly, we will assess the mRNA expression of IL-1β in cathepsin X-

deficient cells. This step is crucial as it will help us determine whether the observed impairment in IL-1β secretion is due to post-translational modifications rather than alterations in mRNA expression.

TMEM176B is a transmembrane protein localised on phagolysosomes [103]. Its localisation indicates a potential interaction with cathepsin X. However, its N and C terminal tails reside outside the phagolysosomal lumen. As a carboxy-monopeptidase, cathepsin X cannot directly cleave TMEM176B. Evidence shows that lysosomal proteases can escape the lysosomal compartment and travel to the cytoplasm to cleave substrates [148]. Whether or not cathepsin X can escape the lysosomes and make a cleavage of TMEM176B needs more investigation. Alternatively, some endopeptidases might make an initial cleavage inside the phagolysosome, generating a neo-c-terminal. Cathepsin X might then be able to cleave TMEM176B at the neo-c-terminal tail. The cleavage needs to be validated using mass-spectrometry techniques, especially C-terminomics [54].

TMEM176B has also been reported to be associated with the immature state of dendritic cells [193]. Condamine et al. showed that BMDCs treated with TLR3 (Poly I:C) and TLR4 (LPS) exhibited downregulated TMEM176B. Our proteomics data showed different results: TMEM176B was increased after TLR9 (CpG) activation. This discrepancy maybe TLR agonist-dependent or cell type-dependent.

Unfortunately, DC1940 ($CD8^+$ dendritic) cells do not have a profound NLRP3 inflammasome activation mechanism. As reported, conventional dendritic cells acquire a mechanism in which transcription factors IRF8 and IRF4 suppress the inflammasome-related genes to maintain their viability to keep priming T cells [108]. We treated the DC1940 cells with two different TLR agonists, CpG and LPS, as the first priming signal for NLRP3 inflammasome activation. LPS is the most used priming agonist in NLRP3 inflammasome; however, DC1940 cells only partially respond to LPS. DC1940 cells exhibit a much greater response to CpG. Although using CpG as the priming signal for NLRP3 inflammasome activation is scarce in the literature, there is evidence showing TLR9 priming can induce NLRP3 inflammasome activation [194]. Our shotgun proteomics data revealed that priming DC1940 cells with CpG significantly increased the protein amount of both IL-1β and NLRP3 (**Figure 4.6F**). We used ATP as the second signal activating the NLRP3 inflammasome. ATP activates the P2X7 receptor and facilitates the efflux of K^+ ions, subsequently activating the inflammasome complex [195, 196]. However, neither

CpG nor LPS with ATP resulted in a substantial secretion of IL-1β. We observed a minor secretion of IL-1β by DC1940 cells treated with CpG alone, but the addition of ATP did not propagate the secretion. Therefore, the involvement of cathepsin X in TMEM176B expression and subsequent inflammasome activation needs to be further validated in the $CD11b^+$ dendritic cell population that has a better ability to form inflammasomes compared to $CD8^+$ dendritic cells or validated in the macrophages which are considered the canonical player in inflammasome activation.

We did not observe significant contributions of cathepsin X to several immune functions of DCs. One possible explanation is the compensatory mechanism in the lysosomal proteolytic environment: the host cell senses the loss of proteolysis and compensates for it by upregulating the expression of related proteases. For example, when legumain activity was lost, primary murine embryonic fibroblast responded to it by increasing the expression of cathepsin A, B, C, L, and X [197]. This compensatory mechanism makes it hard to investigate the role of one particular protease by either chemical or genetic inhibition.

Cathepsin X is not the only exopeptidase in the lysosomes. Cathepsin B is the other cathepsin with exo-dipeptidase activity [189]. The loss of cathepsin X may be compensated by the presence of cathepsin B. Some evidence in the literature showed that inhibiting both cathepsin B and cathepsin X had a synergistic effect [198]. Therefore, genetically knocking out both cathepsin B and X may result in a more obvious defect in lysosomal proteolysis.

The impact of cathepsin X deficiency on the DC lysosomal proteolytic network will be shown and discussed in the next chapter.

Chapter 5. Cathepsin X activity controls cathepsin L processing and nuclear trafficking

5.1 Introduction:

In the previous chapter, I generated a cathepsin X deficient dendritic cell line to investigate the role of cathepsin X in DC function. We examined the impact of cathepsin X deficiency on DC maturation, endocytosis, antigen presentation and cytokine secretion and found that cathepsin X had a limited role in all these DC functions. We eventually conducted shotgun proteomics to broadly investigate the contribution of cathepsin X to DCs. We discovered that cathepsin X-deficient cells exhibited an increased level of TMEM176B. TMEM176B is a transmembrane protein involved with the inhibition of calcium influx. The increased level of TMEM176B in cathepsin X deficient cells resulted in an impaired calcium influx and subsequently halted IL-1β secretion under inflammasome activation.

The loss of one lysosomal proteolytic protease's activity is often accompanied by upregulation of other related lysosomal proteases [175, 197]. This compensatory mechanism may mask the impact of cathepsin X deficiency in dendritic cells and may explain the minimal impact of cathepsin X deficiency on DC function. In this chapter, we focused on the impact of cathepsin X deficiency on the lysosomal proteolytic network.

Lysosomal proteases exist within a sophisticated network and are interconnected with each other. To prevent unwanted protein digestion, cysteine proteases are synthesised as inactive zymogens. Their activation requires proteolytic removal of pro-peptide domain(s) through auto- or trans-activation. Most endopeptidases autoactivate, including cathepsin B, H, L, S, K, V and F. The exopeptidases cathepsin C and cathepsin X require the activity of other proteases for activation. Pro-cathepsin C is cleaved by cathepsin L and S [199]. The catalytic cysteine of cathepsin X forms a disulphide linkage with a cysteine residue in its pro-domain, making its pro-form incapable of autoactivation. In vitro, cathepsin X is activated upon removal of the pro-domain by cathepsin L [43].

Some cathepsins also undergo additional processing. Cathepsin B, C, D, H and L all have a single-chain form after pro-peptide removal. The single chain is subsequently cleaved and processed into a two-chain form consisting of a heavy and light chain (**Figure 5.1A**). The processing of cathepsin B, H, and L single chain to the two-chain form depends on the cysteine

protease legumain. The activities of single-chain and two-chain forms also differ. Upon legumain inhibition, cathepsin B and L exhibited increased proteolytic activity when the single chain accumulated, while cathepsin H activity was diminished [200]. The single-chain and two-chain forms may also have different substrate specificities; the two-chain form of cathepsin L has gelatinolytic activity, while the single-chain form does not [201]. Thus, protease interplay can influence their activity, structure, and substrate specificity.

Inhibition or genetic deletion of a specific protease also alters the expression of other proteases. For example, when the activity of legumain is lost, the host cell can sense the loss of legumain proteolysis and respond to it by upregulating other related proteases, including cathepsin A, B, C, L and X through lysosomal biogenesis [197, 202].

In addition, some proteases have been shown to change the localisation of other proteases. Cathepsin B, a lysosomal cathepsin, has also been detected in the cytosol. The trafficking to the cytosol depends on trypsin, although the mechanism remains unknown. Cathepsin B is active in the neutral pH of the cytosol and can subsequently activate the inflammasome to induce cell death [148].

In this chapter, we analysed the expression and processing of related lysosomal proteases and their inhibitors in the context of cathepsin X deficiency. We discovered that cathepsin X deficiency leads to altered processing of cathepsin L, whereby cathepsin L pro-form and single chain accumulate in cells lacking active cathepsin X. We also showed that cathepsin L is trafficked to the nucleus preferentially in its two-chain form. In the absence of cathepsin X activity, nuclear translocation of cathepsin L heavy chain was diminished, thereby impairing the processing of its nuclear substrates.

5.2 Results

5.2.1 Processing of cathepsin L is altered in cathepsin X deficient cells.

To investigate the impact of cathepsin X deficiency on the lysosomal protease network, we examined the expression and activity of select proteases and their endogenous inhibitors in wild-type and *Ctsz*$^{-/-}$ dendritic cells. Consistent with the results from the previous chapter, cathepsin B and L activity, as detected by BMV109 labelling, was minimal compared to cathepsin S, which was not impacted by the loss of cathepsin X (**Figure 5.1B**). By immunoblot, cathepsin X-deficient cells showed no apparent changes in total expression and processing of cathepsin B and S (**Figure 5.1B**). The processing of cathepsin L, however, was altered: pro-cathepsin L and its single-chain form accumulated in the absence of cathepsin X (1.405-fold, p=0.0112 and 6.855-fold, p=0.0169, respectively) (**Figure 5.1BG**). Using the activity-based probe, FY01, we did not observe any differences in cathepsin C activity (23 kDa) (**Figure 5.1C**). Total expression and processing of cathepsin C by immunoblot were also unchanged (**Figure 5.1C**). Cathepsin H, which exhibits a similar processing mechanism as cathepsin L, was unchanged in the context of cathepsin X deficiency (**Figure 5.1D**).

As legumain is known to mediate the processing of the cathepsin L single chain, we hypothesized that single-chain accumulation in the absence of cathepsin X might be mediated by altered legumain activity. However, using LE28, a legumain-specific activity-based probe, and immunoblotting, we did not observe significant differences in total and active legumain between wild-type and *Ctsz*$^{-/-}$ cells (**Figure 5.1E**). Moreover, we did not observe changes in the expression of cysteine protease inhibitors, including stefin A, stefin B and cystatin C (**Figure 5.1F**).

Collectively, these results suggest that cathepsin X selectively regulates the single-chain processing of cathepsin L in a legumain-independent manner.

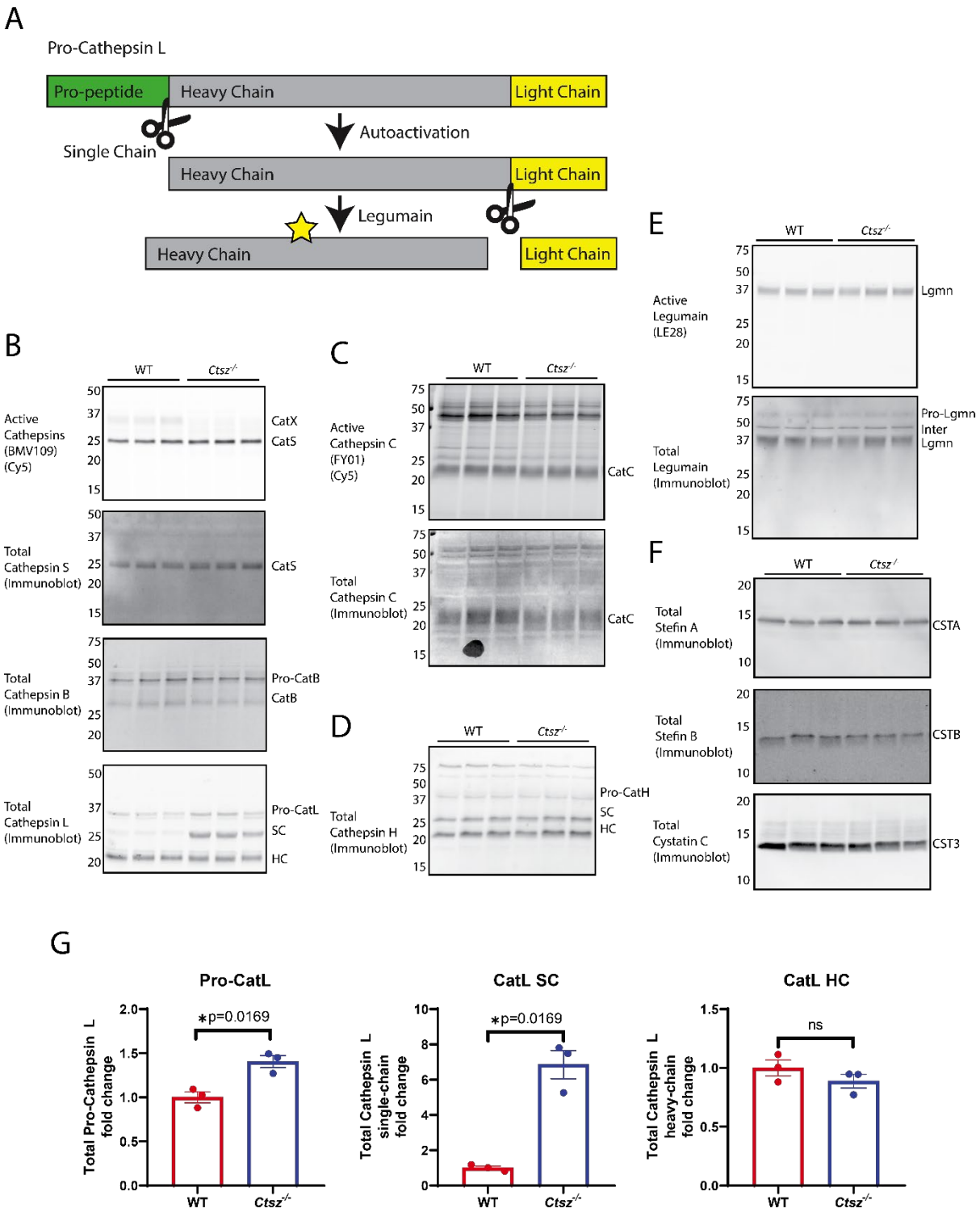
A
Pro-Cathepsin L
Pro-peptide
Heavy Chain
Light Chain
Single Chain
Autoactivation
Heavy Chain
Light Chain
Legumain
Heavy Chain
Light Chain
B
WT
Ctsz-/-
Active Cathepsins (BMV109) (Cy5)
CatX
CatS
Total Cathepsin S (Immunoblot)
CatS
Total Cathepsin B (Immunoblot)
Pro-CatB
CatB
Total Cathepsin L (Immunoblot)
Pro-CatL
SC
HC
C
Active Cathepsin C (FY01) (Cy5)
CatC
Total Cathepsin C (Immunoblot)
CatC
D
Total Cathepsin H (Immunoblot)
Pro-CatH
SC
HC
E
Active Legumain (LE28)
Lgmn
Total Legumain (Immunoblot)
Pro-Lgmn
Inter
Lgmn
F
Total Stefin A (Immunoblot)
CSTA
Total Stefin B (Immunoblot)
CSTB
Total Cystatin C (Immunoblot)
CST3
G
Pro-CatL
Total Pro-Cathepsin L fold change
*p=0.0169
CatL SC
Total Cathepsin L single-chain fold change
*p=0.0169
CatL HC
Total Cathepsin L heavy-chain fold change
ns

Figure 5.1. The processing of related lysosomal proteases and their inhibitors in the context of cathepsin X deficiency. A. The post-translational processing of cathepsin L. **B.** BMV109 labelling of live WT and *Ctsz*$^{-/-}$ DC1940 cells, as shown by in-gel fluorescence. Cathepsin B, S, L immunoblot of WT and *Ctsz*$^{-/-}$ DC1940 cells. **C.** FY01 labelling of live WT and *Ctsz*$^{-/-}$ DC1940 cells, as shown by in-gel fluorescence. Cathepsin C immunoblot of WT and *Ctsz*$^{-/-}$ DC1940 cells. **D.** Cathepsin H immunoblot of WT and *Ctsz*$^{-/-}$ DC1940 cells. **E.** LE28 labelling of live WT and *Ctsz*$^{-/-}$ DC1940 cells, as shown by in-gel fluorescence. Legumain immunoblot of WT and *Ctsz*$^{-/-}$ DC1940 cells. **F.** Stefin A, B and Cystatin C immunoblot of WT and *Ctsz*$^{-/-}$ DC1940 cells. **G.** Densitometry of 35 (pro-cathepsin L), 27 (single chain), and 23 (heavy chain) kDa bands displayed the average intensity relative to the WT (fold change). Statistics were performed using unpaired Student's t-tests. n=3. Error bars represent SEM. ns $P > 0.05$, *$P \leqslant 0.05$, **$P \leqslant 0.01$, ***$P \leqslant 0.001$, **** $P \leqslant 0.0001$.

5.2.2 Cathepsin L pro form and single chain accumulated in cathepsin X-deficient cells and depended on active cathepsin X.

To confirm whether loss of cathepsin X activity or its integrin-binding capabilities were responsible for inducing cathepsin L single chain accumulation, we attempted to rescue the phenotype of the cathepsin X-deficient cells with either wild-type, catalytically dead (R94S) or RGD mutant (R40H) cathepsin X constructs. Re-expression was assessed using the cathepsin X activity-based probe sCy5-Nle-SY and immunoblot. WT (rWT) and R40H (rR40H) construct recovered cathepsin X activity while rC94S was inactive (**Figure 5.2A**). The three rescued cell lines all expressed a similar level of cathepsin X, slightly higher than the WT cells (**Figure 5.2A**).

By cathepsin L immunoblot, cells expressing inactive cathepsin X showed an accumulation of cathepsin L single chain similar to cathepsin X-deficient cells. In contrast, the two cell lines expressing active cathepsin X did not have the accumulation of cathepsin L single chain (**Figure 5.2A**). These results suggest that cathepsin L single-chain accumulation depends on cathepsin X activity, not its RGD motif.

Next, we validated the above discovery with a cathepsin X inhibitor to confirm the loss of cathepsin X activity could impact cathepsin L processing. The cathepsin X inhibitor Biotin-Hex-Nle-SY is derived from its activity-based probe. We switched the sCy5 fluorophore into biotin and added a six-carbon linker between the Norleucine and the biotin. We found that this inhibitor diminished the level of active cathepsin X in both RAW264.7 and DC1940 cell lines, as shown by sCy5-Nle-SY labelling (**Figure 5.2CD)**.

In DC1940 cells, cathepsin X inhibition and its gene deletion caused a slight but significant increase in pro cathepsin L (1.276-fold, p=0.0333- and 1.572-fold, p=0.0035, respectively). Cathepsin L single chain was also significantly increased after both inhibition and deletion of cathepsin X (2.974-fold, p=0.0040- and 3.779-fold, p=0.0006, respectively) (**Figure 5.2CE)**. We found in RAW264.7 macrophages that the inhibitor caused an accumulation of cathepsin L single chain (2.346-fold, p=0.0047), while the pro-form and heavy chain levels remained unchanged (**Figure 5.2DF**).

Collectively, inhibition of cathepsin X activity leads to altered processing of cathepsin L. This phenomenon is not restricted to DCs but could also be observed in macrophages. Accumulation of pro-cathepsin L was only observed in DC1940 cells.

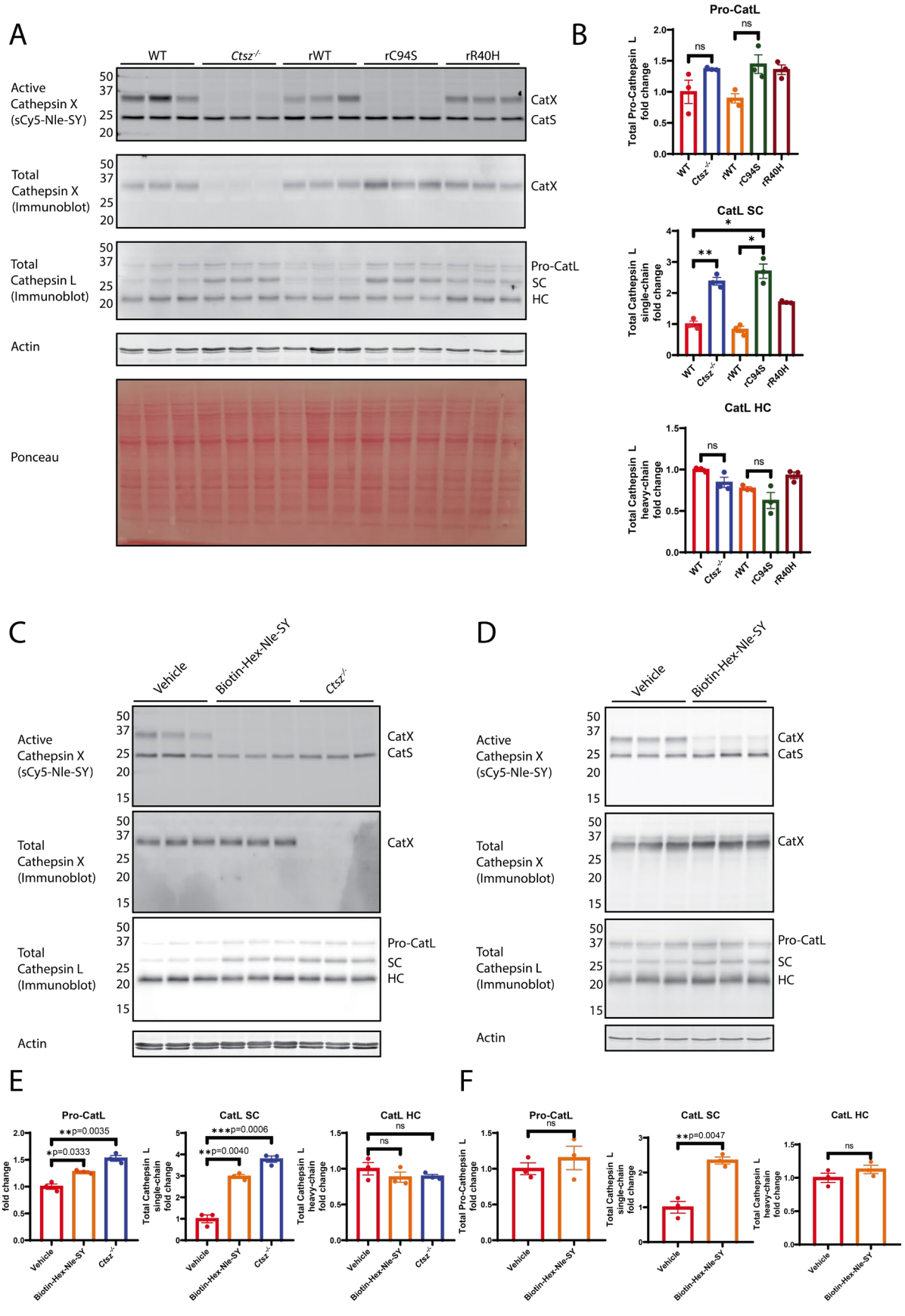
A
WT
Ctsz-/-
rWT
rC94S
rR40H
Active Cathepsin X (sCy5-Nle-SY)
Total Cathepsin X (Immunoblot)
Total Cathepsin L (Immunoblot)
Actin
Ponceau
CatX
CatS
Pro-CatL
SC
HC
50
37
25
20
B
Pro-CatL
Total Pro-Cathepsin L fold change
ns
CatL SC
Total Cathepsin L single-chain fold change
*
**
CatL HC
Total Cathepsin L heavy-chain fold change
C
Vehicle
Biotin-Hex-Nle-SY
Ctsz-/-
15
D
E
**p=0.0035
*p=0.0333
***p=0.0006
**p=0.0040
F
**p=0.0047

Figure 5.2. The altered processing of cathepsin L depends on active cathepsin X. A. sCy5-Nle-SY labelling of live WT, *Ctsz*$^{-/-}$, *Ctsz*$^{-/-}$ re-expressing WT, C94S, and R40H cathepsin X DC1940 cells, as shown by in-gel fluorescence and cathepsin X/L immunoblot. Actin expression was used as a loading control. **B.** Densitometry of 35 (pro-cathepsin L), 27 (single chain), and 23 (heavy chain) kDa bands displayed the average intensity relative to WT (fold change). Statistics were performed using the Brown–Forsythe and Welch ANOVA tests. n=3 **C. D** DC1940 or RAW264.7 cells were pretreated with 50 µM Biotin-Hex-Nle-SY overnight. Active cathepsin X was examined with sCy5-Nle-SY. Total cathepsin X and cathepsin L expression were shown by immunoblot. Actin immunoblot was used as a loading control**. E. F.** Densitometry of 35 (pro-cathepsin L), 27 (single chain), and 23 (heavy chain) kDa bands in DC1940 or RAW264.7 cells displayed the average intensity relative to the vehicle-treated cells (fold change). Statistics were performed using unpaired Student's t-tests. n=3. Error bars represent SEM. ns $P > 0.05$, *$P \leqslant 0.05$, **$P \leqslant 0.01$, ***$P \leqslant 0.001$, **** $P \leqslant 0.0001$.

5.2.3 Cathepsin L single-chain accumulation was not due to direct cathepsin X cleavage, lysosomal oxidative stress, glycosylation or cathepsin L secretion.

Cathepsin X is a carboxy-exopeptidase that is not known to possess endopeptidase activity. While cathepsin L processing depends on cathepsin X activity, we hypothesized that the effect was not likely to be through direct cleavage of cathepsin L by cathepsin X. To eliminate this possibility, we incubated recombinant cathepsin L and cathepsin X in vitro and analysed processing of cathepsin L by immunoblotting. We did not observe the formation of cathepsin L heavy chain in the presence of cathepsin X (**Figure 5.3A**). Conversely, cathepsin L cleaved pro-cathepsin X and processed it into mature cathepsin X at ~35 kDa. Using the BMV109 probe, both the pro-cathepsin X and cathepsin L cleaved cathepsin X were active in vitro, with increased activity for the cleaved cathepsin X (**Figure 5.3B**). This has been observed previously, and cathepsin L is often used to activate recombinant pro-cathepsin X [43]. We observed similar results when Coomassie was used to stain all protein on the gel. No new cathepsin L fragments were produced in the presence of cathepsin X, while cathepsin X was cleaved by cathepsin L, resulting in a slight band shift (**Figure 5.3C**).

Cathepsin L was generally believed to be processed by legumain in the field. Unexpectedly, we found that legumain could not directly cleave cathepsin L into its heavy chain form, though cathepsin L cleaved legumain, resulting in a minor band shift (**Figure 5.D**). On the other hand, legumain cleaved trypsinogen, a previously identified substrate [203], verifying that legumain was active under these reaction conditions (**Figure 5.3E**). These results suggest that processing of cathepsin L single chain into its double chain may not be directly mediated by legumain or cathepsin X, or other factors not captured in our in vitro cleavage assay may be required.

While cathepsin X-deficient cells exhibited accumulation of pro-cathepsin L and cathepsin L single chain, the heavy chain levels remained primarily unchanged. Cathepsin X deficient cells subsequently had more intracellular cathepsin L than WT cells. We next hypothesised that cathepsin X deficient cells may have an increased cathepsin L mRNA expression. Other research groups have shown that loss of proteolytic activity of one lysosomal protease (e.g., legumain) promotes oxidative stress and STAT3-dependent upregulation of the expression of other lysosomal proteases [197, 202].

We used quantitative PCR to measure the mRNA expression of cathepsin L in WT and cathepsin X-deficient cells but observed no significant differences (**Figure 5.3F**). Therefore, the altered level of intracellular cathepsin L is not likely due to increased transcription. Moreover, using CellROX™ Deep Red Reagent and flow cytometry analysis, we did not observe an increase in the lysosomal oxidative stress of *Ctsz*$^{-/-}$ cells compared to WT (**Figure 5.3G**).

We next questioned if the multiple forms of cathepsin L were not proteolytically processed but were different glycosylated forms. We treated WT and *Ctsz*$^{-/-}$ cell lysates with PNGase F and found all three forms of cathepsin L were similarly glycosylated in WT and *Ctsz*$^{-/-}$ cells (**Figure 5.3H)**.

We next hypothesised that cathepsin X deficiency led to impaired secretion of the cathepsin L single chain, which would account for its intracellular accumulation. In wild-type cells, cathepsin L was primarily secreted as the pro-form and, to a lesser extent, in the two-chain form (**Figure 5.3G)**. Single-chain cathepsin L was only secreted from *Ctsz*$^{-/-}$ cells. These results suggest that its intracellular accumulation is not due to impaired secretion without the cathepsin X activity.

Collectively, our results suggest that cathepsin X regulates cathepsin L processing in an activity-dependent manner and that this effect is not likely through direct proteolysis or due to alternations in mRNA expression, oxidative stress, glycosylation, or secretion.

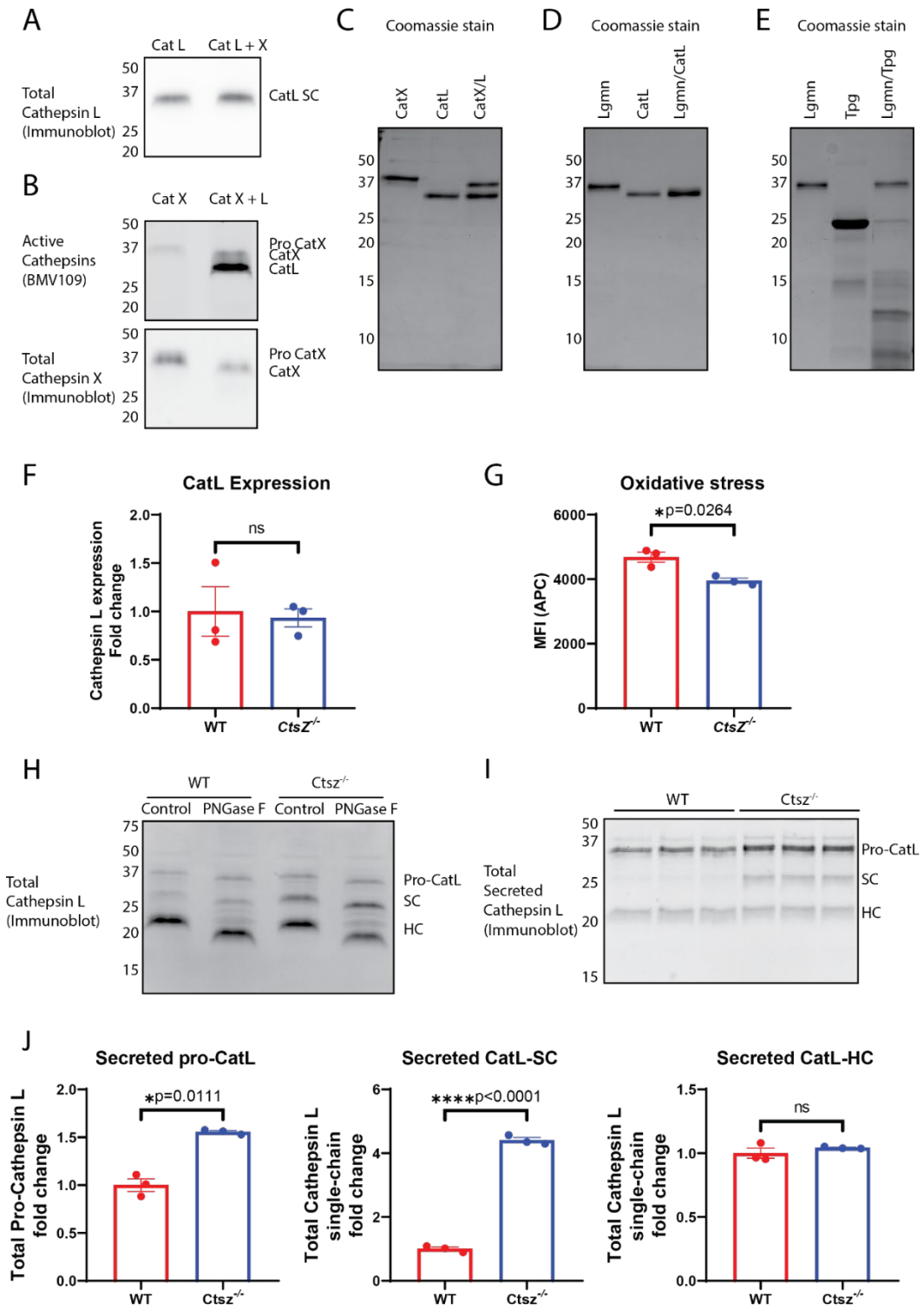
A
Cat L
Cat L + X
Total Cathepsin L (Immunoblot)
CatL SC
B
Cat X
Cat X + L
Active Cathepsins (BMV109)
Pro CatX
CatX
CatL
Total Cathepsin X (Immunoblot)
Pro CatX
CatX
C
Coomassie stain
CatX
CatL
CatX/L
D
Coomassie stain
Lgmn
CatL
Lgmn/CatL
E
Coomassie stain
Lgmn
Tpg
Lgmn/Tpg
F
CatL Expression
Cathepsin L expression Fold change
ns
WT
CtsZ-/-
G
Oxidative stress
*p=0.0264
MFI (APC)
WT
CtsZ-/-
H
WT
Ctsz-/-
Control
PNGase F
Control
PNGase F
Total Cathepsin L (Immunoblot)
Pro-CatL
SC
HC
I
WT
Ctsz-/-
Total Secreted Cathepsin L (Immunoblot)
Pro-CatL
SC
HC
J
Secreted pro-CatL
*p=0.0111
Total Pro-Cathepsin L fold change
WT
Ctsz-/-
Secreted CatL-SC
****p<0.0001
Total Cathepsin L single-chain fold change
WT
Ctsz-/-
Secreted CatL-HC
ns
Total Cathepsin L single-chain fold change
WT
Ctsz-/-

Figure 5.3. Cathepsin L single-chain accumulation was not due to direct cathepsin X cleavage, lysosomal oxidative stress, glycosylation or cathepsin L secretion. A. Cleavage assay of human recombinant cathepsin X on human recombinant cathepsin L single chain form as shown by cathepsin L immunoblot. **B.** Cleavage assay of human recombinant cathepsin L single chain on human recombinant cathepsin X as shown by cathepsin X immunoblot and BMV109 labelling. **C.D.E.** Cleavage assays of cathepsin X on cathepsin L single chain form, legumain on cathepsin L single chain form, and legumain on trypsinogen as shown by Coomassie stain. **F.** Quantitative PCR analysis of cathepsin L mRNA normalised to mouse GAPDH in WT and cathepsin X deficient DC1940 cells relative to WT cells (fold-change). Statistics were performed using the unpaired Student's t-tests. n=3. **G.** Quantification of lysosomal oxidative stress using CellROX™ Deep Red Reagent in WT and cathepsin X deficient DC1940 cells. Statistics were performed using unpaired Student's t-tests. n=3. **H.** Cell lysates were pretreated with PNGase F and shown by cathepsin L immunoblot. **I.** Cathepsin L secretion in WT and *Ctsz*$^{-/-}$ cells, as shown by cathepsin L immunoblot. **J.** Densitometry of secreted 35 (pro-cathepsin L), 27 (single chain), and 23 (heavy chain) kDa bands displayed the average intensity relative to the WT cells (fold change). Statistics were performed using unpaired Student's t-tests. n=3. Error bars represent SEM. ns $P > 0.05$, *$P \leqslant 0.05$, **$P \leqslant 0.01$, ***$P \leqslant 0.001$, **** $P \leqslant 0.0001$.

5.2.4 Cathepsin L can be localised in the nucleus.

In addition to secretion, cathepsin L is known to be trafficked to the nucleus in an importin β-dependent manner (**Figure 5.4A**) [32]. We subsequently did immunofluorescence, looking at the localisation of cathepsin X and L in the DC1940 cells. For cathepsin X, its staining avoided the nucleus, indicating its localisation was mainly in the cytoplasm (lysosomal). The staining of cathepsin L was more dispersed than that of cathepsin X (**Figure 5.4B**). We believed that cathepsin L was present in the cytoplasm and the nucleus. Furthermore, we quantified the cathepsin L that resided in the nucleus in WT and *Ctsz*$^{-/-}$ DC1940 cells and found that the nuclear level of cathepsin L in the *Ctsz*$^{-/-}$ DC1940 cells was significantly less (0.93-fold, p=0.0002) (**Figure 5.4CD**).

The human oral squamous carcinoma cells (HSC-3) were also applied to investigate the localisation of cathepsin L. Unexpectedly, we found a high nuclear cathepsin L localisation in those cells. Conversely, cathepsin X was still mostly cytosolic (**Figure 5.4E**). As HSC-3 cells showed a profound cathepsin L nuclear staining, we treated them with the cathepsin X inhibitor Biotin-Hex-Nle-SY and compared them with DMSO-treated cells. Similarly, we found that cells with cathepsin X inhibition showed a significantly lower nuclear cathepsin L level (0.83-fold, p<0.0001) (**Figure 5.4FG**).

These data showed that the nuclear localisation of cathepsin L is potentially mediated by cathepsin X activity. The loss of cathepsin X activity may result in an impaired cathepsin L nuclear localisation.

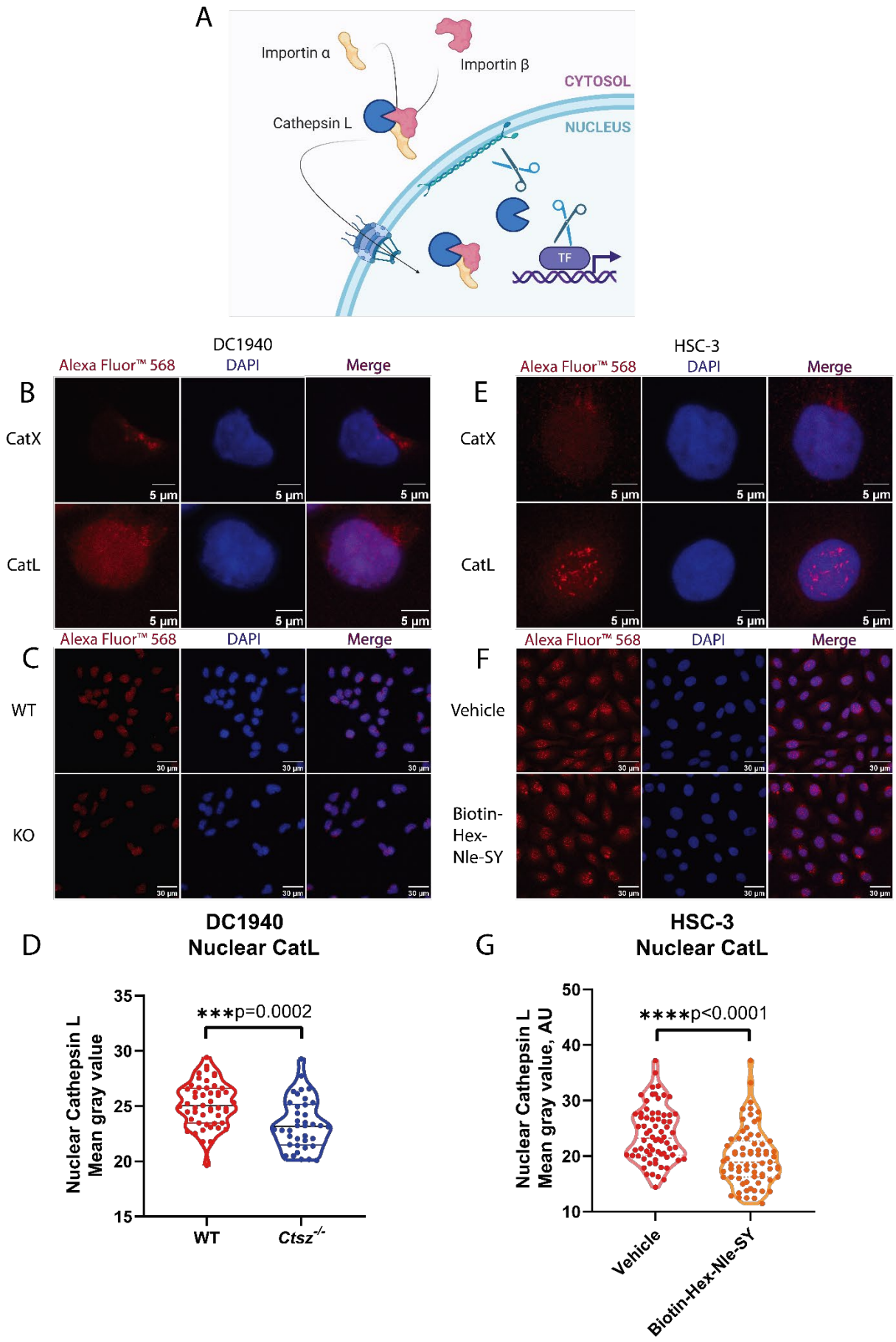
A
Importin α
Importin β
CYTOSOL
NUCLEUS
Cathepsin L
TF
DC1940
HSC-3
Alexa Fluor™ 568
DAPI
Merge
B
CatX
CatL
E
C
WT
KO
F
Vehicle
Biotin-Hex-Nle-SY
5 µm
30 µm
D
DC1940 Nuclear CatL
Nuclear Cathepsin L Mean gray value
***p=0.0002
WT
Ctsz-/-
G
HSC-3 Nuclear CatL
Nuclear Cathepsin L Mean gray value, AU
****p<0.0001
Vehicle
Biotin-Hex-Nle-SY

Figure 5.4. Cathepsin L is also localised in the nucleus. A. Pathway of cathepsin L transportation into the nuclear compartment. Created with BioRender.com. **B.** Intracellular cathepsin X/L in naïve DC1940 cells as shown by immunofluorescence. Scale bar = 5µm. **C.** Intracellular cathepsin L in WT and *Ctsz*$^{-/-}$ DC1940 cells as shown by immunofluorescence. Scale bar = 30µm. **D.** Quantification of nuclear cathepsin L in naïve WT and *Ctsz*$^{-/-}$ DCs. Statistics were performed using unpaired Student's t-tests. **E.** Intracellular cathepsin X/L in HSC-3 human oral squamous carcinoma cells as shown by immunofluorescence. Scale bar = 5µm. **F.** Intracellular cathepsin L in Vehicle treated and cathepsin X inhibitor (Biotin-Hex-Nle-SY) treated HSC-3 cells as shown by immunofluorescence. Scale bar = 30µm. **G.** Quantification of nuclear cathepsin L in HSC-3 cells treated with vehicle or the cathepsin X inhibitor Biotin-Hex-Nle-SY. Statistics were performed using unpaired Student's t-tests.

5.2.5 Cathepsin X-deficient cells exhibited impaired cathepsin L nuclear localisation and nuclear proteolysis.

To confirm the localisation of cathepsin L and X, we fractionated the nucleus and cytosol of DC1940s and looked at the nuclear localisation of several lysosomal proteases. The purity of the cytosolic fraction and the nuclear fraction was confirmed by their specific markers, Tubulin and Lamin A, respectively.

Our data showed that cathepsin B and X were mainly in the cytosolic (lysosome-containing) fraction and were absent in the nuclear fraction (**Figure 5.5A**). Conversely, cathepsin L, H, S and legumain were in cytosolic and nuclear fractions. Legumain was found in the nucleus in its mature form (**Figure 5.5A**). Cathepsin S was in the nucleus with a molecular weight slightly higher than its mature cytosolic form (**Figure 5.5A**). Cathepsin H was in the nucleus only in its single-chain form (**Figure 5.5A**).

Consistent with our previous data, cathepsin L was present in the cytosolic fraction, mainly in its heavy chain form in WT cells. Cathepsin X-deficient cells exhibited an accumulation of cathepsin L single chain in the cytosolic fraction (**Figure 5.5AB**). However, cathepsin L was in the nucleus only in its heavy chain form, regardless of the presence of cathepsin X (**Figure 5.5A**). In addition, we found that the level of nuclear cathepsin L was reduced in cathepsin X-deficient DCs (0.23-fold, p=0.0028, **Figure 5.5C**).

To investigate whether an active cathepsin X was required for cathepsin L nuclear localisation, we fractionated *Ctsz*$^{-/-}$ that re-express WT, C94S or R40H cathepsin X. Cathepsin X-deficient cells and rC94S cells showed significantly lower levels of nuclear cathepsin L than WT, rWT or rR40H cells (**Figure 5.5BC**). Therefore, in the absence of active cathepsin X, the cathepsin L single chain accumulated in the cytoplasm and trafficking of the heavy chain to the nucleus was impaired.

As legumain also alters the processing of cathepsin L, we examined cathepsin L localization in DCs after treatment with a legumain inhibitor, SD134. Legumain inhibition led to a pronounced accumulation of cathepsin L single chain and loss of the heavy chain in the cytosolic fraction (**Figure 5.5D**). Moreover, legumain inhibition significantly reduced nuclear cathepsin L levels (0.60-fold, p=0.0243, **Figure 5.5E**). Inhibiting legumain activity in the context

of cathepsin X deficiency further augmented cathepsin L single chain accumulation and reduced nuclear cathepsin L levels (0.18-fold, p=0.0032, **Figure 5.5E**)

As nuclear cathepsin L has been shown to cleave lamin B1 [35], we subsequently examined lamin B1 processing in cells lacking nuclear cathepsin L due to cathepsin X deficiency, legumain inhibition or both. Full-length lamin B1 (~60 kDa) and its processed form at ~25 kDa were observed. The processed form was diminished in the absence of cathepsin X or legumain activity and even more so in cells lacking the activity of both proteases (**Figure 5.5D**).

Overall, the data showed that the localisation of cathepsin L depends on active cathepsin X and that the processing of nuclear cathepsin L substrates is regulated by cathepsin X and legumain.

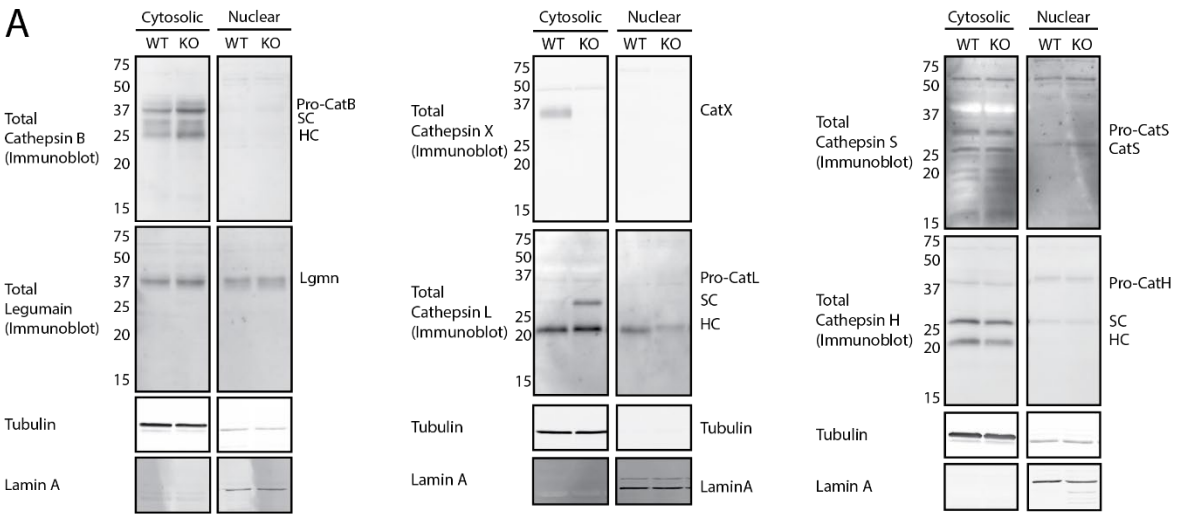
A
Cytosolic
Nuclear
WT KO WT KO
Total Cathepsin B (Immunoblot)
Pro-CatB
SC
HC
Total Legumain (Immunoblot)
Lgmn
Tubulin
Lamin A
Total Cathepsin X (Immunoblot)
CatX
Total Cathepsin L (Immunoblot)
Pro-CatL
SC
HC
LaminA
Total Cathepsin S (Immunoblot)
Pro-CatS
CatS
Total Cathepsin H (Immunoblot)
Pro-CatH
SC
HC
75
50
37
25
20
15

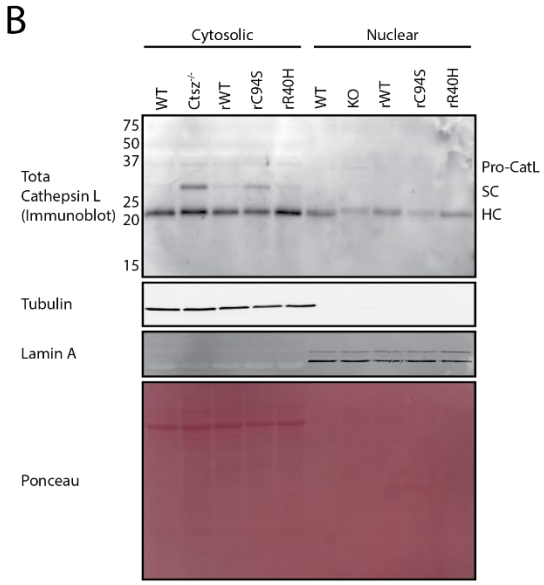
B
Cytosolic
Nuclear
WT
Ctsz-/-
rWT
rC94S
rR40H
KO
Tota Cathepsin L (Immunoblot)
Pro-CatL
SC
HC
Tubulin
Lamin A
Ponceau
75
50
37
25
20
15

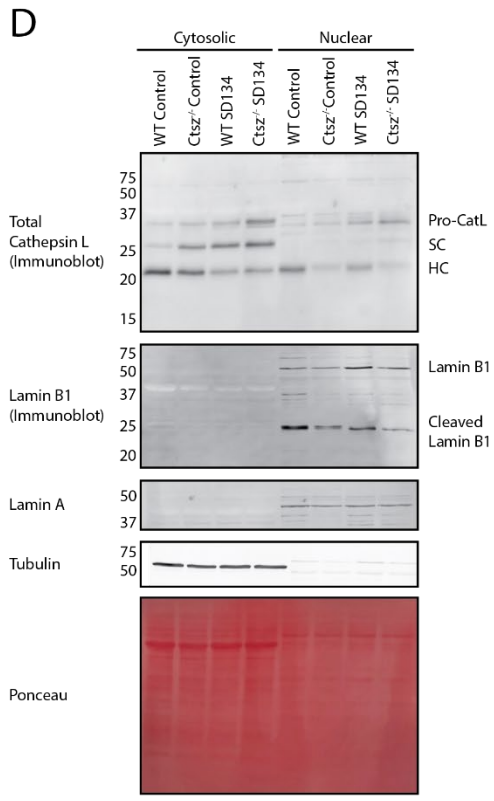
D
Cytosolic
Nuclear
WT Control
Ctsz-/- Control
WT SD134
Ctsz-/- SD134
Total Cathepsin L (Immunoblot)
Pro-CatL
SC
HC
Lamin B1 (Immunoblot)
Lamin B1
Cleaved Lamin B1
Lamin A
Tubulin
Ponceau
75
50
37
25
20

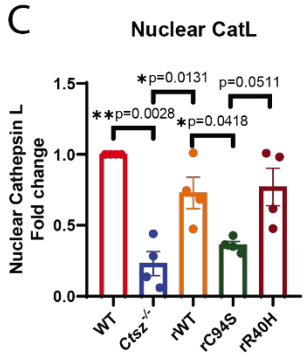
C
Nuclear CatL
Nuclear Cathepsin L Fold change
*p=0.0131
p=0.0511
**p=0.0028
*p=0.0418
1.5
1.0
0.5
0.0
WT
Ctsz-/-
rWT
rC94S
rR40H

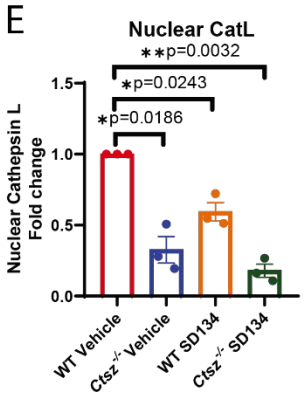
E
Nuclear CatL
Nuclear Cathepsin L Fold change
**p=0.0032
*p=0.0243
*p=0.0186
1.5
1.0
0.5
0.0
WT Vehicle
Ctsz-/- Vehicle
WT SD134
Ctsz-/- SD134

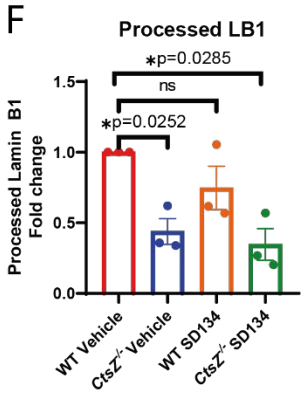
F
Processed LB1
Processed Lamin B1 Fold change
*p=0.0285
ns
*p=0.0252
1.5
1.0
0.5
0.0
WT Vehicle
Ctsz-/- Vehicle
WT SD134
Ctsz-/- SD134

Figure 5.5. Cathepsin X deficiency impaired cathepsin L nuclear localisation and nuclear proteolysis. A. Cathepsin B, H, L, S, X and legumain immunoblot in the cytosolic and nuclear fraction. Tubulin expression was used as a cytosolic marker and loading control. Lamin A expression was used as a nuclear marker and loading control. **B.** Cathepsin L immunoblot in the cytosolic fraction and nuclear fraction of WT, *Ctsz*$^{-/-}$, rWT, rC94S, rR40H DC1940 cells. Tubulin expression was used as a cytosolic marker and loading control. Lamin A expression was used as a nuclear marker and loading control. Ponceau stain was used as a second measure of protein loading. **C.** Densitometry analysis of nuclear 23kDa bands detected by cathepsin L immunoblot displayed the average intensity normalised to WT (fold change). Statistics were performed using unpaired Student's t-tests. n=4. **D.** Cathepsin L and Lamin B1 immunoblot in the cytosolic fraction and nuclear fraction in WT or *Ctsz*$^{-/-}$ cells treated with or without legumain inhibitor SD134 (100 µM). Tubulin expression was used as a cytosolic marker and loading control. Lamin A expression was used as a nuclear marker and loading control. Ponceau stain was used as a second measure of protein loading. **E.** Densitometry analysis of nuclear 23kDa bands detected by cathepsin L immunoblot displayed average intensity normalised to WT control (fold change). Statistics were performed using unpaired Student's t-tests. n=3. Error bars represent SEM. **F.** Densitometry analysis of processed lamin B1 (25 kDa) detected by lamin B1 immunoblot displayed average intensity normalised to WT control (fold change). Statistics were performed using unpaired Student's t-tests. n=3. Error bars represent SEM. ns $P > 0.05$, *$P \leqslant 0.05$, **$P \leqslant 0.01$, ***$P \leqslant 0.001$, **** $P \leqslant 0.0001$.

5.3 Discussion:

In this chapter, we assessed the impact of cathepsin X deficiency on related lysosomal proteases and their inhibitors. Among all the proteases and inhibitors we examined, cathepsin L was the only protein altered by cathepsin X deficiency. Specifically, we observed accumulation of the cathepsin L heavy chain in the absence of cathepsin X, and this effect was confirmed to be dependent on the activity of cathepsin X but not its integrin-binding functions.

Cathepsin L processing from the single chain into its heavy chain has been characterised as legumain dependent. Both legumain inhibition and genetic deletion resulted in the accumulation of cathepsin L single chain and reduced level of cathepsin L heavy chain [203-205]. Legumain expression and activity, however, were not altered in the context of cathepsin X deficiency, suggesting that cathepsin X does not regulate cathepsin L processing through modification of legumain activity.

We also examined differences in cathepsin L processing between cathepsin X deficiency and legumain inhibition. Usually, when a protein is cleaved to produce a more mature form, the loss of its immature form is concomitant with the appearance of the mature form. In legumain-deficient mice, cathepsin L accumulates in its single-chain form, and no heavy chain can be detected [204]. In our legumain inhibition experiments, we also observed accumulation of cathepsin L single chain and loss of the heavy chain. By contrast, however, cathepsin X-deficiency increased the cathepsin L single chain without affecting heavy chain levels. This suggests that legumain and cathepsin X may regulate cathepsin L through distinct mechanisms.

To investigate whether cathepsin X activity is required for its effects on cathepsin L, we first rescued it back into the cathepsin X-deficient cells. We found that cells expressing inactive cathepsin X behaved similarly to cathepsin X-deficient cells, showing an accumulation of cathepsin L single chain. The rescued assay proved that the altered processing of cathepsin L depended on active cathepsin X, whether directly or indirectly.

Cathepsin X is an exopeptidase that cleaves off one amino acid at a time from the carboxy terminus of its substrates. Cathepsin B, the cathepsin most similar to cathepsin X, is primarily a dipeptidyl carboxypeptidase (DPCP) but also exhibits endopeptidase activity [206]. We used a recombinant protein cleavage assay to query whether cathepsin X may have a potential

endopeptidase activity to process the cathepsin L. Our result showed that cathepsin X did not directly cleave cathepsin L single chain to its two-chain form. As a result, although cathepsin X activity may be required for the conversion, the effect is not driven by direct cleavage.

Interestingly, we also found that legumain could not directly cleave cathepsin L single chain to generate its two-chain form. It is widely accepted in the field that cathepsin L processing is stalled by legumain deficiency; however, no studies have proven that legumain performs the cleavage directly. Possibly, the in vitro conditions of our experiment did not fully recapitulate the cellular conditions. Additional chaperones or binding partners may be required to initiate cleavage. Alternatively, legumain may not directly cleave cathepsin L single chain. An intermediate protease might mediate the cleavage of cathepsin L single chain, and legumain plays a role in activating this intermediate unknown protease directly or through the degradation of an inhibitor of that protease. Without legumain activity, the intermediate unknown protease may not be activated, thus unable to process cathepsin L.

However, Colbert and colleagues reconstituted legumain in live macrophages, which could not process the cathepsin L single chain into its heavy-chain form [207]. Briefly, they isolated bone marrow-derived macrophages from legumain-deficient mice and showed accumulation of cathepsin L single chain. They further reconstituted legumain by adding recombinant legumain to the cell culture. The recombinant legumain was endocytosed, and western blot analysis confirmed that the endocytosed pro-legumain was processed into active legumain. Unexpectedly, restoring intracellular legumain reversed the accumulation of single chain cathepsin D but failed to process cathepsin L single chain into the heavy chain [197, 207]. Therefore, whether cathepsin L processing is regulated by legumain activity remains a question and needs further validation. It will be critical to immunoprecipitate cathepsin L in multiple forms and determine the exact cleavage site using mass-spectrometry techniques. This method will tell us whether the C-terminus of the heavy chain ends in asparagine, which would indicate direct cleavage by legumain.

We next sought alternative explanations for the increased total level of cathepsin L in cathepsin X-deficient cells. We first hypothesised that the expression of cathepsin L was increased due to lysosomal oxidative stress. However, we did not observe differences in the mRNA level of cathepsin L between WT and *Ctsz*$^{-/-}$ cells. We also questioned whether cathepsin X deficiency altered cathepsin L secretion and subsequently caused the stalling of a

single chain in the cytosol. By contrast, cathepsin X-deficient cells secreted more cathepsin L pro-form and single chain. As such, the mechanism by which cathepsin X regulates cathepsin L levels remains poorly understood, but we instead turned to identifying possible consequences.

Ultimately, we found cathepsin L could be localised into the nucleus, and when cathepsin L single chain was accumulating in the cell cytosolic fraction, we observed a decreased level of nuclear cathepsin L. This discovery is very striking; however, one crucial question must be solved. Cathepsin L accumulation in the cytosol was in its single-chain form, while cathepsin L localised in the nucleus was already processed into heavy-chain. The relationship between the cytosolic (lysosomal) single chain and the nuclear heavy chain remains unclear.

Another question remains: how exactly cathepsin L is translocated into the nucleus, and how is this dependent on cathepsin X activity? Using the cNLS Mapper (nls-mapper.iab.keio.ac.jp), the nuclear localisation signals recognised by importin α for multiple proteases were summarised in the below table (**Table 5.1**) [208-210]. The search was conducted with a cut-off score of 5: Score $\geqslant$8, and the protein is exclusively localised in the nucleus; 8$\geqslant$Score$\geqslant$6, the protein is partially localised in the nucleus; 6$\geqslant$Score$\geqslant$3, the protein is localised both in the nucleus and in the cytoplasm; Score <3, the proteins is localised in the cytoplasm [208].

We identified that murine cathepsin L contains both a monopartite and a bipartite NLS sequence. The classical NLS can be divided into monopartite NLS and bipartite NLS. The mono partite NLS contains a single cluster of consecutive basic amino acids – K(K/R)X(K/R) [211]. In murine cathepsin L, the monopartite NLS signal contains a string of “KKGR”, which can serve as the NLS signal. On the other hand, bipartite NLS contains two clusters of basic residues and a 10-12 amino acid linker [211]. Cathepsin L contains two possible bipartite NLS sequences with decent scores. The search results indicated that cathepsin L is likely transported to the nucleus in an importin α-dependent pathway. When importin α recognises the cNLS containing cargo, the complex forms a trimer with importin β1 and subsequently gets sent to the nucleus [212].

In contrast, none of the other lysosomal proteases we searched for contained a canonical NLS sequence as predicted by the cNLS mapper. Surprisingly, cathepsin H, S and legumain were found in the DC nuclear fraction even though the cNLS mapper did not observe an NLS

sequence (**Figure 5.5A, Table 5.1**). Cathepsin H exhibited a similar pattern in the cytosolic fraction, consisting of a pro-form, a single chain, and a heave chain. The loss of cathepsin X did not alter the processing of cathepsin H in the cytosol nor its nuclear localisation (**Figure 5.1D, Figure 5.5A**). We also found a species in the nuclear fraction using a cathepsin S-specific antibody. This species, however, has a slightly higher molecular weight than mature cathepsin S (25 kDa) (**Figure 5.5A**). We are currently unsure of the identity of this species and will need further validation using a cathepsin S genetic knockout cell line. Legumain was found in the nuclear fraction in its mature form (**Figure 5.5A**). It remained a question of how these lysosomal proteases were trafficked into the nucleus without a canonical NLS signal. Cathepsin H, S and legumain may contain a non-canonical NLS or be trafficked to the nucleus through an unknown pathway.

Table 5.1 Canonical Nuclear localisation signals of murine lysosomal proteases.

Name	Type	Position	NLS sequence	Score
Cathepsin B	Bipartite	19	DKPSFHPLSDDLINYINKQNTTWQAGRN	2.1
Cathepsin C	-	-	-	-
Cathepsin H	Bipartite	28	IEKFHFKSWMKQHQKTYSSVEYNHRLQMF	2.0
Cathepsin L	Monopartite	96	RHQKHKKGRLFQE	4.0
	Bipartite	96 289	RHQKHKKGRLFQEPLMLKIPK DSNKNKYWLVKNSWGSEWGMEGYIKIAKD	5.0 6.1
Cathepsin S	Bipartite	301	DYWLVKNSWGLNFGDQGYIRMARNNKNHCGI	2.1
Cathepsin X	Bipartite	24	RARLYFRSGQTCYHPIRGDQLALLGRRTYP	2.0
Legumain	-	-	-	-

Proline-tyrosine-NLS (PY-NLS) is the most characterised non-canonical NLS. The consensus sequence is represented as [basic/hydrophobic]-X_n-[R/H/K] -$(X)_{2–5}$-PY, where "X" refers to any amino acid [213]. Such NLS-containing proteins are trafficked to the nucleus through importin β2 [214]. We found that cathepsin H contains a possible PY-NLS sequence: ^{85}**FA**E**IKHKFLW**SEPQNCS**A**T**K**SN**YLR**GTG**PY**^{114}. However, we did not find any PY-NLS in legumain or cathepsin S. There are other types of non-canonical nuclear localisation signals, including KRX(W/F/Y)XXAF and (P/R)XXKR(K/R), which bind directly to importin α [209], and arginine-rich sequences that can bind to importin β1 [215]. However, neither cathepsin S nor legumain contains the above-mentioned NLS. Other chaperone proteins may facilitate the nuclear localisation of these lysosomal proteases.

For cathepsin L, the first NLS could serve as both monopartite NLS or bipartite NLS. The first bipartite NLS sequence is located at the intersection of the activation peptide and the heavy chain, indicating the pro-cathepsin L can be trafficked to the nucleus. Our data showed a high molecular form of cathepsin L at ~40 kDa, which might be the pro-cathepsin L. This needs to be further validated with genetic knockout models or mass-spectrometry. The second bipartite NLS sequence is located at the intersection of the second pro-peptide and the light chain. This location indicates that cathepsin L must be transported into the nucleus in the complete single chain form. However, in our nuclear fraction, we observed that the nuclear cathepsin L was mostly in its heavy chain form. Therefore, there might be some processing of cathepsin L in the nucleus. Legumain still exists in the nuclear fraction, so it may further process cathepsin L (**Figure 5.5A**). Sullivan and colleagues showed that in human colon adenocarcinoma, cathepsin L was localised in the nucleus in both pro-form and heavy chain fo, supporting our data [216].

In DC190 cells, nuclear cathepsin L was mainly in the heavy chain form, which agrees with several other published studies [217, 218]. Burton et al. demonstrated a possible pathway of nuclear localisation of cathepsin L heavy chain through the importin β1 pathway [32]. The trafficking of cathepsin L heavy chain into the nucleus depends on the snail transcription factor. Snail acts as a chaperone protein interacting with cathepsin L. The snail contains an NLS peptide sequence and was found to be critical for the translocation of cathepsin L into the nucleus. Therefore, it seems the nuclear trafficking of cathepsin L is independent of its own

NLS sequences. Whether or not other lysosomal proteases can be sent to the nucleus in a similar pathway needs further validation.

Another research paper proposed a cathepsin L nuclear localisation mechanism by alternative splicing. They showed that a variant of cathepsin L devoid of the signal peptide did not go through canonical trafficking to the lysosomes but to the nucleus [219]. This alternatively spliced form starts at methionine at position 56 and is upstream of the first bipartite NLS sequences. This opened a new route to investigate alternative splicing of cathepsin L in cathepsin X-deficient cells and raised the question of whether different iso-forms of cathepsin L observed in our western blots were cathepsin L alternative splicing forms rather than differentially cleaved forms. As legumain and cathepsin X could not directly cleave cathepsin L single chain, conducting quantitative PCR and RNAseq to investigate alternative splicing of cathepsin L in cathepsin X/legumain deficient cells will be critical.

To determine whether cathepsin L is trafficked directly to the nucleus upon synthesis or first trafficked to the lysosome, the Retention Using Selective Hooks (RUSH) system can be used. The RUSH system consists of a hook protein fused to core streptavidin and stably anchored in the donor compartment, such as the ER or Golgi, and fluorescent-tagged cathepsin L fused with a streptavidin-binding peptide. The addition of biotin will release fluorescent-tagged cathepsin L, allowing us to monitor the trafficking of cathepsin L using live cell imaging [220].

Eventually, we wish to investigate the substrates of nuclear cathepsin L. Several nuclear substrates of cathepsin L were published, including the CCAAT-displacement protein/cut homeobox (CDP/Cux) transcription factor and Lamin B1 [35, 221]. We also validated that the nuclear processing of Lamin B1 was impaired when there was less nuclear cathepsin L due to cathepsin X deficiency or legumain inhibition. To broadly investigate nuclear cathepsin L nuclear substrates, we plan to do N-terminomics with our cathepsin X-deficient cells [54].

Chapter 6. Final discussion:

Cathepsin X is a lysosomal cysteine protease. It is tightly associated with various diseases, including cancer and neuron inflammation [30, 58, 60, 65]. There is also evidence showing cathepsin X may exacerbate the progression of such diseases, and its inhibition leads to mitigation of disease progression [30, 61, 222]. However, the function of cathepsin X in normal physiological conditions remains poorly understood. The expression of cathepsin X is mainly restricted to immune cells, including monocytes, macrophages and dendritic cells [223]. In order to better understand the role of cathepsin X in disease development and ultimately use it as a therapeutic target, more information is required for its role in normal physiology.

We hypothesise that cathepsin X may play a role in dendritic cell immune function. We first characterised cathepsin X in dendritic cells during DC maturation. In **Chapter 3**, we characterised the cathepsin X activity/expression change during CpG-mediated DC maturation using a cathepsin X-specific probe sCy5-Nle-SY. We reported that the level of cathepsin X was significantly increased after CpG priming, and IL-6 caused this upregulation. Although the results seem promising, some issues still need to be addressed.

Firstly, according to Yan et al., IL-6 and IL-10 both activate the STAT3 signalling pathway and increase the expression of cathepsins [21]. Unexpectedly, we only observed an upregulation of cathepsin X after IL-6 treatment but not IL-10. IL-10 is an anti-inflammatory cytokine compared to IL-6, a pro-inflammatory cytokine. Even though both cytokines phosphorylate and activate STAT3, there are some differences in the signalling pathway. IL-6 phosphorylates STAT3, and the phosphorylation declines rapidly. Conversely, IL-10 phosphorylates STAT3 while the phosphorylation remained up to 2 hours post-treatment. These temporal differences resulted in a similar transcriptional response between IL-6 and IL-10 in the initial STAT3 phosphorylation but a significantly different transcriptional response later [224]. The difference between IL-6 and IL-10 STAT3 signalling may explain why only IL-6 – STAT3 signalling induced cathepsin X upregulation. From the perspective of DC immunity, cathepsins are required in various immune responses, including antigen processing, presentation, and cytokine regulation. It seems reasonable to think that a pro-inflammatory cytokine (IL-6) contributes to the upregulation of cathepsins, while an anti-inflammatory cytokine (IL-10) does not.

We previously showed that an NF-κB inhibitor did not blunt the upregulation of cathepsin X upon CpG activation and concluded that the upregulation was independent of NF-κB signalling. However, the expression of pro-inflammatory cytokines is directly regulated by NF-κB signalling. Therefore, when NF-κB signalling was inhibited, we would expect less secretion of pro-inflammatory cytokines and, subsequently, less STAT3 activation. Our explanation is that the NF-κB activation inhibitor we used did not entirely block the expression of IL-6. Even though we saw a significant reduction in IL-6 secretion (**Figure 3.5A**), the reduced level of IL-6 was enough to elicit the upregulation of cathepsin X.

Furthermore, we saw that CpG + IFNϒ co-treatment reverted the upregulation of cathepsin X caused by CpG alone. We first thought the co-treatment might reduce the secretion of IL-6. Conversely, the co-treatment induced a higher transcription and secretion of IL-6, according to our data and Marraco et al. [81]. These results showed that the regulation of cathepsin X by cytokines is sophisticated.

We also investigated the active and total levels of other related lysosomal cysteine proteases and inhibitors during DC maturation. Apart from cathepsin X, we found that the pro- and intermediate forms of cathepsin B and L were significantly increased in CpG-activated cells. Pro-legumain was also upregulated. We speculated that these lysosomal proteases were upregulated similarly through STAT3 activation according to the literature [197, 225]. Cathepsin S, however, was downregulated after CpG activation. Chan and colleagues reported that cathepsin S upregulation could be induced by IFNϒ through STAT1 signalling in human macrophages [183]. They further reported that IL-10 downregulated cathepsin S through STAT3 signalling activation. As described above, although IL-6 and IL-10 both activate the STAT3 signalling pathway, they could exhibit different transcriptional responses over a more extended period. Thus, the different regulation of cathepsin S may suggest that it has a distinct role in DC function compared to other lysosomal cysteine proteases.

Our data showed that the cysteine inhibitor cystatin C was downregulated and agreed upon, as previously reported [174]. Xu and colleagues reported that the expression of Cystatin C depended on the transcription factor IFN regulatory factor 8 (IRF8). IRF8 expression was reduced when IL-10 was secreted from CpG-activated DCs. The reduced IRF8 expression subsequently reduced the level of Cystatin C. Collectively, the upregulation of multiple

lysosomal proteases and the downregulation of cysteine protease inhibitor cystatin C pointed out that lysosomal proteolysis may play a vital role during DC maturation and function.

The apparent upregulation of cathepsin X made us further hypothesise that it might be required by dendritic cells during maturation for their function. We, therefore, generated a cathepsin X deficient cell line and analysed the impact of cathepsin X deficiency on DC function. In **Chapter 4,** we conducted several functional assays to investigate the role of cathepsin X in the DC function. We found that cathepsin X was dispensable for DC maturation, fluid-phase endocytosis, antigen presentation, and secretion of most pro-inflammatory cytokines.

As we did not find any profound impact of cathepsin X deficiency on DC immunity, we conducted shotgun proteomics to broadly investigate the impact of cathepsin X deficiency on DC biology. In the shotgun proteomics, we observed an additional 39 proteins that were significantly enriched in wild-type cells and 17 proteins that were enriched in *Ctsz*$^{-/-}$ cells after CpG activation. We re-expressed cathepsin X in the *Ctsz*$^{-/-}$ cells (rWT) and compared the peptides enriched in rWT cells with *Ctsz*$^{-/-}$ cells after CpG activation. We further validated that 2 proteins were constantly enriched in wild-type and rWT cells. These 2 proteins were Cathepsin X (*Ctsz*) and Nectin-1 (*Nectin-1*). In addition, 4 proteins were significantly enriched in *Ctsz*$^{-/-}$ cells, including Transmembrane protein 176b (*Tmem176b*), Stefin A2 (*Stfa2*), and Anthrax toxin receptor 2 (*Antxr2*), CD302 antigen (*Cd302*).

Transmembrane protein 176b, as mentioned in **Chapter 4,** may provide an alternative explanation for impaired IL-1β secretion in cathepsin X deficient cells. The drawback of the experiment was that conventional DCs did not exhibit profound inflammasome activation. In the shotgun proteomics, we observed a significant enrichment in NLRP3 and Caspase-1, indicating that DC1940 cells had some extent of NLRP3 inflammasome priming upon CpG treatment. However, the level of IL-1β secretion was deficient. We hope to test our hypothesis using other cell types, such as THP1-derived macrophages, splenic cDC2 dendritic cells, and bone marrow-derived macrophages/dendritic cells.

Nectin-1 was significantly enriched in WT cells. Nectin-1 is an immunoglobulin-like cell adhesion molecule located on cell membranes. In the neuronal system, nectin-1 has been found to localize at the presynaptic cell membrane and promote the formation of synapses [226]. Nectin-1 is also involved in other cellular biology, including cell migration, adhesion,

and proliferation [227]. Nectin-1 has been characterised to have a role in herpes simplex virus I (HSV-1) entry on primary murine dermal fibroblasts [228].

Anthrax Toxin Receptor 2 (ANTXR2, also named capillary morphogenesis gene 2 (CMG2)) is significantly enriched in *Ctsz*$^{-/-}$ cells. It is a membrane protein that binds to Anthrax toxin protective antigen and facilitates receptor-mediated endocytosis [229]. Apart from its anthrax toxin binding ability, its mutation causes autosomal recessive syndromes, including Juvenile hyaline fibromatosis (JHF) and infantile systemic hyalinosis (ISH) [230]. Fibroblasts collected from both JHF and ISH patients showed an impaired ability to attach to the Laminin matrix, while attachments to collagen type I and IV were not affected, indicating that ANTXR2 had a potential role in cell adhesion [230].

CD302 belongs to the C-type lectin receptors family. CD302 is highly expressed in macrophages and dendritic cells. CD302 colocalises with F-actin and may have a role in adhesion and migration. In addition, C-type lectin receptors can act as pattern recognition receptors and mediate endocytosis.[231].

It does not look like a coincidence that multiple significantly enriched proteins enriched in the shotgun proteomics were found to be membrane-anchored proteins, including Nectin-1, TMEM176B, ANTXR2, and CD302. Obermajer et al. reported that cathepsin X trafficked the plasma membrane during cell maturation and mediated a cleavage on the Mac-1 surface receptor [3]. However, in **Chapter 3.2.3**, we did not see such a relocation of cathepsin X. In DC1940 cells, cathepsin X likely remained in the cytosolic lysosomes during DC maturation **(Figure 3.3A)**. All the data from our results and the literature suggested that cathepsin X may alter membrane-anchored proteins through its enzymatic activity or an unknown mechanism.

Nectin-1, ANTXR2 and CD302 are all involved in endocytosis and have their specific antigens. In **Chapter 4**, we examined the impact of cathepsin X deficiency in endocytosis using Lucifer Yellow and homemade Cy5-OVA. Both substances were taken up by fluid-phase endocytosis independent of surface receptor binding[232, 233]. This may explain why we did not observe any differences in endocytosis.

Nectin-1, ANTXR3, and CD302 also involve cell adhesion and migration. We investigated whether cathepsin X deficiency altered cell adhesion with or without laminin coating. However, we did not see any differences in cell adhesion. We have not yet examined if

cathepsin X deficiency would alter cell migration. DC migration is an important feature of dendritic cell immune function. After exposure to antigens, DCs need to migrate from inflamed peripheral tissue to the draining lymph nodes to prime naïve T cells [234]. DC migration can be analysed using the Transwell migration assay in the future [235].

Stefin A2 belongs to the A family of cystatins, and there are three different variants of Stefin As, including Stfa1, Stfa2 and Stfa3. Stfa2 is a potent inhibitor for endopeptidase papain and cathepsin L and S [236]. The significant increase of Stfa2 in cathepsin X deficient cells further showed the impact of cathepsin X deficiency on the lysosomal proteolytic network, as we showed in **Chapter 5**. However, how the increased level of Stfa2 affects the overall proteolysis remained to be tested. *Ctsz*$^{-/-}$ cells exhibited increased active cathepsin L single chain level and may increase overall lysosomal proteolysis [200]. The cells may respond to the increased proteolysis and increase the expression of Stfa2 to maintain lysosomal homeostasis.

Overall, we found cathepsin X was dispensable for most immune functions we investigated. In **Chapter 3**, we saw that the upregulation of cathepsin X occurs late (24-32h post activation). The late response may explain the dispensable role of cathepsin X in these immediate immune functions. DC maturation markers and cytokine expression are directly promoted by NF-κB signalling (https://www.bu.edu/nf-kb/gene-resources/target-genes/) and are transcribed much earlier. Therefore, according to the timeline, cathepsin X may not affect earlier immune responses, and we will assess the role of cathepsin X in an extended period of time in DC function [191, 192].

Alternatively, we suspected that the minor impact of cathepsin X on DC function was due to the compensatory mechanism of lysosomal proteases. Briefly, when the proteolytic activities of one or several proteases are diminished either by chemical inhibition or genetic deletion, the lysosomes become incapable of conducting proteolysis and may be overloaded with substrates. The host cells will respond to it by upregulating the expression of other related proteases to overcome the loss of proteolysis [175, 197].

Cathepsin B, an exo-dipeptidase in the cysteine cathepsin family, may compensate for the loss of the exo-monopeptidase activity of cathepsin X. Double deficiency of cathepsin B and cathepsin X had a synergistic role in preventing breast cancer metastasis and progression, indicating these two cathepsins may have some functional overlap [198].

In **Chapter 5**, we demonstrated that cathepsin X deficiency resulted in an accumulation of cathepsin L single chain. The accumulation of cathepsin L may also compensate for the loss of cathepsin X. Shirahama-Noda et al. reported that cathepsin L exhibited increased proteolytic activity when the single chain accumulated [200]. Therefore, in future experiments, it would be necessary to generate cathepsin B/X or cathepsin L/X double knockout cells to investigate further the role of lysosomal cathepsins in DC immune function.

Other than cathepsin L, in **Chapter 5**, we discussed the impact of cathepsin X on the general lysosomal proteolytic network. We screened and investigated the expression/processing of multiple lysosomal proteases and their inhibitors. However, we revealed that the loss of cathepsin X deficiency specially resulted in an increased level of single chain cathepsin L. Further investigation showed that the accumulation of cathepsin L single chain was not due to direct cathepsin X cleavage nor altered legumain, which had been shown in the literature to facilitate cathepsin L processing. We also showed that recombinant legumain could not process recombinant cathepsin L single chain into the heavy chain form. More and more evidence suggests that cathepsin L processing is not directly related to legumain cleavage [207]. We thus had a bold assumption that the different forms of cathepsin L were different spliced forms of cathepsin L. Cathepsin L alternative splicing had been studied in human fibroblasts and breast cancer cells [219, 237]. We hope to observe the cathepsin L splicing variant with RNA-Seq and explore the processing of cathepsin with different spliced forms.

Even though we did not have an explanation for the altered cathepsin L processing in cathepsin X deficient cells, we further found that cathepsin X deficient cells exhibited accumulation of cathepsin L single chain in the cytosolic fraction (including lysosomes). In contrast, the nuclear cathepsin L level was reduced. The reduced nuclear cathepsin L further impacted the proteolysis of nuclear proteins such as Lamin B1. However, we are still investigating how the accumulated lysosomal cathepsin L single chain affects nuclear cathepsin L, which is in the heavy chain form.

Studies of the mis-localisation of lysosomal proteases are emerging. In **Chapter 3**, we showed that CpG activation induced an increased secretion of cathepsin X, but we are currently unable to explain how cathepsin X was secreted and why its secretion was increased during DC maturation. Several hypotheses in the field uncover lysosomal protease secretion. Dongyao and colleagues raised the first hypothesis. They proposed that pro-inflammatory cytokines,

including IL-4, IL-6, and IL-10 cytokines, activate the unfolded protein response (UPR) and facilitate the secretion of cathepsins in their pro-forms. They showed that cathepsin B, L and S mainly were secreted under this mechanism. The secreted proteases could degrade the extracellular matrix and promote cancer cell invasion and inhibition of UPR-impaired cancer progression [212]. This hypothesis seemed to fit my data that during DC maturation, the cells start to secrete pro-inflammatory cytokines, increasing the expression of lysosomal proteases and their secretion. However, $CD8^+$ dendritic cells do not express IL-4. Even though they do express IL-4 receptors, we did not see IL-4 treatment alter cathepsin levels. This pathway may differ in different cell types.

There is a more recent proposed explanation of lysosomal protein secretion. Lysosomal proteins are trafficked into the lysosomes under the M6PR pathway. Several research groups showed that LYSET (TMEM251) was responsible for the stability of GlcNAc-1-phosphotransferase. The loss of LYSET failed M6P tagging and, subsequently, the secretion of lysosomal proteins, including lysosomal proteases [23, 238, 239]. Inspired by their fantastic research techniques and data, I wonder if the increased secretion of cathepsin X was due to the increased expression of cathepsin X. When cathepsin X expression was largely increased, the GlcNAc-1-phosphotransferase could not efficiently tag the excessive cathepsin X and resulted in the untagged cathepsin X getting secreted. However, this bold hypothesis needs further experimental validation. We could overexpress the GlcNAc-1-phosphotransferase and investigate whether a higher expression of GlcNAc-1-phosphotransferase could reduce the secretion of cathepsin X under CpG activation.

Nuclear localisation of lysosomal proteases is another example of mis-localisation and is not rare. A variety of research has reported the existence of nuclear localised lysosomal proteases. These nuclear proteases may cleave nuclear substrates and affect cell functions [31-37].

We also found that the nuclear localisation of lysosomal proteases differed in different cell lines. We did not observe nuclear cathepsin B in DC1940 cells. However, in HSC-3 human squamous carcinoma cells, we could spot nuclear cathepsin B (data not shown). Interestingly, research showed nuclear localisation of most lysosomal cathepsins, including cathepsin X, in kidney cells. They also found that the level of nuclear lysosomal proteases differs between normal and cancerous kidney cells, indicating that the nuclear localisation of lysosomal proteases may also indicate a role in disease progression [240].

Our knowledge of the route for lysosomal protease trafficking to the nucleus is scarce. We conducted a cNLS signal search and found that only cathepsin L had canonical NLS signals. However, other lysosomal proteases were also observed in the nucleus, and therefore, the nuclear localisation of those lysosomal proteases is not solely dependent on canonical NLS. The complexity of non-canonical NLS and cell line discrepancies make it hard to investigate the nuclear trafficking pathway. The RUSH system can be used as a powerful tool to track the trafficking of cathepsin L to the nucleus [220]. We hope future studies will give us more insights into the mechanism of nuclear localisation of lysosomal proteases.

Collectively, the data we generated may have some future implications for pathophysiology. We first showed that cathepsin X was primarily secreted as pro-forms. Pro-cathepsin X contains an RGD motif located on its pro-peptide sequence. The RGD motif can interact with β2 integrin receptors to promote pancreatic cancer cell proliferation and invasiveness through FAK/Src signalling [48]. The cancer microenvironment is usually coupled with increased infiltration of immune cells. Our result showed that cathepsin X was secreted by dendritic cells even in their naïve state. Therefore, more RGD-containing pro-cathepsin X may be released into the extracellular matrix, with more immune cells accumulating in the tumour microenvironment. Whether or not the proliferation/invasiveness of other cancer types can be triggered by RGD-FAK/Src signalling needs future validation. The level of secreted cathepsin X can potentially become a biomarker for cancer prognosis and a therapeutic target.

Cathepsin B is a carboxy-exo-dipeptidase. Therefore, it exhibited a similar proteolytic mechanism as cathepsin X. Regarding breast cancer, both cathepsin B and cathepsin X were found to play a role in cancer progression and metastasis. Co-inhibition/silencing of cathepsin B and cathepsin X has been shown to elicit a synergistic effect on preventing cancer progression and invasion [60, 198]. Therefore, when evaluating cathepsin X as a therapeutic target in cancer treatment, co-inhibition of both cathepsin B and X should be considered.

The data generated from the shotgun proteomics also indicated some new directions involving cathepsin X and disease progression. Nectin-1, an immunoglobulin-like cell adhesion molecule, is decreased in cathepsin X-deficient cells. Nectin-1 has been implicated in HSV-1 entry [228]. Therefore, the absence of cathepsin X may result in lower expression of Nectin-1 and subsequently reduce viral entry. ANTXR2, similar to Nectin-1, mediates Anthrax toxin endocytosis [229]. Conversely, its protein level was increased in cathepsin X-deficient cells.

Therefore, cathepsin X may play a protective role in preventing the endocytosis of Anthrax toxin.

In addition, cathepsin X has been reported to regulate IL-β secretion in the neuroinflammation model [30, 64]. Cathepsin X deficiency resulted in a reduction in IL-1β secretion while the mRNA expression of IL-1β remained constant. In addition, the literature reported that the modulation mechanism is through the integrin binding ability of pro-cathepsin X. We proposed a different mechanism in which cathepsin X modulates inflammasome activation through TMEM176B. We hypothesised that cathepsin X modulated IL-1β secretion through modulating calcium influx and was independent of pro-IL-1β mRNA expression. However, more evidence is required of how cathepsin X changes the expression of TMEM176B. Our data, consistent with Allan and colleagues' data, showed that cathepsin X deficiency reduced the secretion of IL-1β and may play a protective role in neuron inflammation diseases [30].

Furthermore, both cathepsin L and X have been reported to be overexpressed in neuroinflammation [30, 35]. Distortion of nuclear lamina structure is a newly discovered factor contributing to the progression of neuronal inflammation. Abnormally increased level of nuclear cathepsin L has been reported in AD patients' tissues and contribute to the excessive cleavage of Lamin B1, exacerbating AD progression. Our results showed a novel linkage between cathepsin L and X. The loss of cathepsin X activity resulted in the stalling of cathepsin L single chain in the cytosol and preventing cathepsin L heavy chain translocation into the nucleus. When cells regained functional cathepsin X, the cytosolic stalling disappeared, and the nuclear cathepsin L level was also restored. This may have a link within the context of neuroinflammation. Neuroinflammation is characterised by an increased expression of cathepsin X [30]. The increased activity of cathepsin X may facilitate an increased nuclear localisation of cathepsin L, resulting in excessive degradation of Lamin B1, eventually leading to exacerbated neuroinflammation.

In conclusion, this study showed that DC maturation was accompanied by cathepsin X regulation through an IL-6 – Stat3 dependent manner. We further proposed that cathepsin X may modulate the secretion of IL-1β through TMEM176B. We eventually showed a modification of lysosomal cathepsin L processing by active cathepsin X and a novel lysosomal and nuclear proteolysis connection. These data, collectively, may contribute to disease progression, especially in the context of cancer and neuron inflammation.

7. References

1. Jevnikar, Z., et al., *The role of cathepsin X in the migration and invasiveness of T lymphocytes.* J Cell Sci, 2008. **121**(Pt 16): p. 2652-61.
2. Hsing, L.C. and A.Y. Rudensky, *The lysosomal cysteine proteases in MHC class II antigen presentation.* Immunological Reviews, 2005. **207**: p. 229-241.
3. Obermajer, N., et al., *Maturation of dendritic cells depends on proteolytic cleavage by cathepsin X.* J Leukoc Biol, 2008. **84**(5): p. 1306-15.
4. Chapman, H.A., R.J. Riese, and G.P. Shi, *Emerging roles for cysteine proteases in human biology.* Annual Review Of Physiology, 1997. **59**: p. 63-88.
5. López-Otín, C. and J.S. Bond, *Proteases: multifunctional enzymes in life and disease.* J Biol Chem, 2008. **283**(45): p. 30433-7.
6. Hagemann, S., et al., *The human cysteine protease cathepsin V can compensate for murine cathepsin L in mouse epidermis and hair follicles.* Eur J Cell Biol, 2004. **83**(11-12): p. 775-80.
7. Tisljar, K., J. Deussing, and C. Peters, *Cathepsin J, a novel murine cysteine protease of the papain family with a placenta-restricted expression.* FEBS Lett, 1999. **459**(3): p. 299-304.
8. von Figura, K., *Molecular recognition and targeting of lysosomal proteins.* Curr Opin Cell Biol, 1991. **3**(4): p. 642-6.
9. Watts, C., *Capture and processing of exogenous antigens for presentation on MHC molecules.* Annu Rev Immunol, 1997. **15**: p. 821-50.
10. Qi, R., D. Singh, and C.C. Kao, *Proteolytic Processing Regulates Toll-like Receptor 3 Stability and Endosomal Localization*.* Journal of Biological Chemistry, 2012. **287**(39): p. 32617-32629.
11. Honey, K. and A.Y. Rudensky, *Lysosomal cysteine proteases regulate antigen presentation.* Nature Reviews. Immunology, 2003. **3**(6): p. 472-482.
12. Tu, N.H., et al., *Legumain Induces Oral Cancer Pain by Biased Agonism of Protease-Activated Receptor-2.* J Neurosci, 2021. **41**(1): p. 193-210.
13. Vasiljeva, O., et al., *Recombinant human procathepsin S is capable of autocatalytic processing at neutral pH in the presence of glycosaminoglycans.* FEBS Lett, 2005. **579**(5): p. 1285-90.
14. Yoon, M.C., et al., *Selective Neutral pH Inhibitor of Cathepsin B Designed Based on Cleavage Preferences at Cytosolic and Lysosomal pH Conditions.* ACS Chem Biol, 2021. **16**(9): p. 1628-1643.
15. Almeida, P.C., et al., *Cysteine proteinase activity regulation. A possible role of heparin and heparin-like glycosaminoglycans.* J Biol Chem, 1999. **274**(43): p. 30433-8.
16. Yadati, T., et al., *The Ins and Outs of Cathepsins: Physiological Function and Role in Disease Management.* Cells, 2020. **9**(7).
17. Campden, R.I. and Y. Zhang, *The role of lysosomal cysteine cathepsins in NLRP3 inflammasome activation.* Arch Biochem Biophys, 2019. **670**: p. 32-42.
18. Li, S., et al., *Cathepsin B contributes to autophagy-related 7 (Atg7)-induced nod-like receptor 3 (NLRP3)-dependent proinflammatory response and aggravates lipotoxicity in rat insulinoma cell line.* J Biol Chem, 2013. **288**(42): p. 30094-30104.
19. Niemi, K., et al., *Serum amyloid A activates the NLRP3 inflammasome via P2X7 receptor and a cathepsin B-sensitive pathway.* J Immunol, 2011. **186**(11): p. 6119-28.
20. Orlowski, G.M., et al., *Multiple Cathepsins Promote Pro-IL-1β Synthesis and NLRP3-Mediated IL-1β Activation.* J Immunol, 2015. **195**(4): p. 1685-97.
21. Yan, D., et al., *STAT3 and STAT6 Signaling Pathways Synergize to Promote Cathepsin Secretion from Macrophages via IRE1α Activation.* Cell reports, 2016. **16**(11): p. 2914-2927.
22. Jiang, T., et al., *Cathepsin L-containing exosomes from α-synuclein-activated microglia induce neurotoxicity through the P2X7 receptor.* npj Parkinson's Disease, 2022. **8**(1): p. 127.
23. Richards, C.M., et al., *The human disease gene LYSET is essential for lysosomal enzyme transport and viral infection.* Science, 2022. **378**(6615): p. eabn5648.

24. Marschner, K., et al., *A Key Enzyme in the Biogenesis of Lysosomes Is a Protease That Regulates Cholesterol Metabolism.* Science, 2011. **333**(6038): p. 87-90.
25. Raposo, G. and W. Stoorvogel, *Extracellular vesicles: Exosomes, microvesicles, and friends.* Journal of Cell Biology, 2013. **200**(4): p. 373-383.
26. Turola, E., et al., *Microglial microvesicles secretion and intercellular signalling.* Frontiers in Physiology, 2012. **3**.
27. Yan, S., M. Sameni, and B.F. Sloane, *Cathepsin B and human tumor progression.* Biol Chem, 1998. **379**(2): p. 113-23.
28. Yan, X., et al., *Stromal expression of cathepsin K in squamous cell carcinoma.* J Eur Acad Dermatol Venereol, 2011. **25**(3): p. 362-5.
29. Dall, E. and H. Brandstetter, *Mechanistic and structural studies on legumain explain its zymogenicity, distinct activation pathways, and regulation.* Proc Natl Acad Sci U S A, 2013. **110**(27): p. 10940-5.
30. Allan, E.R.O., et al., *A role for cathepsin Z in neuroinflammation provides mechanistic support for an epigenetic risk factor in multiple sclerosis.* Journal of Neuroinflammation, 2017. **14**: p. 1-11.
31. Al-Hashimi, A., et al., *Significance of nuclear cathepsin V in normal thyroid epithelial and carcinoma cells.* Biochimica et Biophysica Acta (BBA) - Molecular Cell Research, 2020. **1867**(12): p. 118846.
32. Burton, L.J., et al., *Snail transcription factor NLS and importin β1 regulate the subcellular localization of Cathepsin L and Cux1.* Biochem Biophys Res Commun, 2017. **491**(1): p. 59-64.
33. Haugen, M.H., et al., *Nuclear legumain activity in colorectal cancer.* PLoS One, 2013. **8**(1): p. e52980.
34. Pan, T., et al., *Cathepsin L promotes angiogenesis by regulating the CDP/Cux/VEGF-D pathway in human gastric cancer.* Gastric Cancer, 2020. **23**(6): p. 974-987.
35. Islam, M.I., et al., *Regulatory role of cathepsin L in induction of nuclear laminopathy in Alzheimer's disease.* Aging Cell, 2022. **21**(1): p. e13531.
36. Tamhane, T., et al., *Nuclear cathepsin L activity is required for cell cycle progression of colorectal carcinoma cells.* Biochimie, 2016. **122**: p. 208-18.
37. Solberg, R., et al., *The Mammalian Cysteine Protease Legumain in Health and Disease.* Int J Mol Sci, 2022. **23**(24).
38. Colbert, J.D., et al., *Diverse regulatory roles for lysosomal proteases in the immune response.* Eur J Immunol, 2009. **39**(11): p. 2955-65.
39. Amenta, J.S. and S.C. Brocher, *Role of lysosomes in protein turnover: Catch-up proteolysis after release from NH4Cl inhibition.* Journal of Cellular Physiology, 1980. **102**(2): p. 259-266.
40. Kos, J., Z. Jevnikar, and N. Obermajer, *The role of cathepsin X in cell signaling.* Cell Adhesion & Migration, 2009. **3**(2): p. 164-166.
41. Deussing, J., I. von Olshausen, and C. Peters, *Murine and human cathepsin Z: cDNA-cloning, characterization of the genes and chromosomal localization.* Biochimica et Biophysica Acta (BBA) - Gene Structure and Expression, 2000. **1491**(1): p. 93-106.
42. Nägler, D.K. and R. Ménard, *Human cathepsin X: A novel cysteine protease of the papain family with a very short proregion and unique insertions1NRCC Publication No. 41436. The nucleotide sequence reported in this paper has been submitted to the GenBank/EMBL data bank under GenBank accession number AF073890.1.* FEBS Letters, 1998. **434**(1): p. 135-139.
43. Nägler, D.K., et al., *Human cathepsin X: A cysteine protease with unique carboxypeptidase activity.* Biochemistry, 1999. **38**(39): p. 12648-12654.
44. Puzer, L., et al., *Recombinant human cathepsin X is a carboxymonopeptidase only: a comparison with cathepsins B and L.* Biol Chem, 2005. **386**(11): p. 1191-5.
45. Klemenčič, I., et al., *Biochemical characterization of human cathepsin X revealed that the enzyme is an exopeptidase, acting as carboxymonopeptidase or carboxydipeptidase.* European Journal of Biochemistry, 2000. **267**(17): p. 5404-5412.

46. Edgington, L.E., M. Verdoes, and M. Bogyo, *Functional imaging of proteases: recent advances in the design and application of substrate-based and activity-based probes.* Curr Opin Chem Biol, 2011. **15**(6): p. 798-805.
47. Zavasnik-Bergant, T. and B. Turk, *Cysteine cathepsins in the immune response.* Tissue Antigens, 2006. **67**(5): p. 349-55.
48. Akkari, L., et al., *Distinct functions of macrophage-derived and cancer cell-derived cathepsin Z combine to promote tumor malignancy via interactions with the extracellular matrix.* Genes Dev, 2014. **28**(19): p. 2134-50.
49. Sivaraman, J., et al., *Crystal structure of human procathepsin X: a cysteine protease with the proregion covalently linked to the active site cysteine1 1Edited by I. A. Wilson.* Journal of Molecular Biology, 2000. **295**(4): p. 939-951.
50. Staudt, N.D., et al., *Cathepsin X is secreted by human osteoblasts, digests CXCL-12 and impairs adhesion of hematopoietic stem and progenitor cells to osteoblasts.* Haematologica, 2010. **95**(9): p. 1452-1460.
51. Devanathan, G., et al., *Carboxy-monopeptidase substrate specificity of human cathepsin X.* Biochemical and Biophysical Research Communications, 2005. **329**(2): p. 445-452.
52. Obermajer, N., et al., *Cathepsin X cleaves the C-terminal dipeptide of alpha- and gamma-enolase and impairs survival and neuritogenesis of neuronal cells.* The International Journal of Biochemistry & Cell Biology, 2009. **41**(8): p. 1685-1696.
53. Pečar Fonović, U. and J. Kos, *Cathepsin X Cleaves Profilin 1 C-Terminal Tyr139 and Influences Clathrin-Mediated Endocytosis.* PLOS ONE, 2015. **10**(9): p. e0137217.
54. Marino, G., U. Eckhard, and C.M. Overall, *Protein Termini and Their Modifications Revealed by Positional Proteomics.* ACS Chem Biol, 2015. **10**(8): p. 1754-64.
55. Edgington, L.E., et al., *Functional Imaging of Legumain in Cancer Using a New Quenched Activity-Based Probe.* Journal of the American Chemical Society, 2013. **135**(1): p. 174-182.
56. Mountford, S.J., et al., *Application of a sulfoxonium ylide electrophile to generate cathepsin X-selective activity-based probes.* ACS Chem Biol, 2020.
57. Jian, W., et al., *Overexpression of Cathepsin Z Contributes to Tumor Metastasis by Inducing Epithelial-Mesenchymal Transition in Hepatocellular Carcinoma.* PLoS ONE, 2011. **6**(9): p. 1-9.
58. Pišlar, A., et al., *Upregulation of Cysteine Protease Cathepsin X in the 6-Hydroxydopamine Model of Parkinson's Disease.* Frontiers in Molecular Neuroscience, 2018. **11**.
59. Yang, W.-E., et al., *Cathepsin B Expression and the Correlation with Clinical Aspects of Oral Squamous Cell Carcinoma.* PLoS ONE, 2016. **11**(3): p. 1-11.
60. Mitrovic, A., U.P. Fonovic, and J. Kos, *Cysteine cathepsins B and X promote epithelial-mesenchymal transition of tumor cells.* European Journal of Cell Biology, 2017(6): p. 622.
61. Mitrović, A., et al., *Evaluation of novel cathepsin-X inhibitors in vitro and in vivo and their ability to improve cathepsin-B-directed antitumor therapy.* Cell Mol Life Sci, 2022. **79**(1): p. 34.
62. Krueger, S., et al., *Induction of premalignant host responses by cathepsin x/z-deficiency in Helicobacter pylori-infected mice.* PLoS One, 2013. **8**(7): p. e70242.
63. Pišlar, A., et al., *Neuroinflammation-Induced Upregulation of Glial Cathepsin X Expression and Activity in vivo.* Frontiers in Molecular Neuroscience, 2020. **13**.
64. Campden, R.I., et al., *Extracellular cathepsin Z signals through the α(5) integrin and augments NLRP3 inflammasome activation.* J Biol Chem, 2022. **298**(1): p. 101459.
65. Wang, J., et al., *Overexpression of cathepsin Z contributes to tumor metastasis by inducing epithelial-mesenchymal transition in hepatocellular carcinoma.* PLoS One, 2011. **6**(9): p. e24967.
66. Majc, B., et al., *Upregulation of Cathepsin X in Glioblastoma: Interplay with γ-Enolase and the Effects of Selective Cathepsin X Inhibitors.* Int J Mol Sci, 2022. **23**(3).
67. Banchereau, J., et al., *IMMUNOBIOLOGY OF DENDRITIC CELLS*. 2000, ANNUAL REVIEWS INC: United States. p. 767.

68. Park, B., et al., *Proteolytic cleavage in an endolysosomal compartment is required for activation of Toll-like receptor 9.* Nat Immunol, 2008. **9**(12): p. 1407-14.
69. Riese, R.J., et al., *Essential Role for Cathepsin S in MHC Class II–Associated Invariant Chain Processing and Peptide Loading.* Immunity, 1996. **4**(4): p. 357-366.
70. Ha, S.-D., et al., *Cathepsin B Is Involved in the Trafficking of TNF-α-Containing Vesicles to the Plasma Membrane in Macrophages.* The Journal of Immunology, 2008. **181**(1): p. 690-697.
71. Yin, X., et al., *Human Blood CD1c+ Dendritic Cells Encompass CD5high and CD5low Subsets That Differ Significantly in Phenotype, Gene Expression, and Functions.* J Immunol, 2017. **198**(4): p. 1553-1564.
72. Villani, A.C., et al., *Single-cell RNA-seq reveals new types of human blood dendritic cells, monocytes, and progenitors.* Science, 2017. **356**(6335).
73. Collin, M., N. McGovern, and M. Haniffa, *Human dendritic cell subsets.* Immunology, 2013. **140**(1): p. 22-30.
74. Haniffa, M., et al., *Human tissues contain CD141hi cross-presenting dendritic cells with functional homology to mouse CD103+ nonlymphoid dendritic cells.* Immunity, 2012. **37**(1): p. 60-73.
75. McGovern, N., et al., *Human dermal CD14^{+} cells are a transient population of monocyte-derived macrophages.* Immunity, 2014. **41**(3): p. 465-477.
76. Bakdash, G., et al., *Expansion of a BDCA1+CD14+ Myeloid Cell Population in Melanoma Patients May Attenuate the Efficacy of Dendritic Cell Vaccines.* Cancer Res, 2016. **76**(15): p. 4332-46.
77. Mueller, C.G. and B. Voisin, *Of skin and bone: did Langerhans cells and osteoclasts evolve from a common ancestor?* Journal of Anatomy, 2019. **235**(2): p. 412-417.
78. Romani, N., P.M. Brunner, and G. Stingl, *Changing views of the role of Langerhans cells.* J Invest Dermatol, 2012. **132**(3 Pt 2): p. 872-81.
79. Cohn, L., et al., *Antigen delivery to early endosomes eliminates the superiority of human blood BDCA3+ dendritic cells at cross presentation.* Journal of Experimental Medicine, 2013. **210**(5): p. 1049-1063.
80. Embgenbroich, M. and S. Burgdorf, *Current Concepts of Antigen Cross-Presentation.* Frontiers in Immunology, 2018. **9**.
81. Fuertes Marraco, S., et al., *Novel Murine Dendritic Cell Lines: A Powerful Auxiliary Tool for Dendritic Cell Research.* Frontiers in Immunology, 2012. **3**(331).
82. Rakoff-Nahoum, S. and R. Medzhitov, *Toll-like receptors and cancer.* Nature Reviews Cancer, 2008. **9**: p. 57.
83. Meylan, E., J. Tschopp, and M. Karin, *Intracellular pattern recognition receptors in the host response.* Nature, 2006. **442**(7098): p. 39-44.
84. Martinon, F., K. Burns, and J. Tschopp, *The inflammasome: a molecular platform triggering activation of inflammatory caspases and processing of proIL-beta.* Mol Cell, 2002. **10**(2): p. 417-26.
85. Levinsohn, J.L., et al., *Anthrax lethal factor cleavage of Nlrp1 is required for activation of the inflammasome.* PLoS Pathog, 2012. **8**(3): p. e1002638.
86. Bauernfeind, F.G., et al., *Cutting edge: NF-kappaB activating pattern recognition and cytokine receptors license NLRP3 inflammasome activation by regulating NLRP3 expression.* J Immunol, 2009. **183**(2): p. 787-91.
87. de Zoete, M.R., et al., *Inflammasomes.* Cold Spring Harb Perspect Biol, 2014. **6**(12): p. a016287.
88. Elinav, E., et al., *NLRP6 inflammasome regulates colonic microbial ecology and risk for colitis.* Cell, 2011. **145**(5): p. 745-57.
89. Wlodarska, M., et al., *NLRP6 inflammasome orchestrates the colonic host-microbial interface by regulating goblet cell mucus secretion.* Cell, 2014. **156**(5): p. 1045-59.

90. Zaki, M.H., et al., *The NOD-like receptor NLRP12 attenuates colon inflammation and tumorigenesis.* Cancer Cell, 2011. **20**(5): p. 649-60.
91. Allen, I.C., et al., *NLRP12 suppresses colon inflammation and tumorigenesis through the negative regulation of noncanonical NF-κB signaling.* Immunity, 2012. **36**(5): p. 742-54.
92. Miao, E.A., et al., *Innate immune detection of the type III secretion apparatus through the NLRC4 inflammasome.* Proc Natl Acad Sci U S A, 2010. **107**(7): p. 3076-80.
93. Kofoed, E.M. and R.E. Vance, *Innate immune recognition of bacterial ligands by NAIPs determines inflammasome specificity.* Nature, 2011. **477**(7366): p. 592-5.
94. Sharma, D. and T.-D. Kanneganti, *The cell biology of inflammasomes: Mechanisms of inflammasome activation and regulation.* Journal of Cell Biology, 2016. **213**(6): p. 617-629.
95. Morrone, S.R., et al., *Cooperative assembly of IFI16 filaments on dsDNA provides insights into host defense strategy.* Proc Natl Acad Sci U S A, 2014. **111**(1): p. E62-71.
96. Schnappauf, O., et al., *The Pyrin Inflammasome in Health and Disease.* Frontiers in Immunology, 2019. **10**.
97. Kayagaki, N., et al., *Caspase-11 cleaves gasdermin D for non-canonical inflammasome signalling.* Nature, 2015. **526**(7575): p. 666-71.
98. Shi, J., et al., *Cleavage of GSDMD by inflammatory caspases determines pyroptotic cell death.* Nature, 2015. **526**(7575): p. 660-5.
99. Muñoz-Planillo, R., et al., *K^+ efflux is the common trigger of NLRP3 inflammasome activation by bacterial toxins and particulate matter.* Immunity, 2013. **38**(6): p. 1142-53.
100. Lee, G.S., et al., *The calcium-sensing receptor regulates the NLRP3 inflammasome through Ca2+ and cAMP.* Nature, 2012. **492**(7427): p. 123-7.
101. Di, A., et al., *The TWIK2 Potassium Efflux Channel in Macrophages Mediates NLRP3 Inflammasome-Induced Inflammation.* Immunity, 2018. **49**(1): p. 56-65.e4.
102. Murakami, T., et al., *Critical role for calcium mobilization in activation of the NLRP3 inflammasome.* Proc Natl Acad Sci U S A, 2012. **109**(28): p. 11282-7.
103. Segovia, M., et al., *Targeting TMEM176B Enhances Antitumor Immunity and Augments the Efficacy of Immune Checkpoint Blockers by Unleashing Inflammasome Activation.* Cancer Cell, 2019. **35**(5): p. 767-781.e6.
104. Lebreton, F., et al., *NLRP3 inflammasome is expressed and regulated in human islets.* Cell Death & Disease, 2018. **9**(7): p. 726.
105. Helft, J., et al., *GM-CSF Mouse Bone Marrow Cultures Comprise a Heterogeneous Population of CD11c+MHCII+ Macrophages and Dendritic Cells.* Immunity, 2015. **42**(6): p. 1197-1211.
106. Erlich, Z., et al., *Macrophages, rather than DCs, are responsible for inflammasome activity in the GM-CSF BMDC model.* Nature Immunology, 2019. **20**(4): p. 397-406.
107. Chakraborty, R., et al., *CD8+ lineage dendritic cells determine adaptive immune responses to inflammasome activation upon sterile skin injury.* Experimental Dermatology, 2018. **27**(1): p. 71-79.
108. McDaniel, M.M., et al., *Suppression of Inflammasome Activation by IRF8 and IRF4 in cDCs Is Critical for T Cell Priming.* Cell Rep, 2020. **31**(5): p. 107604.
109. Neefjes, J., et al., *Towards a systems understanding of MHC class I and MHC class II antigen presentation.* Nat Rev Immunol, 2011. **11**(12): p. 823-36.
110. Joffre, O.P., et al., *Cross-presentation by dendritic cells.* Nature Reviews Immunology, 2012(8): p. 557.
111. Shortman, K. and W.R. Heath, *The CD8+ dendritic cell subset.* Immunological Reviews, 2010. **234**(1): p. 18-31.
112. Nagahama, M., K. Kobayashi, and M. Takehara, *Cathepsin Release from Lysosomes Promotes Endocytosis of Clostridium perfringens Iota-Toxin.* Toxins, 2021. **13**(10): p. 721.
113. Witke, W., et al., *In mouse brain profilin I and profilin II associate with regulators of the endocytic pathway and actin assembly.* Embo j, 1998. **17**(4): p. 967-76.

114. Zhao, M.-M., et al., *Cathepsin L plays a key role in SARS-CoV-2 infection in humans and humanized mice and is a promising target for new drug development.* Signal Transduction and Targeted Therapy, 2021. **6**(1): p. 134.
115. Garcia-Cattaneo, A., et al., *Cleavage of Toll-like receptor 3 by cathepsins B and H is essential for signaling.* Proceedings of the National Academy of Sciences, 2012. **109**(23): p. 9053-9058.
116. Sepulveda, F.E., et al., *Critical Role for Asparagine Endopeptidase in Endocytic Toll-like Receptor Signaling in Dendritic Cells.* Immunity, 2009. **31**(5): p. 737-748.
117. Ewald, S.E., et al., *Nucleic acid recognition by Toll-like receptors is coupled to stepwise processing by cathepsins and asparagine endopeptidase.* J Exp Med, 2011. **208**(4): p. 643-51.
118. Shen, Z., et al., *Cloned dendritic cells can present exogenous antigens on both MHC class I and class II molecules.* J Immunol, 1997. **158**(6): p. 2723-30.
119. Obermajer, N., et al., *Cathepsin X-mediated beta2 integrin activation results in nanotube outgrowth.* Cell Mol Life Sci, 2009. **66**(6): p. 1126-34.
120. Rodriguez, G.M. and S. Diment, *Role of cathepsin D in antigen presentation of ovalbumin.* Journal Of Immunology (Baltimore, Md.: 1950), 1992. **149**(9): p. 2894-2898.
121. Jan, D., et al., *Cathepsins B and D are Dispensable for Major Histocompatibility Complex Class II-Mediated Antigen Presentation.* Proceedings of the National Academy of Sciences of the United States of America, 1998. **95**(8): p. 4516.
122. Bennett, K., et al., *Antigen processing for presentation by class II major histocompatibility complex requires cleavage by cathepsin E.* European Journal Of Immunology, 1992. **22**(6): p. 1519-1524.
123. Honey, K., et al., *Cathepsin L regulates CD4+ T cell selection independently of its effect on invariant chain: a role in the generation of positively selecting peptide ligands.* The Journal of experimental medicine, 2002. **195**(10): p. 1349-1358.
124. Pluger, E.B., et al., *Specific role for cathepsin S in the generation of antigenic peptides in vivo.* Eur J Immunol, 2002. **32**(2): p. 467-76.
125. Antoniou, A.N., et al., *Control of Antigen Presentation by a Single Protease Cleavage Site.* Immunity, 2000. **12**(4): p. 391-398.
126. Manoury, B., et al., *Asparagine Endopeptidase Can Initiate the Removal of the MHC Class II Invariant Chain Chaperone.* Immunity, 2003. **18**(4): p. 489-498.
127. Nakagawa, T.Y. and A.Y. Rudensky, *The role of lysosomal proteinases in MHC class II-mediated antigen processing and presentation.* Immunological Reviews, 1999. **172**: p. 121-129.
128. Nakagawa, T., W. Roth, and A.Y. Rudensky, *Cathespin L: critical role in Ii degradation and CD4 cell selection in the thymus.* Science, 1998. **280**: p. 450+.
129. Kostura, M.J., et al., *Identification of a monocyte specific pre-interleukin 1 beta convertase activity.* Proceedings of the National Academy of Sciences, 1989. **86**(14): p. 5227-5231.
130. Ghayur, T., et al., *Caspase-1 processes IFN-γ-inducing factor and regulates LPS-induced IFN- γ production.* Nature, 1997. **386**(6625): p. 619-623.
131. Lamkanfi, M. and V.M. Dixit, *Mechanisms and functions of inflammasomes.* Cell, 2014. **157**(5): p. 1013-22.
132. Tsutsui, H., et al., *Caspase-1-Independent, Fas/Fas Ligand–Mediated IL-18 Secretion from Macrophages Causes Acute Liver Injury in Mice.* Immunity, 1999. **11**(3): p. 359-367.
133. Black, R.A., et al., *Generation of biologically active interleukin-1 beta by proteolytic cleavage of the inactive precursor.* J Biol Chem, 1988. **263**(19): p. 9437-42.
134. Hazuda, D.J., et al., *Processing of precursor interleukin 1 beta and inflammatory disease.* J Biol Chem, 1990. **265**(11): p. 6318-22.
135. Cavalli, G., et al., *Interleukin 1α: a comprehensive review on the role of IL-1α in the pathogenesis and treatment of autoimmune and inflammatory diseases.* Autoimmunity Reviews, 2021. **20**(3): p. 102763.
136. Afonina, Inna S., et al., *Granzyme B-Dependent Proteolysis Acts as a Switch to Enhance the Proinflammatory Activity of IL-1α.* Molecular Cell, 2011. **44**(2): p. 265-278.

137. Schmitz, J., et al., *IL-33, an Interleukin-1-like Cytokine that Signals via the IL-1 Receptor-Related Protein ST2 and Induces T Helper Type 2-Associated Cytokines.* Immunity, 2005. **23**(5): p. 479-490.
138. Lüthi, A.U., et al., *Suppression of Interleukin-33 Bioactivity through Proteolysis by Apoptotic Caspases.* Immunity, 2009. **31**(1): p. 84-98.
139. Kumar, S., et al., *Interleukin-1F7B (IL-1H4/IL-1F7) is processed by caspase-1 and mature IL-1F7B binds to the IL-18 receptor but does not induce IFN-gamma production.* Cytokine, 2002. **18**(2): p. 61-71.
140. Sharma, S., et al., *The IL-1 Family Member 7b Translocates to the Nucleus and Down-Regulates Proinflammatory Cytokines.* The Journal of Immunology, 2008. **180**(8): p. 5477-5482.
141. Bulau, A.-M., et al., *Role of caspase-1 in nuclear translocation of IL-37, release of the cytokine, and IL-37 inhibition of innate immune responses.* Proceedings of the National Academy of Sciences, 2014. **111**(7): p. 2650.
142. Shi, J., et al., *Inflammatory caspases are innate immune receptors for intracellular LPS.* Nature, 2014. **514**(7521): p. 187-92.
143. He, W.-t., et al., *Gasdermin D is an executor of pyroptosis and required for interleukin-1β secretion.* Cell Research, 2015. **25**(12): p. 1285-1298.
144. Sagulenko, V., et al., *AIM2 and NLRP3 inflammasomes activate both apoptotic and pyroptotic death pathways via ASC.* Cell Death Differ, 2013. **20**(9): p. 1149-60.
145. Rauch, I., et al., *NAIP-NLRC4 Inflammasomes Coordinate Intestinal Epithelial Cell Expulsion with Eicosanoid and IL-18 Release via Activation of Caspase-1 and -8.* Immunity, 2017. **46**(4): p. 649-659.
146. Lee, B.L., et al., *ASC- and caspase-8-dependent apoptotic pathway diverges from the NLRC4 inflammasome in macrophages.* Sci Rep, 2018. **8**(1): p. 3788.
147. Chevriaux, A., et al., *Cathepsin B Is Required for NLRP3 Inflammasome Activation in Macrophages, Through NLRP3 Interaction.* Frontiers in Cell and Developmental Biology, 2020. **8**.
148. Talukdar, R., et al., *Release of Cathepsin B in Cytosol Causes Cell Death in Acute Pancreatitis.* Gastroenterology, 2016. **151**(4): p. 747-758.e5.
149. Burgener, S.S., et al., *Cathepsin G Inhibition by Serpinb1 and Serpinb6 Prevents Programmed Necrosis in Neutrophils and Monocytes and Reduces GSDMD-Driven Inflammation.* Cell Rep, 2019. **27**(12): p. 3646-3656.e5.
150. Jun, H.-K., et al., *Integrin α5β1 Activates the NLRP3 Inflammasome by Direct Interaction with a Bacterial Surface Protein.* Immunity, 2012. **36**(5): p. 755-768.
151. Thinwa, J., et al., *Integrin-mediated first signal for inflammasome activation in intestinal epithelial cells.* J Immunol, 2014. **193**(3): p. 1373-82.
152. Mortimer, L., et al., *The NLRP3 Inflammasome Is a Pathogen Sensor for Invasive Entamoeba histolytica via Activation of α5β1 Integrin at the Macrophage-Amebae Intercellular Junction.* PLoS Pathog, 2015. **11**(5): p. e1004887.
153. Mócsai, A., et al., *Syk Is Required for Integrin Signaling in Neutrophils.* Immunity, 2002. **16**(4): p. 547-558.
154. Song, N. and T. Li, *Regulation of NLRP3 Inflammasome by Phosphorylation.* Frontiers in Immunology, 2018. **9**.
155. Kayagaki, N., et al., *Noncanonical inflammasome activation by intracellular LPS independent of TLR4.* Science, 2013. **341**(6151): p. 1246-9.
156. Manoury, B., et al., *An asparaginyl endopeptidase processes a microbial antigen for class II MHC presentation.* Nature, 1998. **396**(6712): p. 695-699.
157. Vremec, D., *The isolation of mouse dendritic cells from lymphoid tissues and the identification of dendritic cell subtypes by multiparameter flow cytometry.* Methods Mol Biol, 2010. **595**: p. 205-29.

158. Wilson, K.R., et al., *MARCH1-mediated ubiquitination of MHC II impacts the MHC I antigen presentation pathway.* PLoS One, 2018. **13**(7): p. e0200540.
159. Raschke, W.C., et al., *Functional macrophage cell lines transformed by Abelson leukemia virus.* Cell, 1978. **15**(1): p. 261-7.
160. Momose, F., et al., *Variant sublines with different metastatic potentials selected in nude mice from human oral squamous cell carcinomas.* J Oral Pathol Med, 1989. **18**(7): p. 391-5.
161. Graham, F.L., et al., *Characteristics of a human cell line transformed by DNA from human adenovirus type 5.* J Gen Virol, 1977. **36**(1): p. 59-74.
162. Mountford, S.J., et al., *Application of a Sulfoxonium Ylide Electrophile to Generate Cathepsin X-Selective Activity-Based Probes.* ACS Chemical Biology, 2020. **15**(3): p. 718-727.
163. Verdoes, M., et al., *Improved quenched fluorescent probe for imaging of cysteine cathepsin activity.* J Am Chem Soc, 2013. **135**(39): p. 14726-30.
164. Yuan, F., et al., *A selective activity-based probe for the papain family cysteine protease dipeptidyl peptidase I/cathepsin C.* J Am Chem Soc, 2006. **128**(17): p. 5616-7.
165. Edgington, L.E., et al., *Functional imaging of legumain in cancer using a new quenched activity-based probe.* J Am Chem Soc, 2013. **135**(1): p. 174-82.
166. Anderson, B.M., et al., *Application of a chemical probe to detect neutrophil elastase activation during inflammatory bowel disease.* Sci Rep, 2019. **9**(1): p. 13295.
167. Edgington-Mitchell, L.E., et al., *Fluorescent diphenylphosphonate-based probes for detection of serine protease activity during inflammation.* Bioorg Med Chem Lett, 2017. **27**(2): p. 254-260.
168. Liu, Y., M.P. Patricelli, and B.F. Cravatt, *Activity-based protein profiling: the serine hydrolases.* Proc Natl Acad Sci U S A, 1999. **96**(26): p. 14694-9.
169. Hewitt, E., et al., *Selective Cathepsin S Inhibition with MIV-247 Attenuates Mechanical Allodynia and Enhances the Antiallodynic Effects of Gabapentin and Pregabalin in a Mouse Model of Neuropathic Pain.* J Pharmacol Exp Ther, 2016. **358**(3): p. 387-96.
170. Lee, J. and M. Bogyo, *Synthesis and evaluation of aza-peptidyl inhibitors of the lysosomal asparaginyl endopeptidase, legumain.* Bioorg Med Chem Lett, 2012. **22**(3): p. 1340-3.
171. Hogquist, K.A., et al., *T cell receptor antagonist peptides induce positive selection.* Cell, 1994. **76**(1): p. 17-27.
172. Barnden, M.J., et al., *Defective TCR expression in transgenic mice constructed using cDNA-based alpha- and beta-chain genes under the control of heterologous regulatory elements.* Immunol Cell Biol, 1998. **76**(1): p. 34-40.
173. Kirschke, H. and B. Wiederanders, *[34] Cathepsin S and related lysosomal endopeptidases*, in *Methods in Enzymology*. 1994, Academic Press. p. 500-511.
174. Xu, Y., et al., *IL-10 Controls Cystatin C Synthesis and Blood Concentration in Response to Inflammation through Regulation of IFN Regulatory Factor 8 Expression*. 2011, American Association of Immunologists: United States. p. 3666.
175. Akkari, L., et al., *Combined deletion of cathepsin protease family members reveals compensatory mechanisms in cancer.* Genes Dev, 2016. **30**(2): p. 220-32.
176. Tobe, M., et al., *Discovery of quinazolines as a novel structural class of potent inhibitors of NF-κB activation.* Bioorganic & Medicinal Chemistry, 2003. **11**(3): p. 383-391.
177. Katunuma, N., *Posttranslational processing and modification of cathepsins and cystatins.* J Signal Transduct, 2010. **2010**: p. 375345.
178. Yamamoto, M., et al., *Role of Adaptor TRIF in the MyD88-Independent Toll-Like Receptor Signaling Pathway.* Science, 2003. **301**(5633): p. 640-643.
179. Maelfait, J., L. Liverpool, and J. Rehwinkel, *Nucleic Acid Sensors and Programmed Cell Death.* J Mol Biol, 2020. **432**(2): p. 552-568.
180. Tatematsu, M., et al., *Toll-like receptor 3 recognizes incomplete stem structures in single-stranded viral RNA.* Nat Commun, 2013. **4**: p. 1833.

181. Karikó, K., et al., *mRNA is an endogenous ligand for Toll-like receptor 3.* J Biol Chem, 2004. **279**(13): p. 12542-50.
182. West, N.R., *Coordination of Immune-Stroma Crosstalk by IL-6 Family Cytokines.* Front Immunol, 2019. **10**: p. 1093.
183. Chan, L.L.Y., et al., *A role for STAT3 and cathepsin S in IL-10 down-regulation of IFN-γ-induced MHC class II molecule on primary human blood macrophages.* Journal of Leukocyte Biology, 2010. **88**(2): p. 303-311.
184. Sepulveda, F.E., et al., *Critical Role for Asparagine Endopeptidase in Endocytic Toll-like Receptor Signaling in Dendritic Cells.* Immunity, 2009. **31**(5): p. 737-748.
185. Matsumoto, F., et al., *Cathepsins are required for Toll-like receptor 9 responses.* Biochemical and Biophysical Research Communications, 2008. **367**(3): p. 693-699.
186. Liu, Z. and P.A. Roche, *Macropinocytosis in phagocytes: regulation of MHC class-II-restricted antigen presentation in dendritic cells.* Front Physiol, 2015. **6**: p. 1.
187. Platt, C.D., et al., *Mature dendritic cells use endocytic receptors to capture and present antigens.* Proc Natl Acad Sci U S A, 2010. **107**(9): p. 4287-92.
188. Burgdorf, S., V. Lukacs-Kornek, and C. Kurts, *The mannose receptor mediates uptake of soluble but not of cell-associated antigen for cross-presentation.* J Immunol, 2006. **176**(11): p. 6770-6.
189. Brasel, K., et al., *Generation of murine dendritic cells from flt3-ligand-supplemented bone marrow cultures.* Blood, 2000. **96**(9): p. 3029-39.
190. Hirano, T., *Interleukin 6 and its receptor: ten years later.* Int Rev Immunol, 1998. **16**(3-4): p. 249-84.
191. Park, S.J., et al., *IL-6 regulates in vivo dendritic cell differentiation through STAT3 activation.* J Immunol, 2004. **173**(6): p. 3844-54.
192. Kitamura, H., et al., *IL-6-STAT3 Controls Intracellular MHC Class II αβ Dimer Level through Cathepsin S Activity in Dendritic Cells.* Immunity, 2005. **23**(5): p. 491-502.
193. Condamine, T., et al., *Tmem176B and Tmem176A are associated with the immature state of dendritic cells.* Journal of Leukocyte Biology, 2010. **88**(3): p. 507-515.
194. Kim, S.K., K.Y. Park, and J.Y. Choe, *Toll-Like Receptor 9 Is Involved in NLRP3 Inflammasome Activation and IL-1β Production Through Monosodium Urate-Induced Mitochondrial DNA.* Inflammation, 2020. **43**(6): p. 2301-2311.
195. Franceschini, A., et al., *The P2X7 receptor directly interacts with the NLRP3 inflammasome scaffold protein.* Faseb j, 2015. **29**(6): p. 2450-61.
196. Di Virgilio, F., et al., *The P2X7 Receptor in Infection and Inflammation.* Immunity, 2017. **47**(1): p. 15-31.
197. Martínez-Fábregas, J., et al., *Lysosomal protease deficiency or substrate overload induces an oxidative-stress mediated STAT3-dependent pathway of lysosomal homeostasis.* Nature Communications, 2018. **9**(1): p. 5343.
198. Sevenich, L., et al., *Synergistic antitumor effects of combined cathepsin B and cathepsin Z deficiencies on breast cancer progression and metastasis in mice.* Proc Natl Acad Sci U S A, 2010. **107**(6): p. 2497-502.
199. Dahl, S.W., et al., *Human Recombinant Pro-dipeptidyl Peptidase I (Cathepsin C) Can Be Activated by Cathepsins L and S but Not by Autocatalytic Processing.* Biochemistry, 2001. **40**(6): p. 1671-1678.
200. Shirahama-Noda, K., et al., *Biosynthetic Processing of Cathepsins and Lysosomal Degradation Are Abolished in Asparaginyl Endopeptidase-deficient Mice **.* Journal of Biological Chemistry, 2003. **278**(35): p. 33194-33199.
201. Mattock, K.L., et al., *Legumain and cathepsin-L expression in human unstable carotid plaque.* Atherosclerosis, 2010. **208**(1): p. 83-9.
202. Wang, D., et al., *Loss of legumain induces premature senescence and mediates aging-related renal fibrosis.* Aging Cell, 2022. **21**(3): p. e13574.

203. Edgington-Mitchell, L.E., et al., *Legumain is activated in macrophages during pancreatitis*. 2016. p. G548-G560.
204. Maehr, R., et al., *Asparagine Endopeptidase Is Not Essential for Class II MHC Antigen Presentation but Is Required for Processing of Cathepsin L in Mice.* The Journal of Immunology, 2005. **174**(11): p. 7066-7074.
205. Anderson, B.M., et al., *N-Terminomics/TAILS Profiling of Macrophages after Chemical Inhibition of Legumain.* Biochemistry, 2020. **59**(3): p. 329-340.
206. Yoon, M.C., V. Hook, and A.J. O'Donoghue, *Cathepsin B Dipeptidyl Carboxypeptidase and Endopeptidase Activities Demonstrated across a Broad pH Range.* Biochemistry, 2022. **61**(17): p. 1904-1914.
207. Colbert, J.D., et al., *Internalization of exogenous cystatin F supresses cysteine proteases and induces the accumulation of single-chain cathepsin L by multiple mechanisms.* J Biol Chem, 2011. **286**(49): p. 42082-42090.
208. Kosugi, S., et al., *Systematic identification of cell cycle-dependent yeast nucleocytoplasmic shuttling proteins by prediction of composite motifs.* Proc Natl Acad Sci U S A, 2009. **106**(25): p. 10171-6.
209. Kosugi, S., et al., *Six classes of nuclear localization signals specific to different binding grooves of importin alpha.* J Biol Chem, 2009. **284**(1): p. 478-485.
210. Kosugi, S., et al., *Design of peptide inhibitors for the importin alpha/beta nuclear import pathway by activity-based profiling.* Chem Biol, 2008. **15**(9): p. 940-9.
211. Nguyen Ba, A.N., et al., *NLStradamus: a simple Hidden Markov Model for nuclear localization signal prediction.* BMC Bioinformatics, 2009. **10**(1): p. 202.
212. Hodel, M.R., A.H. Corbett, and A.E. Hodel, *Dissection of a nuclear localization signal.* J Biol Chem, 2001. **276**(2): p. 1317-25.
213. Mallet, P.L. and F. Bachand, *A proline-tyrosine nuclear localization signal (PY-NLS) is required for the nuclear import of fission yeast PAB2, but not of human PABPN1.* Traffic, 2013. **14**(3): p. 282-94.
214. Lee, B.J., et al., *Rules for nuclear localization sequence recognition by karyopherin beta 2.* Cell, 2006. **126**(3): p. 543-58.
215. Truant, R. and B.R. Cullen, *The arginine-rich domains present in human immunodeficiency virus type 1 Tat and Rev function as direct importin beta-dependent nuclear localization signals.* Mol Cell Biol, 1999. **19**(2): p. 1210-7.
216. Sullivan, S., et al., *Localization of nuclear cathepsin L and its association with disease progression and poor outcome in colorectal cancer.* International Journal of Cancer, 2009. **125**(1): p. 54-61.
217. Tamhane, T., et al., *Nuclear cathepsin L activity is required for cell cycle progression of colorectal carcinoma cells.* Biochimie, 2016. **122**: p. 208-218.
218. Burton, L.J., et al., *Targeting the Nuclear Cathepsin L CCAAT Displacement Protein/Cut Homeobox Transcription Factor-Epithelial Mesenchymal Transition Pathway in Prostate and Breast Cancer Cells with the Z-FY-CHO Inhibitor.* Molecular and Cellular Biology, 2017. **37**(5): p. e00297-16.
219. Goulet, B., et al., *A Cathepsin L Isoform that Is Devoid of a Signal Peptide Localizes to the Nucleus in S Phase and Processes the CDP/Cux Transcription Factor.* Molecular Cell, 2004. **14**(2): p. 207-219.
220. Boncompain, G., et al., *Synchronization of secretory protein traffic in populations of cells.* Nature Methods, 2012. **9**(5): p. 493-498.
221. Goulet, B., et al., *Increased expression and activity of nuclear cathepsin L in cancer cells suggests a novel mechanism of cell transformation.* Mol Cancer Res, 2007. **5**(9): p. 899-907.
222. Pišlar, A., et al., *Cysteine Peptidase Cathepsin X as a Therapeutic Target for Simultaneous TLR3/4-mediated Microglia Activation.* Molecular Neurobiology, 2022. **59**(4): p. 2258-2276.

223. Kos, J., et al., *Carboxypeptidases cathepsins X and B display distinct protein profile in human cells and tissues*. 2005, Elsevier Science B.V., Amsterdam: United States. p. 103.
224. Braun, D.A., M. Fribourg, and S.C. Sealfon, *Cytokine response is determined by duration of receptor and signal transducers and activators of transcription 3 (STAT3) activation.* J Biol Chem, 2013. **288**(5): p. 2986-93.
225. Kreuzaler, P.A., et al., *Stat3 controls lysosomal-mediated cell death in vivo.* Nature Cell Biology, 2011. **13**(3): p. 303-309.
226. Mizoguchi, A., et al., *Nectin: an adhesion molecule involved in formation of synapses.* J Cell Biol, 2002. **156**(3): p. 555-65.
227. Takai, Y., et al., *The immunoglobulin-like cell adhesion molecule nectin and its associated protein afadin.* Annu Rev Cell Dev Biol, 2008. **24**: p. 309-42.
228. Petermann, P., et al., *Role of Nectin-1 and Herpesvirus Entry Mediator as Cellular Receptors for Herpes Simplex Virus 1 on Primary Murine Dermal Fibroblasts.* J Virol, 2015. **89**(18): p. 9407-16.
229. Sun, J. and P. Jacquez, *Roles of Anthrax Toxin Receptor 2 in Anthrax Toxin Membrane Insertion and Pore Formation.* Toxins (Basel), 2016. **8**(2): p. 34.
230. Dowling, O., et al., *Mutations in capillary morphogenesis gene-2 result in the allelic disorders juvenile hyaline fibromatosis and infantile systemic hyalinosis.* Am J Hum Genet, 2003. **73**(4): p. 957-66.
231. Kato, M., et al., *The Novel Endocytic and Phagocytic C-Type Lectin Receptor DCL-1/CD302 on Macrophages Is Colocalized with F-Actin, Suggesting a Role in Cell Adhesion and Migration1.* The Journal of Immunology, 2007. **179**(9): p. 6052-6063.
232. Baluška, F., et al., *Actin‐dependent fluid‐phase endocytosis in inner cortex cells of maize root apices.* Journal of Experimental Botany, 2004. **55**(396): p. 463-473.
233. Lin, H.-P., et al., *Receptor-independent fluid-phase macropinocytosis promotes arterial foam cell formation and atherosclerosis.* Science Translational Medicine, 2022. **14**(663): p. eadd2376.
234. Martín-Fontecha, A., A. Lanzavecchia, and F. Sallusto, *Dendritic cell migration to peripheral lymph nodes.* Handb Exp Pharmacol, 2009(188): p. 31-49.
235. Justus, C.R., et al., *In vitro cell migration and invasion assays.* J Vis Exp, 2014(88).
236. Mihelič, M., et al., *Mouse stefins A1 and A2 (Stfa1 and Stfa2) differentiate between papain-like endo- and exopeptidases.* FEBS Letters, 2006. **580**(17): p. 4195-4199.
237. Caserman, S., et al., *Cathepsin L splice variants in human breast cell lines.* Biol Chem, 2006. **387**(5): p. 629-34.
238. Pechincha, C., et al., *Lysosomal enzyme trafficking factor LYSET enables nutritional usage of extracellular proteins.* Science, 2022. **378**(6615): p. eabn5637.
239. Zhang, W., et al., *GCAF(TMEM251) regulates lysosome biogenesis by activating the mannose-6-phosphate pathway.* Nat Commun, 2022. **13**(1): p. 5351.
240. Frolova, A.S., et al., *Expression, Intracellular Localization, and Maturation of Cysteine Cathepsins in Renal Embryonic and Cancer Cell Lines.* Biochemistry (Moscow), 2023. **88**(7): p. 1034-1044.